NOAA Data Report ERL PMEL-12

RELATIONSHIPS BETWEEN SURFACE OBSERVATIONS OVER THE GLOBAL OCEANS AND THE SOUTHERN OSCILLATION

Peter B. Wright
Joint Institute for Study of the Atmosphere and Ocean
University of Washington

Todd P. Mitchell
Department of Atmospheric Sciences
University of Washington

John M. Wallace
Joint Institute for Study of the Atmosphere and Ocean
and
Department of Atmospheric Sciences
University of Washington

Pacific Marine Environmental Laboratory
Seattle, Washington
January 1985

UNITED STATES DEPARTMENT OF COMMERCE

Malcolm Baldrige, Secretary

NATIONAL OCEANIC AND ATMOSPHERIC ADMINISTRATION

Environmental Research Laboratories

Vernon E. Derr, Director

NOTICE

Mention of a commercial company or product does not constitute an endorsement by NOAA/ERL. Use of information from this publication concerning proprietary products or the tests of such products for publicity or advertising purposes is not authorized.

CONTENTS

LIST OF TABLES

LIST OF FIGURES

1. INTRODUCTION

This atlas contains maps of correlation and regression coefficients between seasonal anomalies of surface meteorological fields over the global oceans and Darwin, Australia (12°S,131°E) annual-mean sea-level pressure anomalies. The statistics were calculated for six consecutive seasons defined relative to the Darwin index. The resulting charts provide a description of the time evolution of meteorological anomalies associated with the Southern Oscillation over the global oceans.

Darwin lies within the region of large year-to-year pressure variability associated with the Southern Oscillation over the Indian Ocean, Indonesia, and the western Pacific Ocean, and its annual-mean sea-level pressure is highly correlated with other indices of the Southern Oscillation (Wright, 1984). In many previous studies, Darwin pressure data have been used in combination with pressure data from stations in the southeast Pacific to form indices of the strength of the pressure gradient that drives the south Pacific tradewind circulation [e.g., Trenberth (1976), Quinn *et al.* (1978)]. We have chosen to use Darwin data alone as a reference time series so as to avoid imposing any spatial structure on the resulting correlation patterns. The negative correlations between Darwin pressure and pressures in the southeastern Pacific emerge spontaneously in the patterns based on Darwin alone. Note that the year-to-year fluctuations in Darwin pressure are of opposite polarity to those of most conventional Southern Oscillation indices, which are defined such that positive values denote an abnormally strong south Pacific tradewind circulation.

The twelve-month average for the index is taken from April of one year through March of the next. This choice of months maximizes the year-to-year variability of the index and locates the months of strongest autocorrelation (July through December) near the middle of the averaging period.

The fields correlated with and regressed on the Darwin pressure index are seasonal anomalies of sea surface temperatures (SST), SST minus air tem-

perature, pressure, surface wind, and cloudiness over the global oceans for the period 1950 to 1979. Figure 1 shows the six three-month seasons for which statistics are calculated: the first season is December-January-February (DJF1) several months prior to the start of the Darwin average; MAM1 begins one month previous to the Darwin year; JJA, SON, and DJF2 are successive seasons within; and MAM2 begins in the last month of the Darwin year. For example, in calculating a correlation coefficient for SST in MAM1 at a particular gridpoint, the SST values for March-May 1950, 1951,...,1979 were paired with the Darwin pressure values for April 1950 - March 1951, April 1951 - March 1952,...,April 1979 - March 1980.

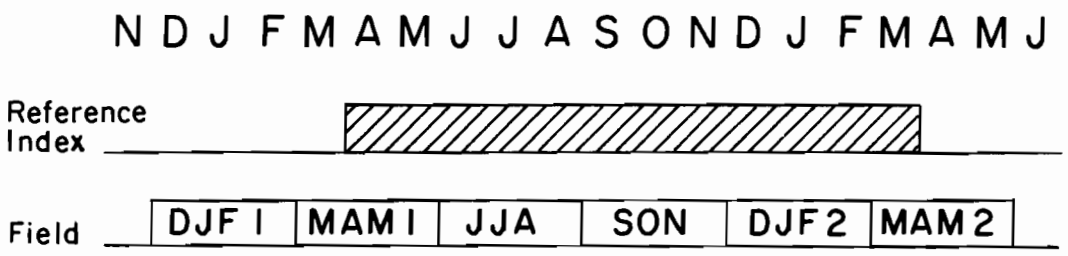

Fig. 1. Averaging periods used in study.

Two different statistical approaches have been adopted in previous studies in which an index of the Southern Oscillation has been related to fields of various meteorological variables over large regions of the globe. In one approach, correlation and/or regression coefficients are found between a Southern Oscillation index and the fields in question. Some studies [e.g., Egger et al. (1981)] examined only simultaneous relationships,

whereas others [e.g., Wright (1977), Angell (1981), Newell et al. (1982)] described both simultaneous and lag relationships. This approach treats the Southern Oscillation as a phenomenon with a continuous range of variation and is most appropriate if relationships between the fields and the Southern Oscillation index are linear.

In the other approach, a set of years is selected according to some criterion, e.g., SST anomaly in a certain area greater than some threshold value, and the mean value of the field over those years (the "composite") is calculated [e.g., Rasmusson and Carpenter (1982), Arkin (1982), Pan and Oort (1983)]. The compositing approach is most appropriate if the Southern Oscillation consists of a sequence of discrete "events" separated by periods within which the variations are of less interest.

The present analysis contains elements of both approaches. It is formally of the first type in that correlations and regressions are generated. It differs from most previous studies based on regressions and correlations in that it takes account of the strong link between the anomalies and the annual cycle. The present study also resembles the composite approach in that the Southern Oscillation is treated in terms of a sequence of annual "events". It differs from the composite studies cited above in the sense that it takes account of all years, not just those in which a particular threshold is passed. The regression fields presented here are equivalent to composites in which every year is used, each weighted according to its value of the Darwin pressure anomaly.

2. DATA

The data used were the "untrimmed" version of the Comprehensive Ocean - Atmosphere Data Set (COADS) [Fletcher et al. (1983)], kindly supplied by J. O. Fletcher. The data for each field, month, and two degree latitude by two degree longitude grid box consisted of the mean, the median, the number of observations, and other statistics. Data for the fields of SST, air temperature, pressure, cloudiness in oktas (eighths of the sky covered), and

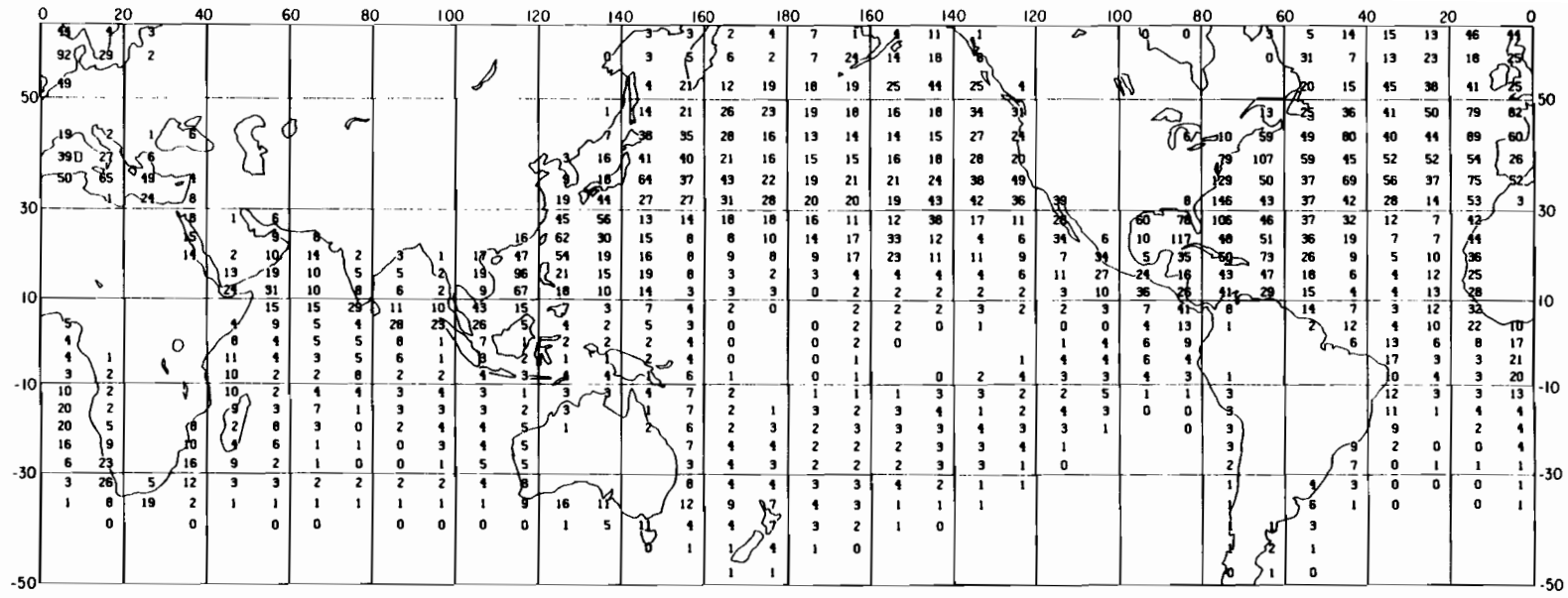

Figure 2. AVERAGE NUMBER OF OBSERVATIONS (DIVIDED BY TEN) PER MONTH IN EACH 4° x 10° REGION.

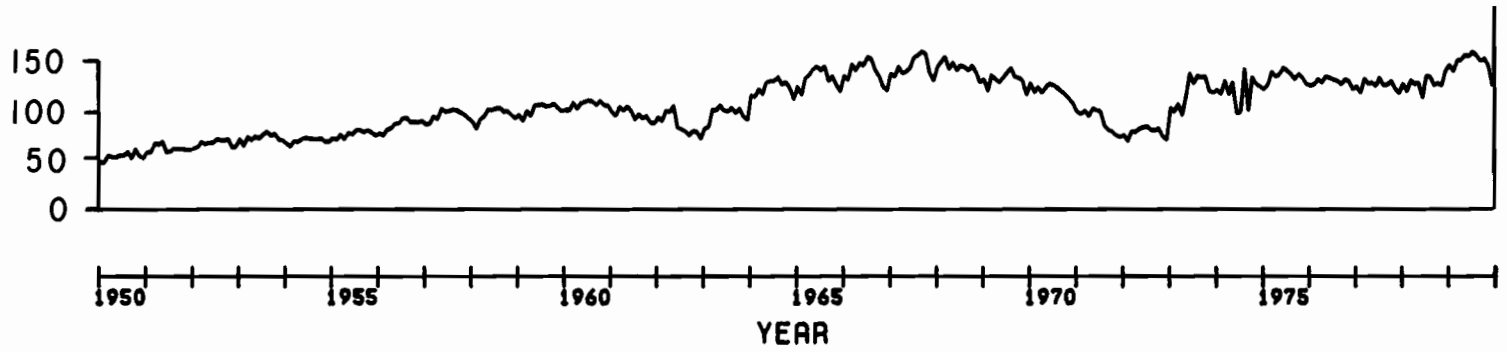

Figure 3. NUMBER OF OBSERVATIONS OF SST (DIVIDED BY ONE THOUSAND) IN EACH MONTH OVER THE GLOBAL OCEANS.

zonal and meridional components of the surface wind for the period 1950-79 were extracted. Figures 2 and 3 give some indication of the data coverage in space and time. Coverage in most of the Northern Hemisphere is more than adequate, but over much of the tropics and Southern Hemisphere, adequate coverage is restricted to the major shipping lanes. Data density averaged over the globe nearly tripled during the study period.

3. GENERATION OF SEASONAL MEAN ANOMALIES

The raw data for this study comprised the monthly means of each variable in each of the two degree by two degree grid boxes. A climatological monthly mean was calculated for each variable, calendar month, and two degree by two degree area, provided that at least ten of the thirty years contributed to the mean. Each field of climatological monthly means was then smoothed, interpolated, and extrapolated to enhance the coverage and smooth the field. The smoothing, interpolation, and extrapolation process was performed first along latitude circles, then along meridians, and finally along latitude circles again. The smoothing employed was a 1-2-1 filter. The interpolation scheme consisted of replacing the value at a single missing gridpoint by the average of the values at the two neighboring points. The extrapolation scheme (applied along latitude circles only) reduced the extent of the larger gaps and extended the coverage into blank regions by one 2-degree by 2-degree area. The extrapolation involved in total only the two grid boxes nearest the data on each end of the gap.

For purposes of display, the climatological mean fields were averaged in space and time to form four degree latitude by ten degree longitude seasonal mean fields. These fields are presented in Figures 4-8 in the maps section. The units of the means are given in the figure titles, and only the last two digits of the pressure in mb are printed.

Two degree by two degree anomalies were calculated by subtracting from each monthly mean the corresponding climatological mean for that month. The

anomaly was treated as missing if either the montnly mean or the climatological monthly mean was missing. If the magnitude of the anomaly was found to be greater than specified thresholds (Table 1) it was treated as missing. The 2°x2° anomalies were then averaged, weighted by the number of observations, to form four degree latitude by ten degree longitude anomalies. If the total number of observations was less than a specified threshold (Table 1), the 4°x10° anomaly was treated as missing. Finally, monthly anomalies were averaged in groups of three sequential months to form seasonal anomalies. If fewer than two monthly anomalies were available for a given season, the seasonal anomaly was treated as missing. The first season in the sequence was the mean of only two months, January and February 1950.

Table 1. Thresholds used in calculating 2°x2° and 4°x10° anomalies. 2°x2° anomalies were treated as missing if the absolute value of the anomaly was greater than A, or if the absolute value of the anomaly was greater than B and there were less than C observations in the month. 4°x10° anomalies were treated as missing if the total number of observations was less than D.

	Threshold			
Field	A	B	C	D
Sea Surface Temperature	8°C	5°C	3	4
Air Temperature	8°C	5°C	3	4
Pressure	40 mb	30 mb	4	6
Cloudiness	7 oktas	4 oktas	4	6
Zonal Wind	15 m/s	10 m/s	6	4
Meridional Wind	15 m/s	10 m/s	6	4

4. REFERENCE INDEX

Darwin pressure data were obtained from the NCAR "World Climatology" tape with isolated corrections made following Parker (1983). Monthly values

of Darwin pressure anomaly and the corresponding annual mean values derived from them are shown in Figure 9.

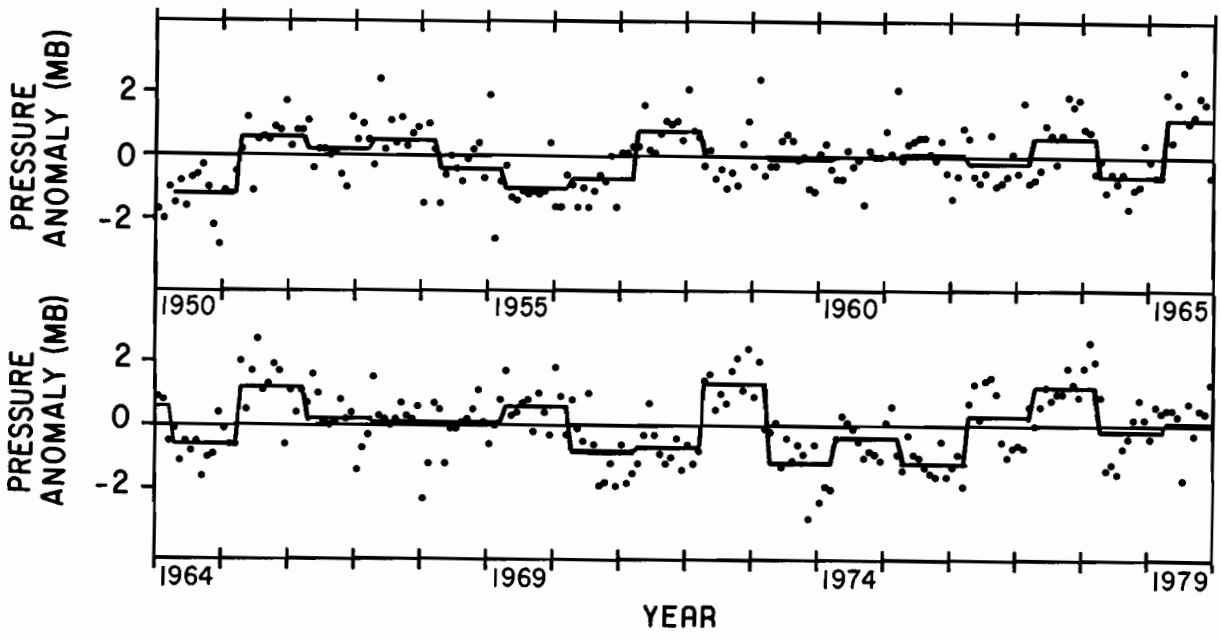

Figure 9. TIME SERIES OF DARWIN MONTHLY PRESSURE ANOMALIES (DOTS) AND THE PRESSURE INDEX (SOLID LINE).

5. GENERATION AND INTERPRETATION OF MAPS

For each 4°x10° area in each field and for each of the six seasons relative to the twelve months of the Darwin index (Fig. 1), a correlation coefficient, C, and regression coefficient, R, were calculated. Coefficients were calculated only for 4°x10° areas with at least ten years of data. The charts are presented in Figures 10-51 of the maps section.

A positive correlation indicates that a positive anomaly tends to be associated with a year of positive Darwin pressure anomaly, which corresponds to a "year of low Southern Oscillation index", a "warm episode", or an "El Nino event;" a positive correlation also implies that a negative anomaly in the same place tends to accompany a year of negative Darwin pressure anomaly. The correlation coefficients provide a measure of statistical significance. For thirty independent samples, an individual correlation coefficient must be stronger than 0.36 (0.46) for the null hypothesis of no relationship to be rejected at the 95% (99%) confidence level. The correlation coefficient squared indicates the fraction of the year-to-year variability of a field in a particular season that is associated with year-to-year fluctuations of the reference index, e.g., a correlation coefficient stronger than 0.71 implies that, during 1950-79, more than half of the season's variance was associated with fluctuations in the Darwin pressure index.

The correlation coefficients were rounded to tenths and plotted as follows:

i) 1.00 to 0.25 as 10 to 3 in red.
ii) 0.24 to 0.01 as + in red.
iii) 0.00 as + in black.
iv) -0.01 to -0.24 as - in black.
v) -0.25 to -1.00 as -3 to -10 in black.

The regression coefficient of field F on index I is related to the correlation coefficient by

$$R = \frac{C\sigma_F}{\sigma_I}$$

where σ is the standard deviation. The regression coefficient can be interpreted as the anomaly that tends, on average, to be associated with an annual mean pressure at Darwin that is one millibar above normal. The units of the plotted regression coefficients are as follows:

SST, SST - air temperature: tenths of °C per mb Darwin pressure anomaly.

Pressure: tenths of mb per mb Darwin pressure anomaly.

Zonal wind: tenths of m/s per mb Darwin pressure anomaly.

Cloudiness: tenths of an okta per mb Darwin pressure anomaly.

6. REGIONAL INDICES

There are several regions, apparent from this and previous studies, in which anomalies tend to be spatially coherent and strongly related to the Southern Oscillation. We defined monthly indices to represent some of these regional phenomena by taking the means of all the 4°x10° anomalies within certain specified regions. Figure 52 shows the regions chosen, and Figure 53 presents time series of seasonal mean values of the indices. Tables 2 and 3 present correlation and regression coefficients, respectively, with the Darwin pressure index for each index in each of the six seasons shown in Fig. 1. Table 4 presents the standard deviations of the indices in eacn calendar season.

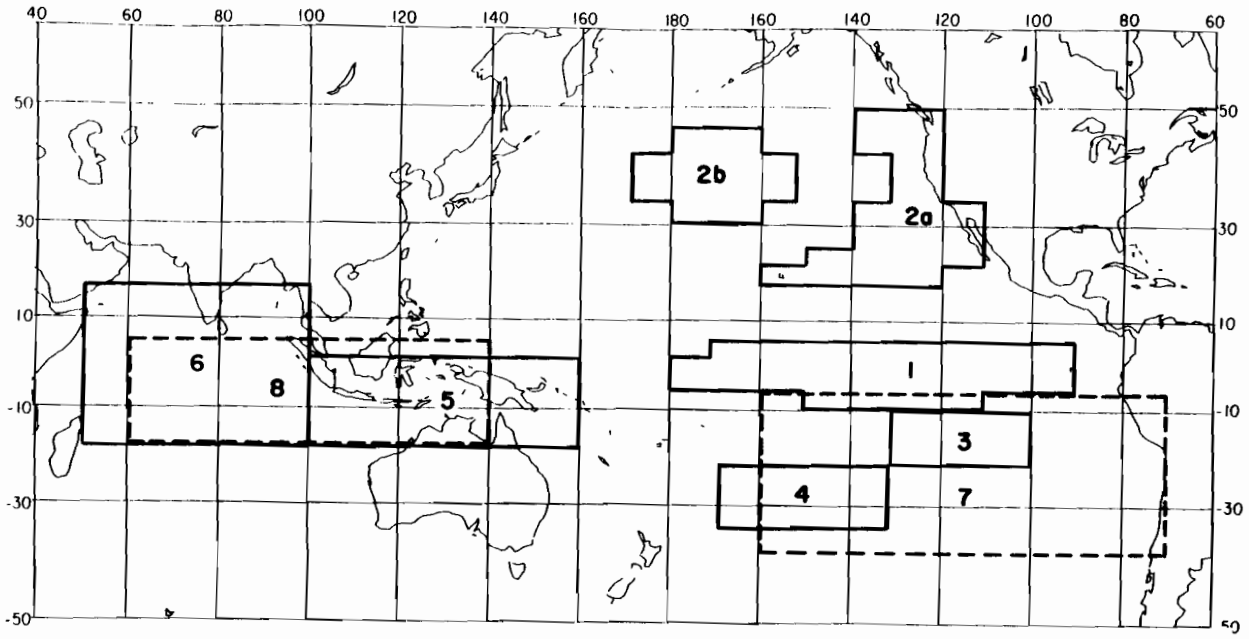

Figure 52. REGIONS USED FOR THE INDICES WHOSE TIME SERIES ARE PLOTTED IN FIGURE 53.

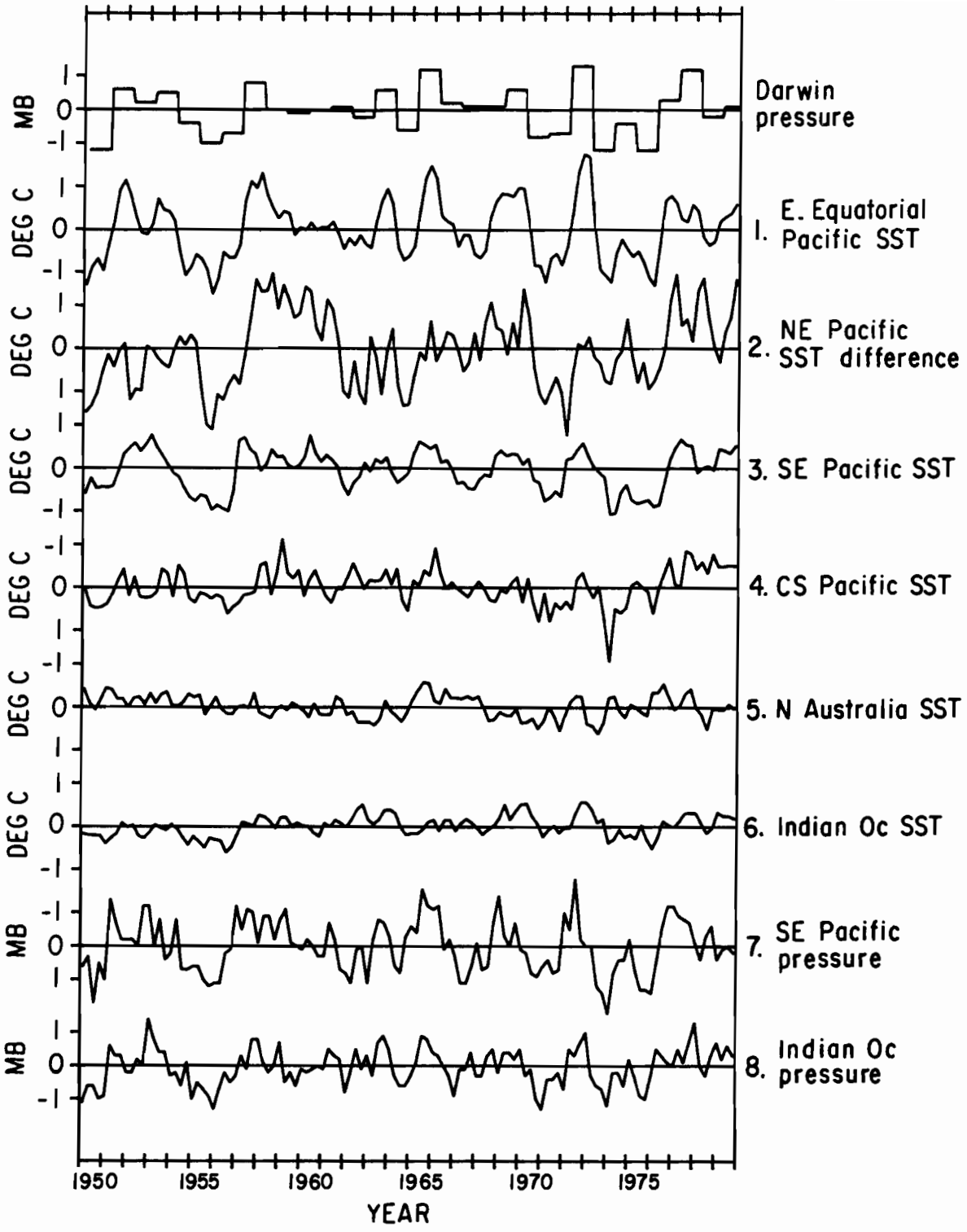

Figure 53. TIME SERIES OF THE INDICES FOR THE SELECTED REGIONS INDICATED IN FIGURE 52.

Index 1 is an index based on equatorial Pacific SST shown by Wright (1984) to be correlated with the simultaneous seasonal mean Darwin pressure with a value of 0.78.

Index 2 represents the SST difference between two regions of the north Pacific shown by Namias (1972) to be inversely correlated and related to climatic anomalies over North America. Weare et al. (1976) showed in an eigenvector analysis that this difference pattern tends to accompany equatorial Pacific SST anomalies. Table 2 shows correlations reaching 0.55, implying that up to 30% of the variance of seasonal means of this pattern is associated with Southern Oscillation fluctuations.

Index 3 represents SST in a region of the southeast Pacific notable for its precursor relationship to the Southern Oscillation. Table 2 shows a correlation of 0.53 between this index in DJF and Darwin pressure averaged over the year beginning two months later.

Indices 4 and 5 both represent SST in regions in which it exhibits a strong negative correlation with Darwin pressure in SON. Table 2 shows that both regions behave similarly in prior seasons, but in DJF2 a dramatic change occurs in the north Australia region where the correlation flips to significantly positive. These characteristics were also apparent in the composite charts presented by Rasmusson and Carpenter (1982).

Index 6 represents the SST over a large region of the Indian Ocean. This index exhibits a strong relationship to the Southern Oscillation but lags the other strongly related indices by about one season. This lag relationship had previously been noted by Navato et al. (1981).

Indices 7 and 8 represent the pressure in the two sides of the familiar Southern Oscillation pressure "see-saw". The strongest correlation on the Pacific side occurs in JJA, whereas on the Indian Ocean side it occurs in SON, about a season later, consistent with results of Trenberth (1976).

Table 2. Correlation coefficients x 100 between seasonal values of indices and mean Darwin pressure anomaly over the twelve months running from April of one year through March of the next year.

	Season Relative to Darwin					
Index	DJF1	MAM1	JJA	SON	DJF2	MAM2
(1) E Equatorial Pacific SST	7	67	89	91	86	23
(2) NE Pacific SST diff.	-1	22	41	55	50	43
(3) SE Pacific SST	53	58	76	79	50	40
(4) CS Pacific SST	-6	-1	-56	-69	-55	-56
(5) N Australia SST	-6	-29	-59	-66	42	55
(6) Indian Oc SST	-15	7	39	58	81	60
(7) SE Pacific SLP	-43	-50	-88	-72	-44	-16
(8) Indian Oc SLP	6	73	77	88	69	-7

Table 3. Regression coefficients of seasonal values of indices on mean Darwin pressure anomaly for the twelve months running from April of one year to March of the next year.

	Season Relative to Darwin					
	DJF1	MAM1	JJA	SON	DJF2	MAM2
(1) E Equatorial Pacific SST (0.01°C/mb)	8	46	88	110	96	15
(2) NE Pacific SST diff. (0.01°C/mb)	-1	25	47	67	68	46
(3) SE Pacific SST (0.01°C/mb)	40	43	46	49	37	29
(4) CS Pacific SST (0.01°C/mb)	-4	0	-28	-43	-38	-28
(5) N Australia SST (0.01°C/mb)	-2	-9	-25	-26	13	18
(6) Indian Oc SST (0.01°C/mb)	-6	3	13	22	31	20
(7) SE Pacific pressure (0.01 mb/mb)	-53	-51	-112	-77	-54	-16
(8) Indian Oc pressure (0.01 mb/mb)	7	41	49	73	75	-4

Table 4. Standard deviation of seasonal mean indices by season.

Index	Season			
	DJF	MAM	JJA	SON
(1) E Equatorial Pacific SST (hundredths °C)	80	48	68	84
(2) NE Pacific SST difference (hundredths °C)	98	78	78	85
(3) SE Pacific SST (hundredths °C)	52	51	42	43
(4) CS Pacific SST (hundredths °C)	48	35	35	43
(5) N Australia SST (hundredths °C)	23	22	30	27
(6) Indian Oc SST (hundredths °C)	27	24	22	26
(7) SE Pacific pressure (hundredths mb)	85	70	88	74
(8) Indian Oc pressure (hundredths mb)	75	39	44	57

7. ACKNOWLEDGMENTS

The preparation and publication of this atlas were carried out under the sponsorship of a grant from the NOAA Equatorial Pacific Ocean Climate Studies (EPOCS) program. T. P. Mitchell's participation in the project was sponsored by the Climate Dynamics Program of the National Science Foundation under Grant Number ATM 8318853. We would also like to acknowledge the contributions of Mr. Ryan Whitney and Mr. Roger Coghlan of the Pacific Marine Environmental Laboratory of NOAA, and Mr. David Obitts of the Mountain Area Service Center of NOAA.

8. REFERENCES

Angell, J. K., 1981: Comparison of variations in atmospheric quantities with sea surface temperature variations in the equatorial eastern Pacific. Mon. Wea. Rev., 109, 230-243.

Arkin, P. A., 1982: The relationship between interannual variability in the 200 mb tropical wind field and the Southern Oscillation. Mon. Wea. Rev., 110, 1393-1404.

Egger, J., G. Meyers, and P. B. Wright, 1981: Pressure, wind, and cloudiness in the tropical Pacific related to the Southern Oscillation. Mon. Wea. Rev., 109, 1139-1149.

Fletcher, J. O., R. J. Slutz, and S. D. Woodruff, 1983: Towards a comprehensive ocean-atmospheric data set. Trop. Ocean-Atmos. Newslett., 20, 13-14.

Namias, J., 1972: Large-scale and long-term fluctuations in some atmospheric and oceanic variables. In: Nobel Symposium 20, D. Dyrssen and D. Jagner, eds., Almqvist and Wiksell, Stockholm, 27-48.

Navato, A. R., R. E. Newell, J. C. Hsiung, and C. B. Billing, Jr., 1981: Tropospheric mean temperature and its relationship to the oceans and atmospheric aerosols. Mon. Wea. Rev., 109, 244-254.

Newell, R. E., R. Selkirk, and W. Ebisuzaki, 1982: The Southern Oscillation: Sea surface temperature and wind relationships in a 100 year data set. J. Climatol., 2, 357-373.

Pan, Y. H., and A. H. Oort, 1983: Global climate variations connected with sea surface temperature anomalies in the eastern equatorial Pacific Ocean for the 1958-73 period. Mon. Wea. Rev., 111, 1244-1258.

Parker, D. E., 1983: Documentation of a Southern Oscillation index. Met. Mag., 112, 184-188.

Quinn, W. H., D. O. Zopf, K. S. Short, and R. T. W. Kuo Yang, 1978: Historical trends and statistics of the Southern Oscillation, El Nino, and Indonesian droughts. Fish. Bull., 76, 663-678.

Rasmusson, E. M., and T. H. Carpenter, 1982: Variations in tropical sea surface temperature and surface wind fields associated with the

Southern Oscillation/El Nino. Mon. Wea. Rev., 110, 354-384.

Trenberth, K. E., 1976: Spatial and temporal variations of the Southern Oscillation. Quart. J. Roy. Meteor. Soc., 102, 639-653.

Weare, B. C., A. R. Navato, and R. E. Newell, 1976: Empirical orthogonal analysis of Pacific sea surface temperatures. J. Phys. Oceanogr., 6, 671-678.

Wright, P. B., 1977: The Southern Oscillation - patterns and mechanisms of the teleconnections and the persistence. HIG-77-13. Hawaii Institute of Geophysics, Honolulu, HI 96822. 107 pp.

_____, 1984: Relationships between indices of the Southern Oscillation. Mon. Wea. Rev., 112, 1913-1919.

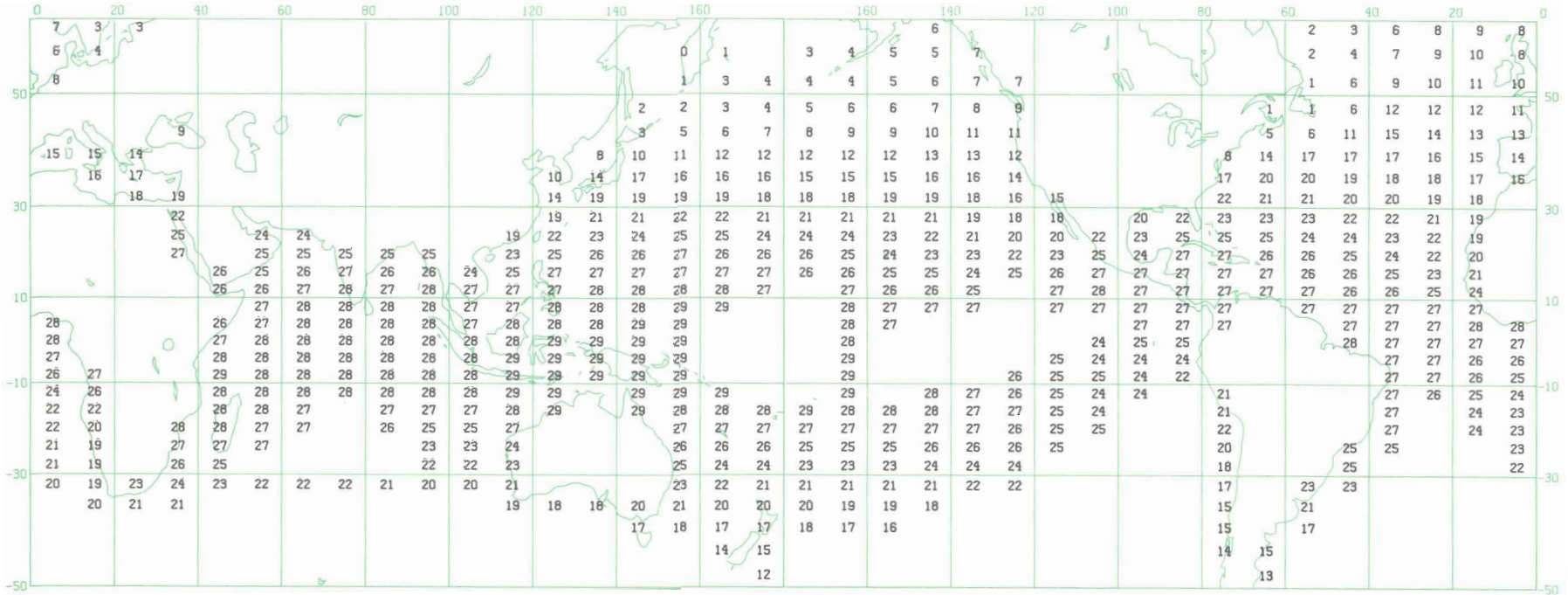

Figure 4a. SST SEASONAL MEAN DJF °C

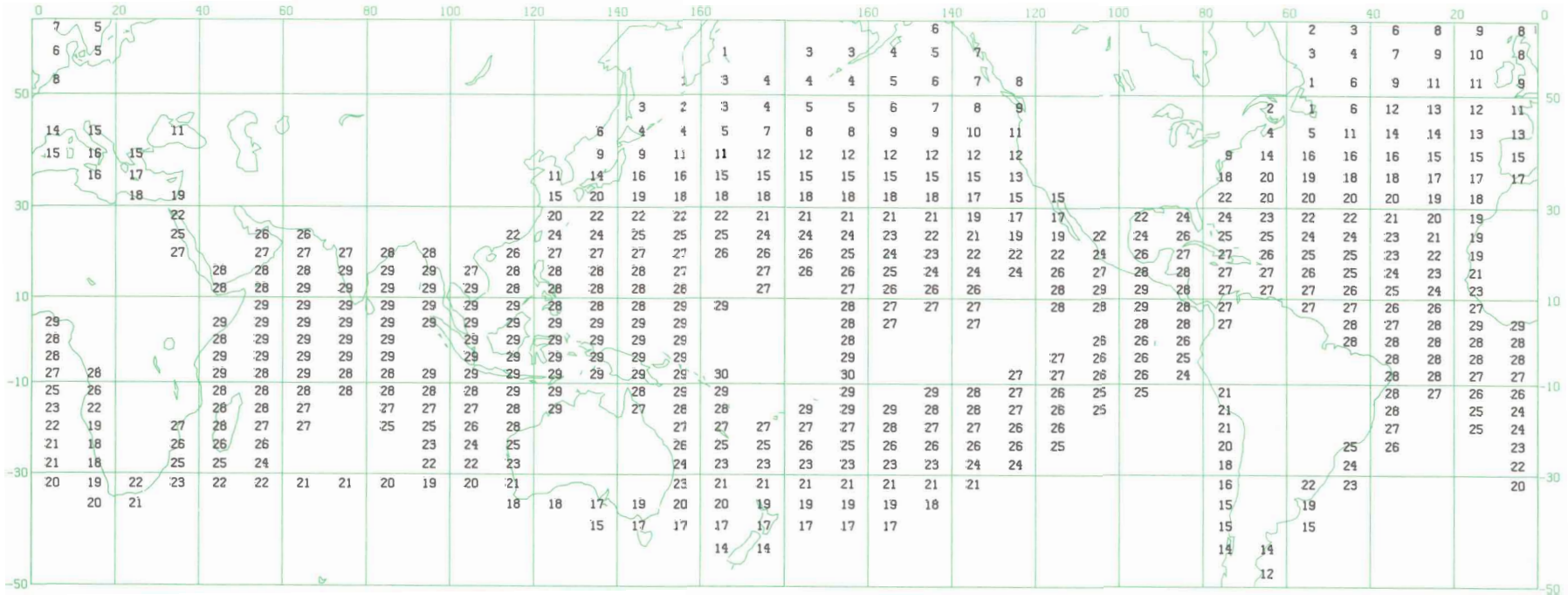

Figure 4b. SST SEASONAL MEAN MAM °C

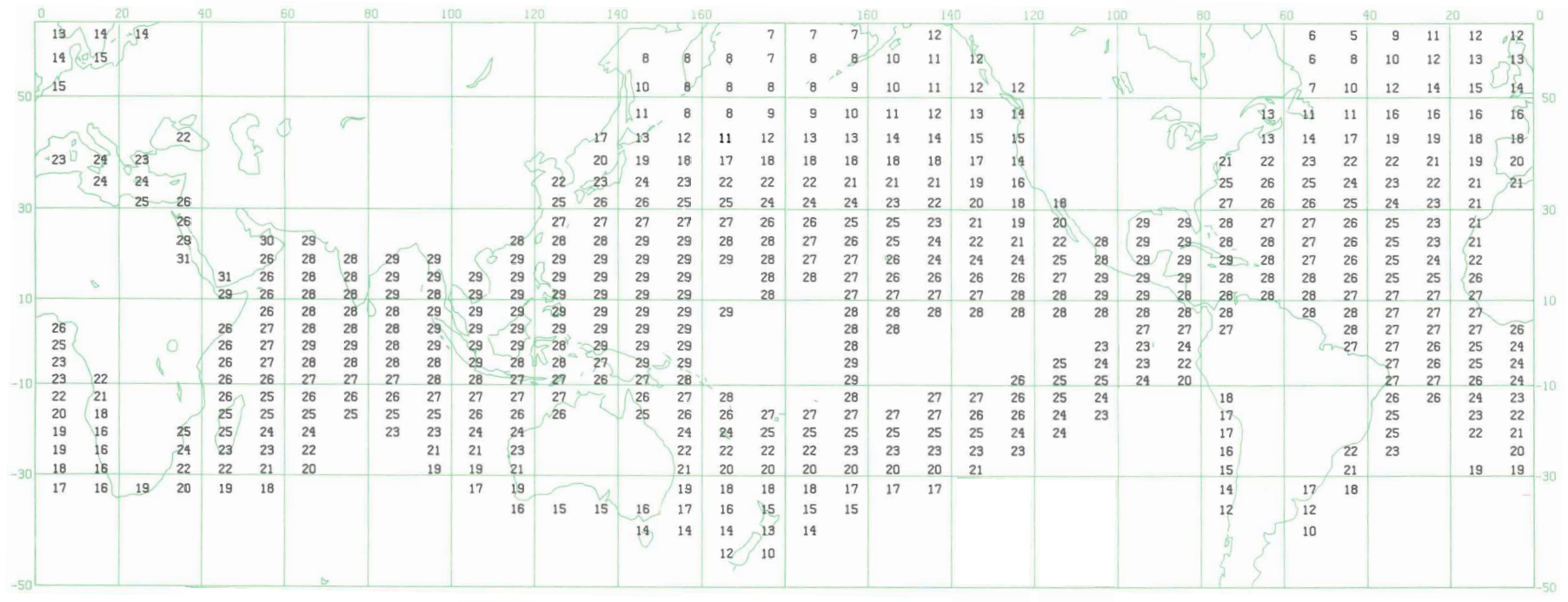

Figure 4c. SST SEASONAL MEAN JJA °C

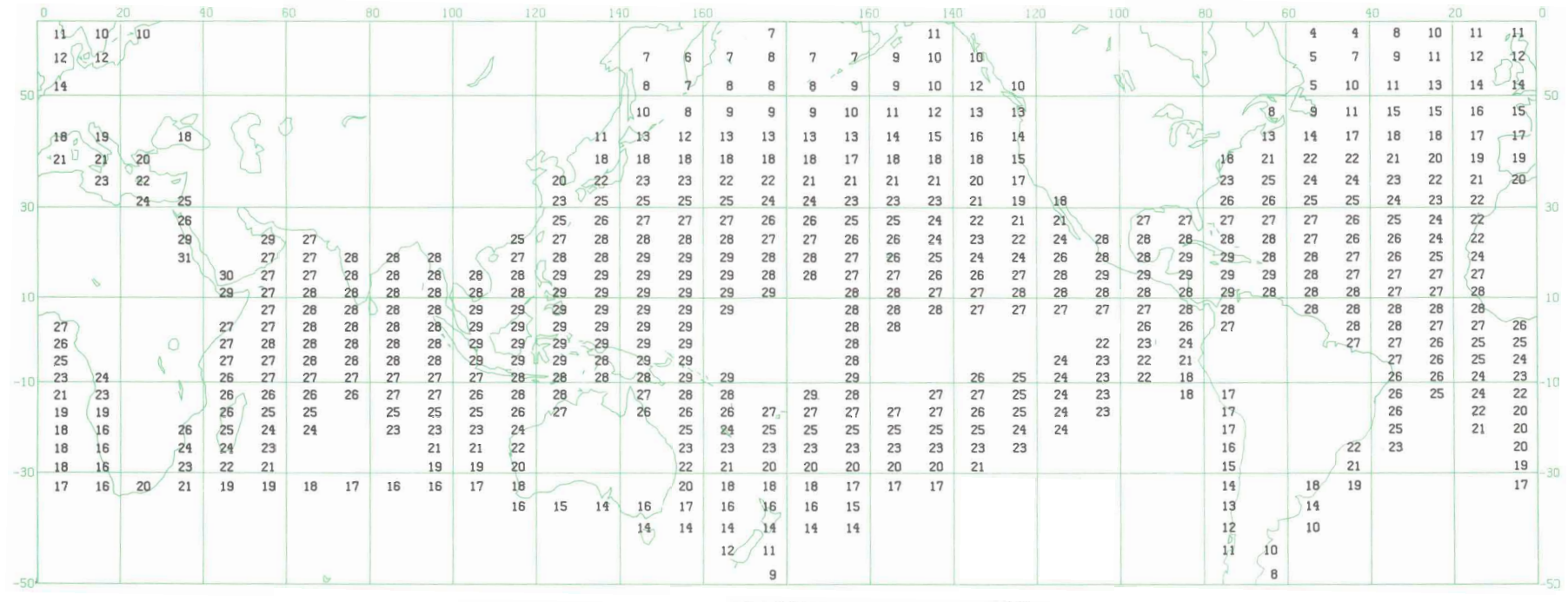

Figure 4d. SST SEASONAL MEAN SON °C

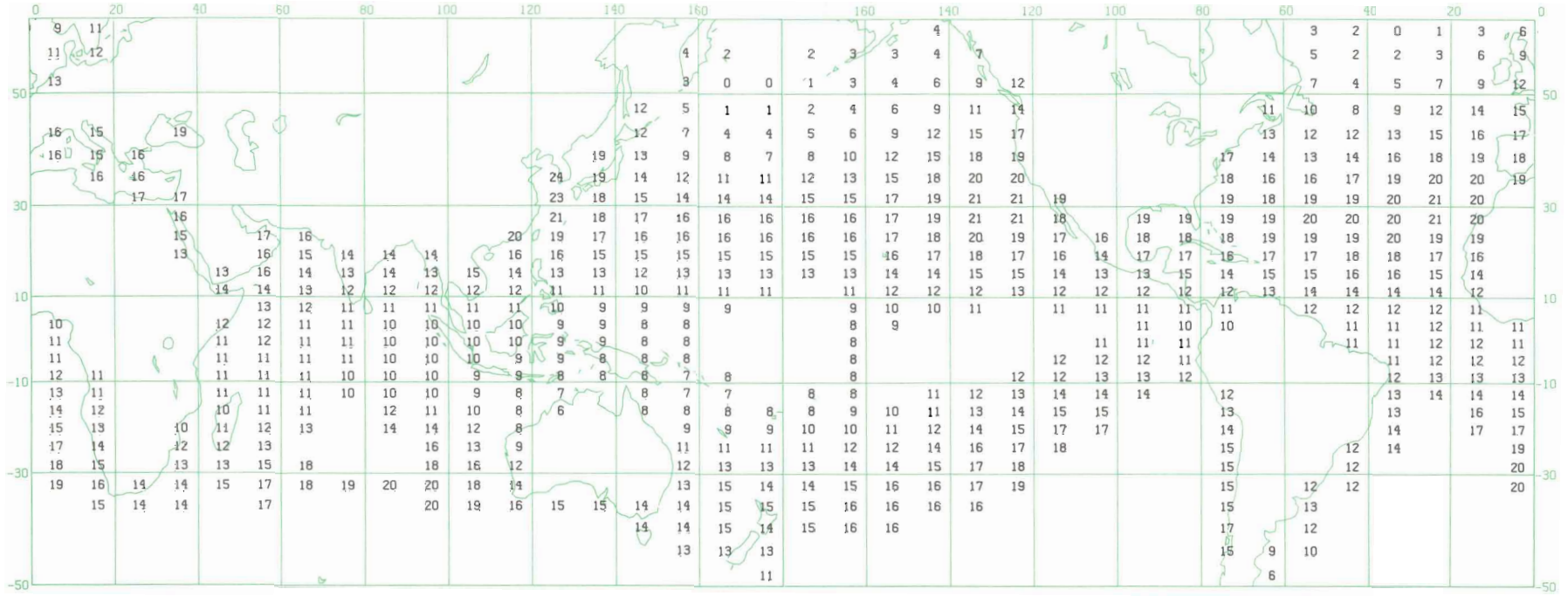

Figure 5a. PRESSURE SEASONAL MEAN DJF MB

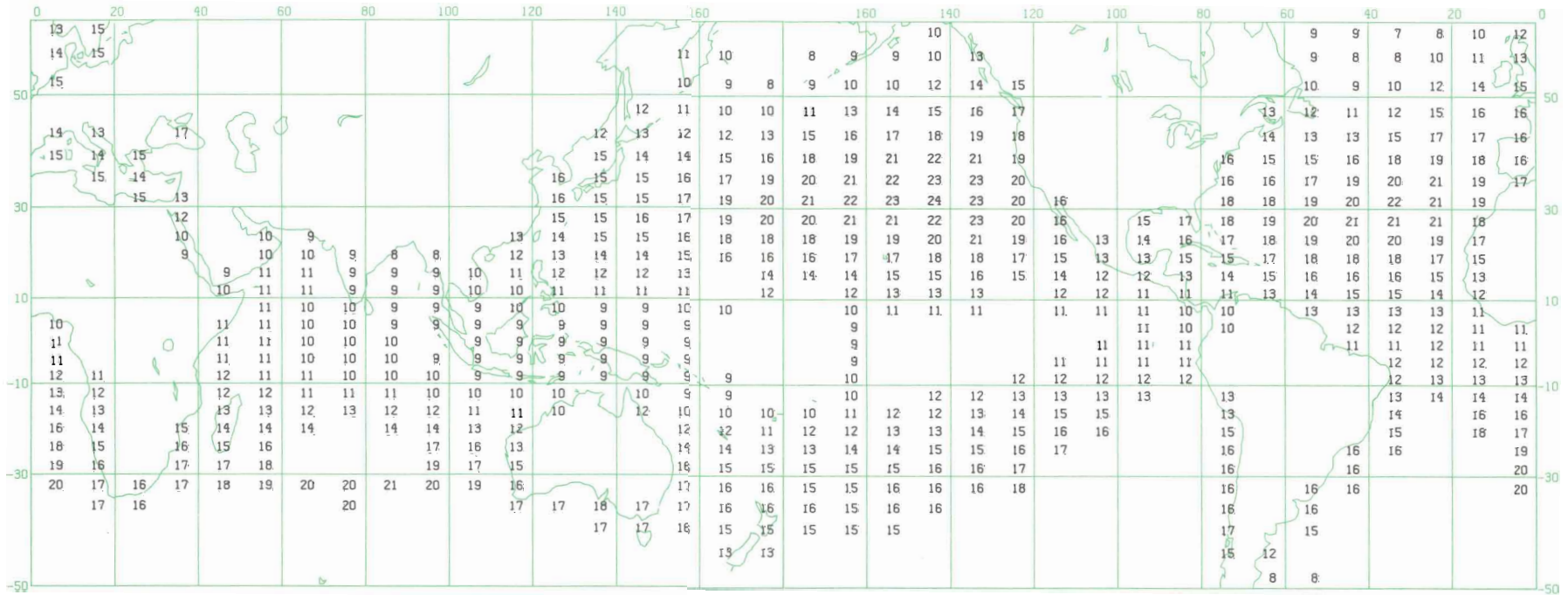

Figure 5b. PRESSURE SEASONAL MEAN MAM MB

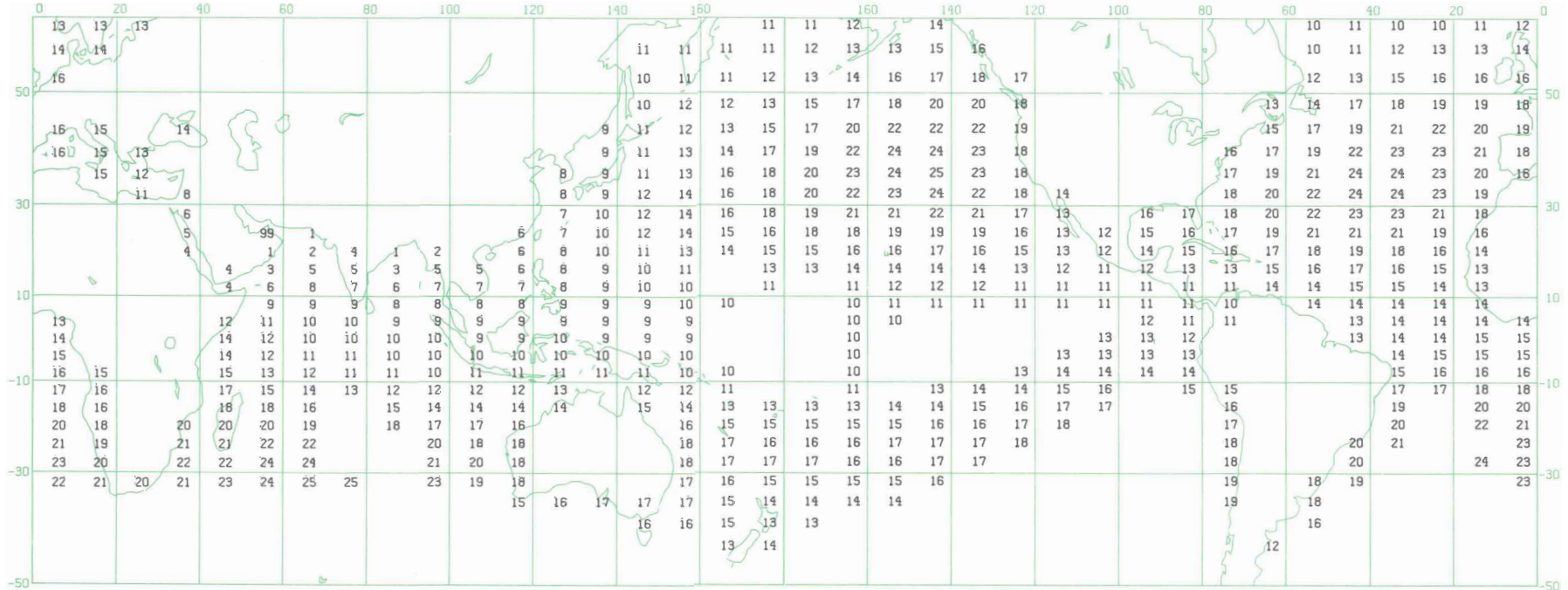

Figure 5c. PRESSURE SEASONAL MEAN JJA MB

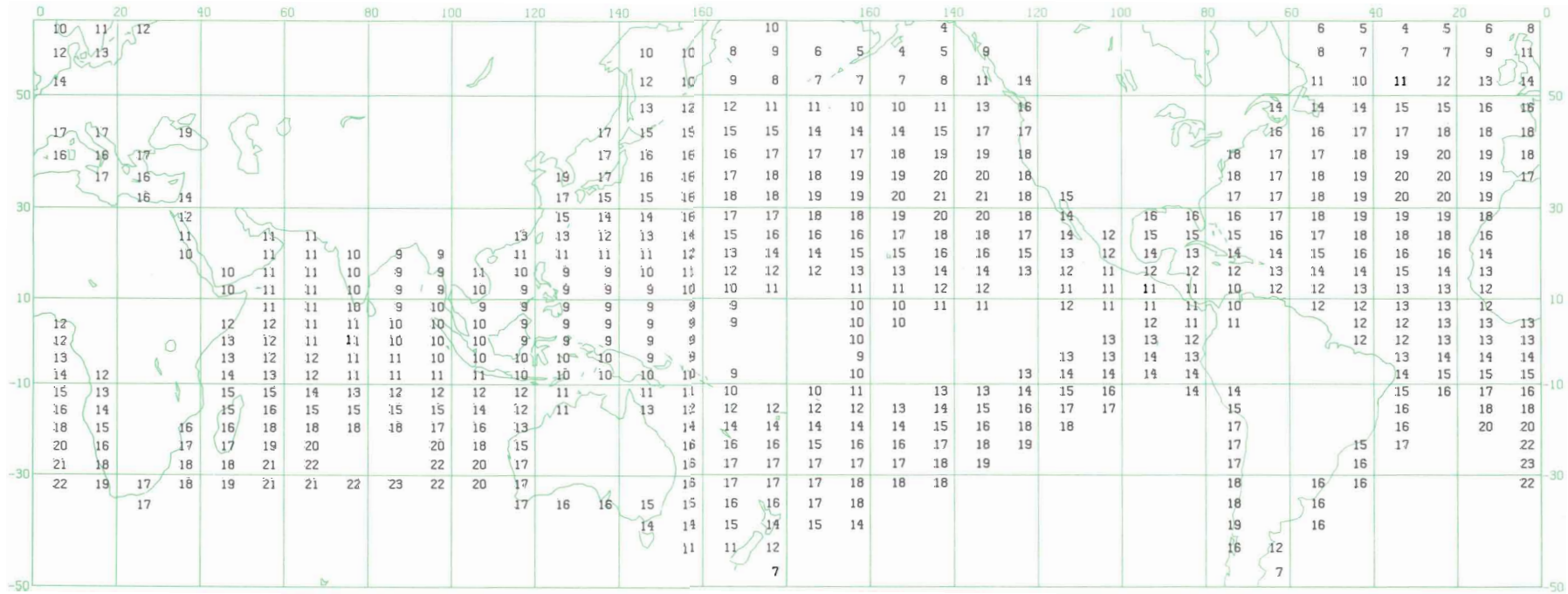

Figure 5d. PRESSURE SEASONAL MEAN SON MB

Figure 6a. SST MINUS AIR TEMP SEASONAL MEAN DJF °C

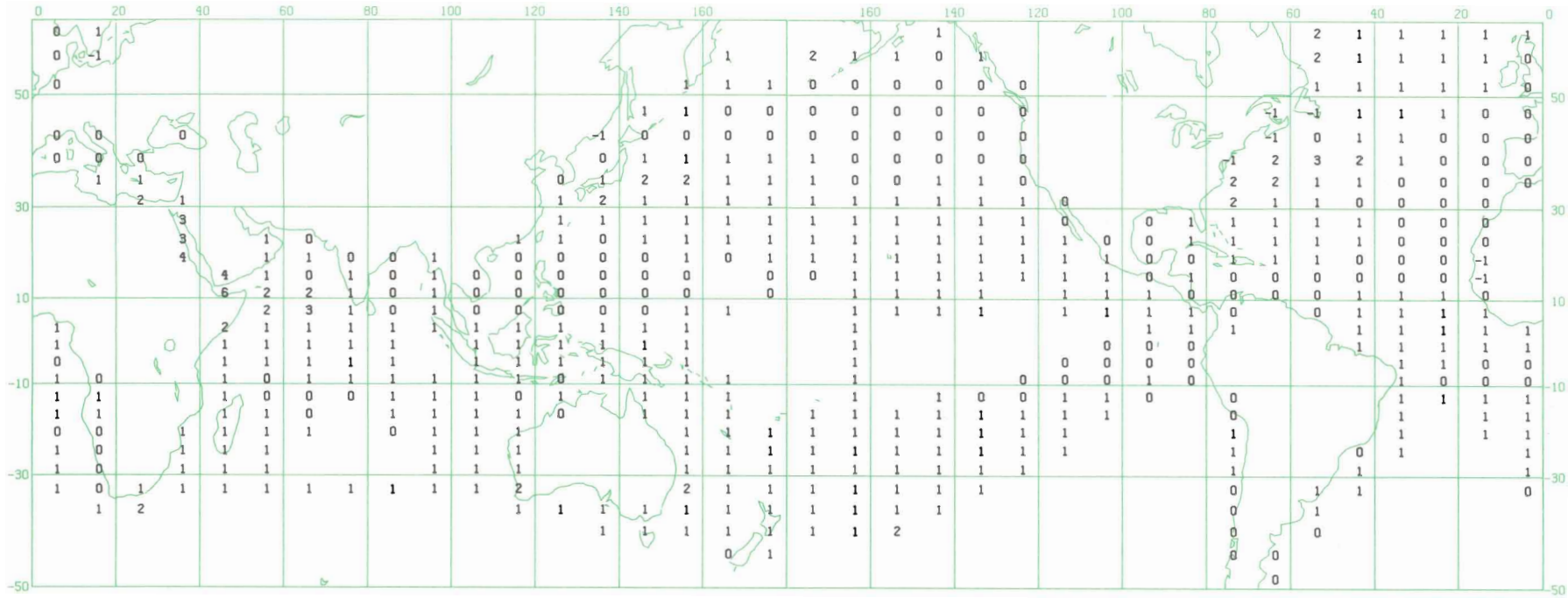

Figure 6b. SST MINUS AIR TEMP SEASONAL MEAN MAM °C

Figure 6c. SST MINUS AIR TEMP SEASONAL MEAN JJA °C

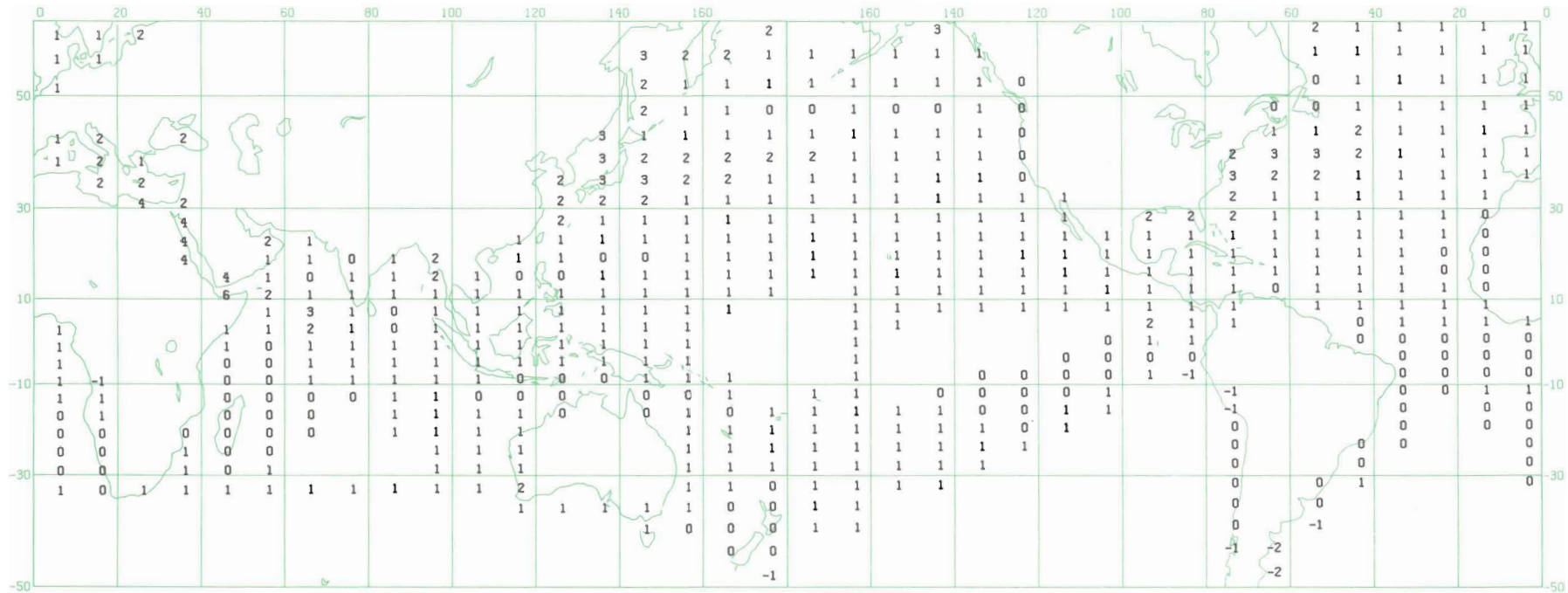

Figure 6d. SST MINUS AIR TEMP SEASONAL MEAN SON °C

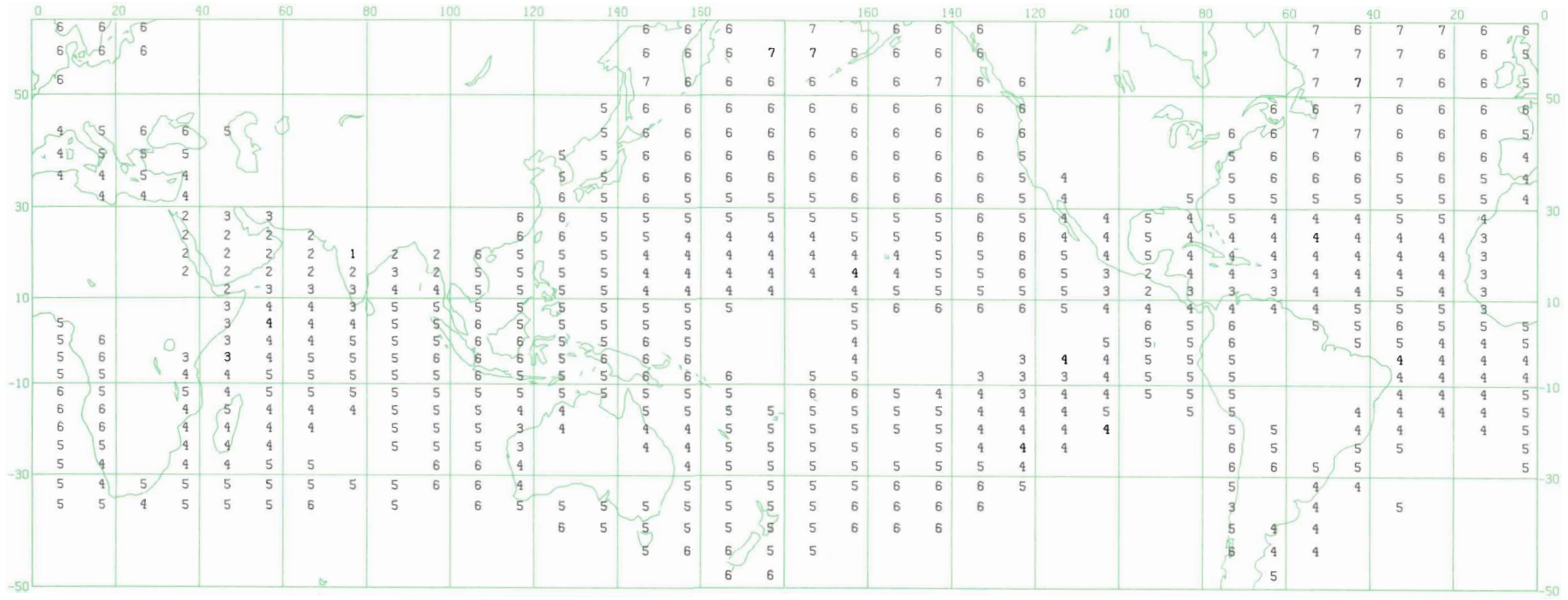

Figure 7a. CLOUDINESS SEASONAL MEAN DJF OKTAS

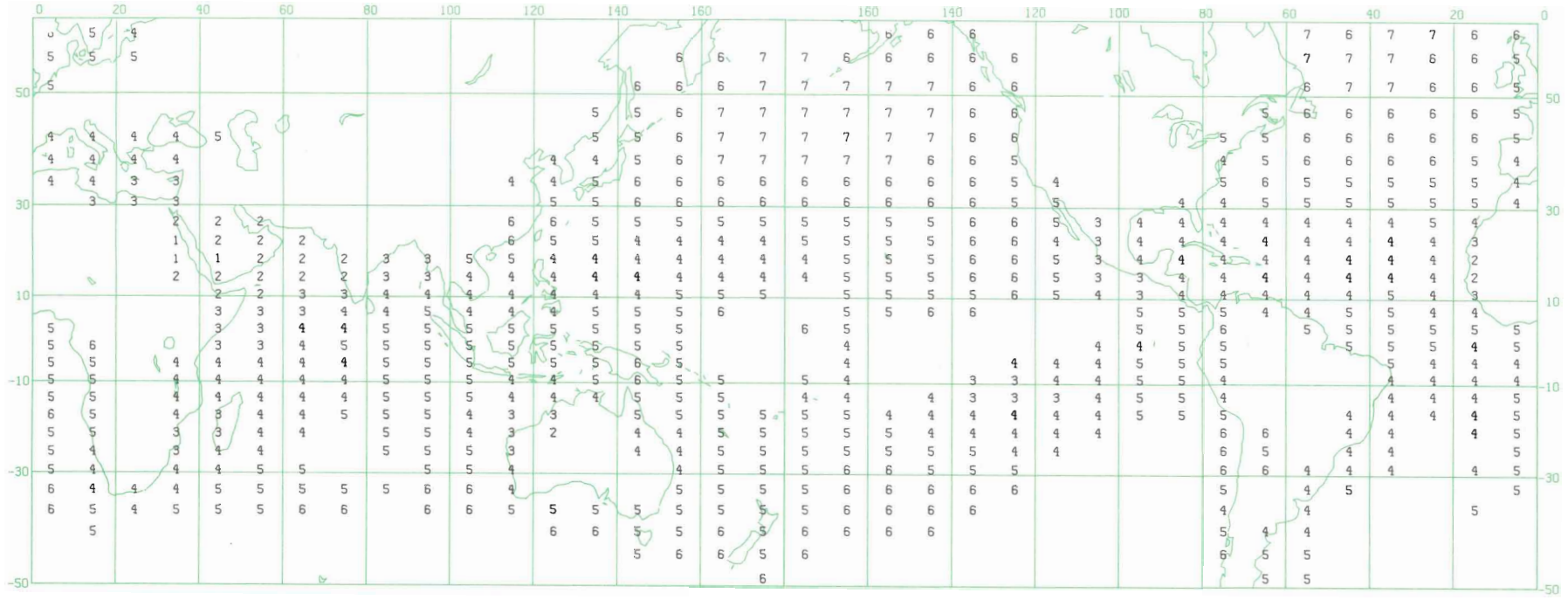

Figure 7b. CLOUDINESS SEASONAL MEAN MAM OKTAS

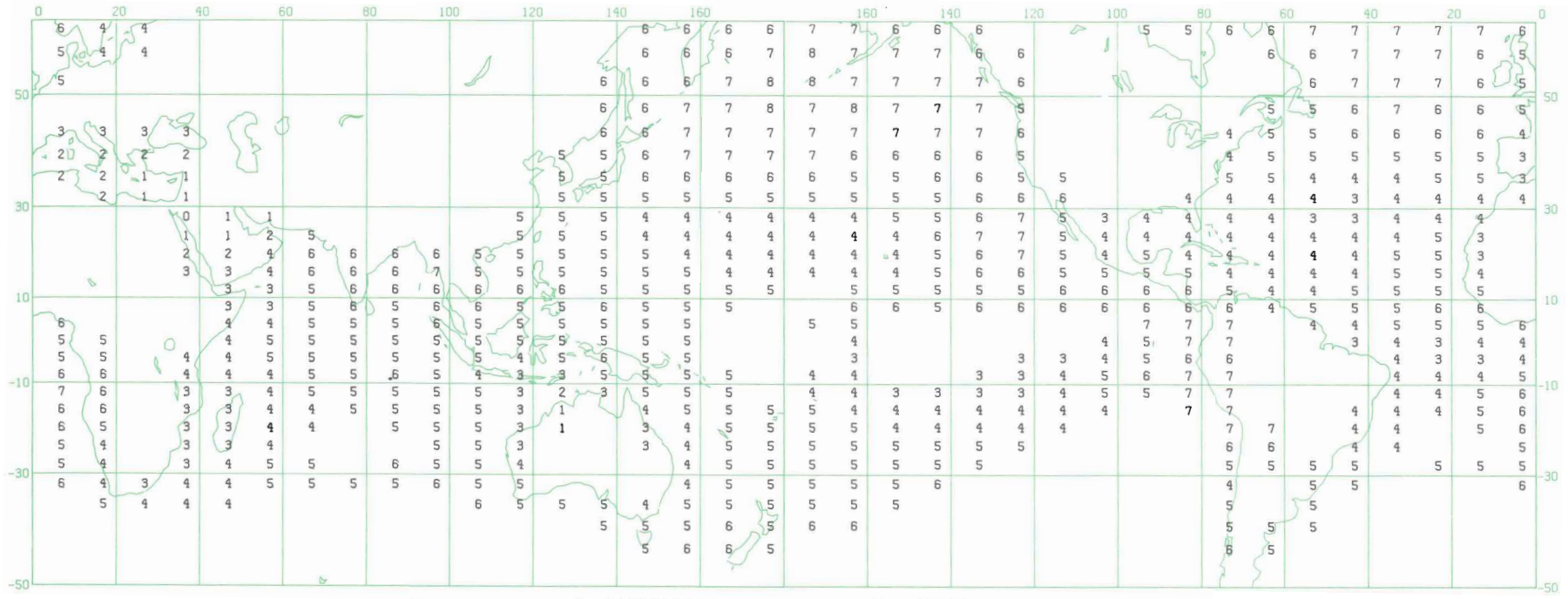

Figure 7c. CLOUDINESS SEASONAL MEAN JJA OKTAS

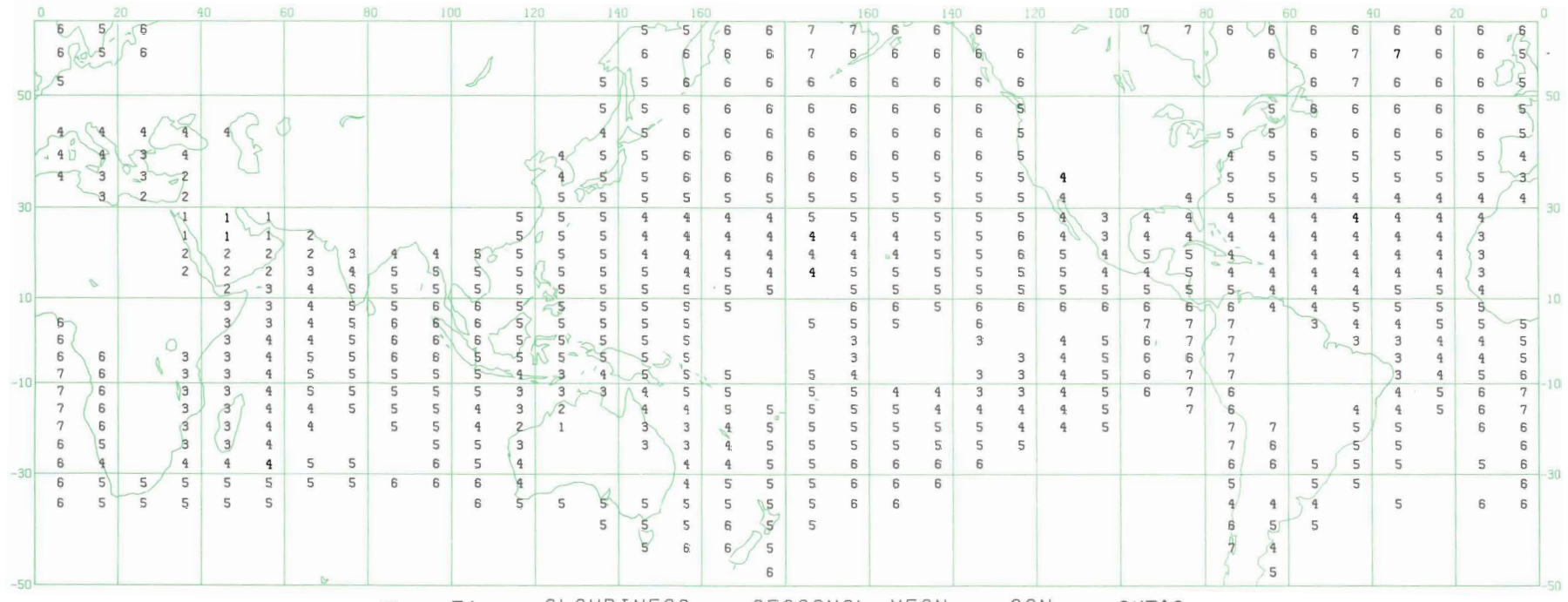

Figure 7d. CLOUDINESS SEASONAL MEAN SON OKTAS

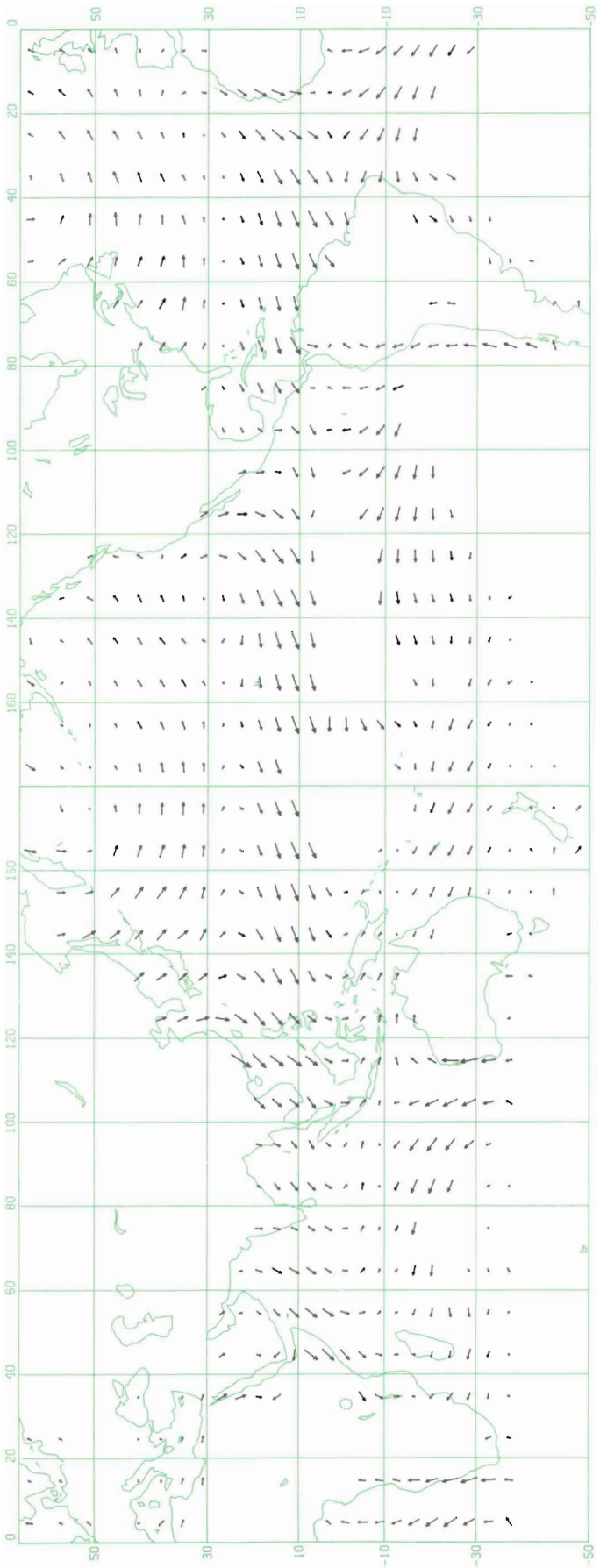

Figure 8a.

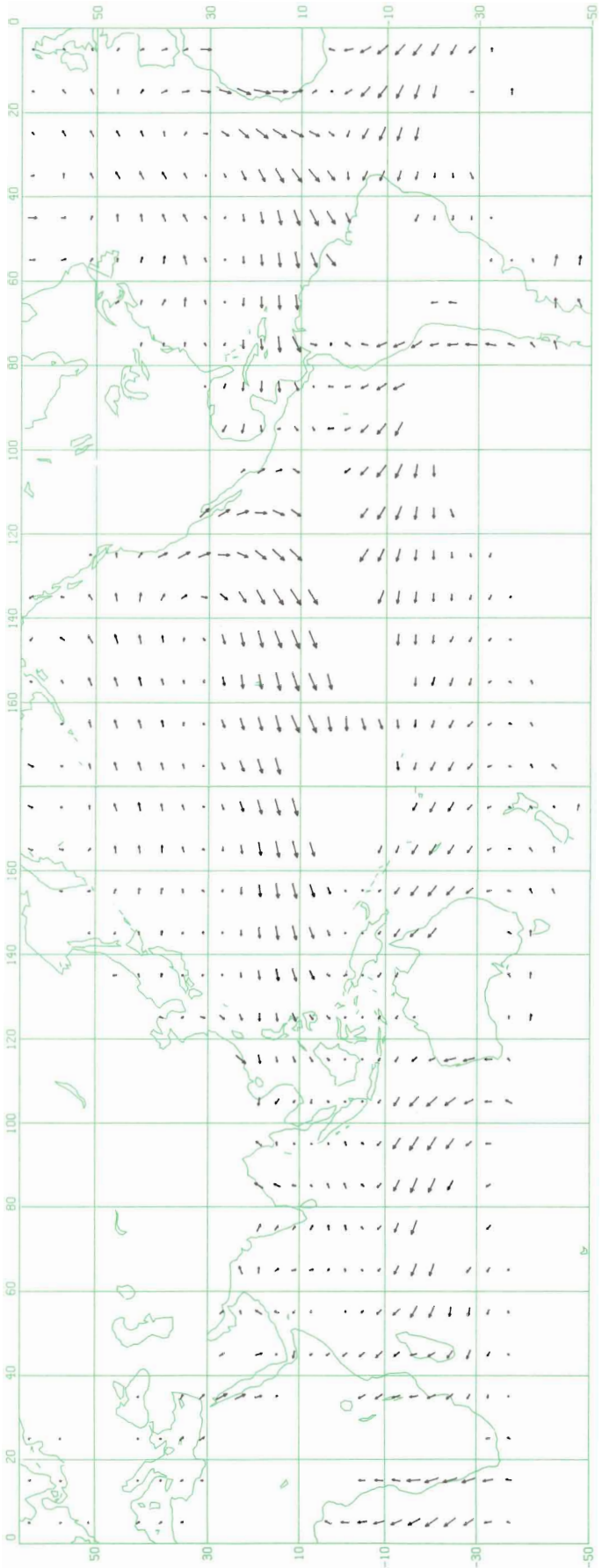

Figure 8b.

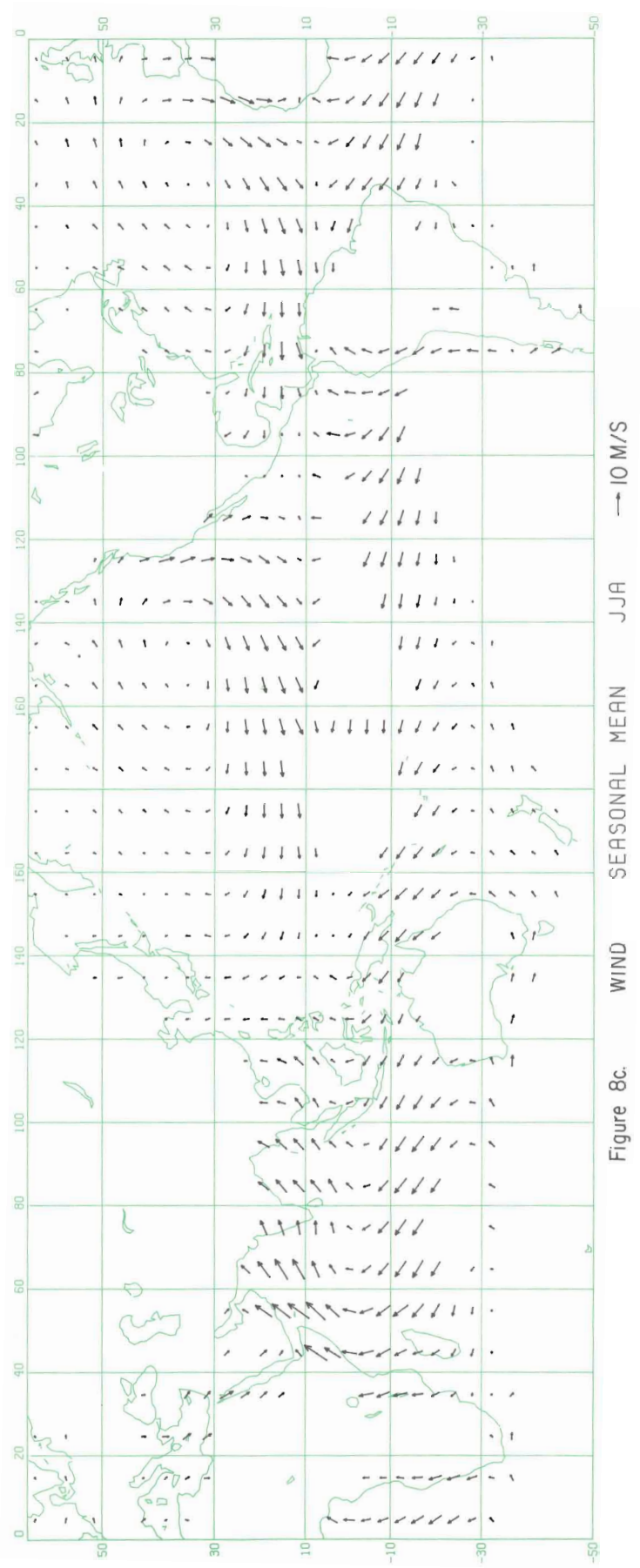

Figure 8c. WIND SEASONAL MEAN JJA → 10 M/S

Figure 8d. WIND SEASONAL MEAN SON → 10 M/S

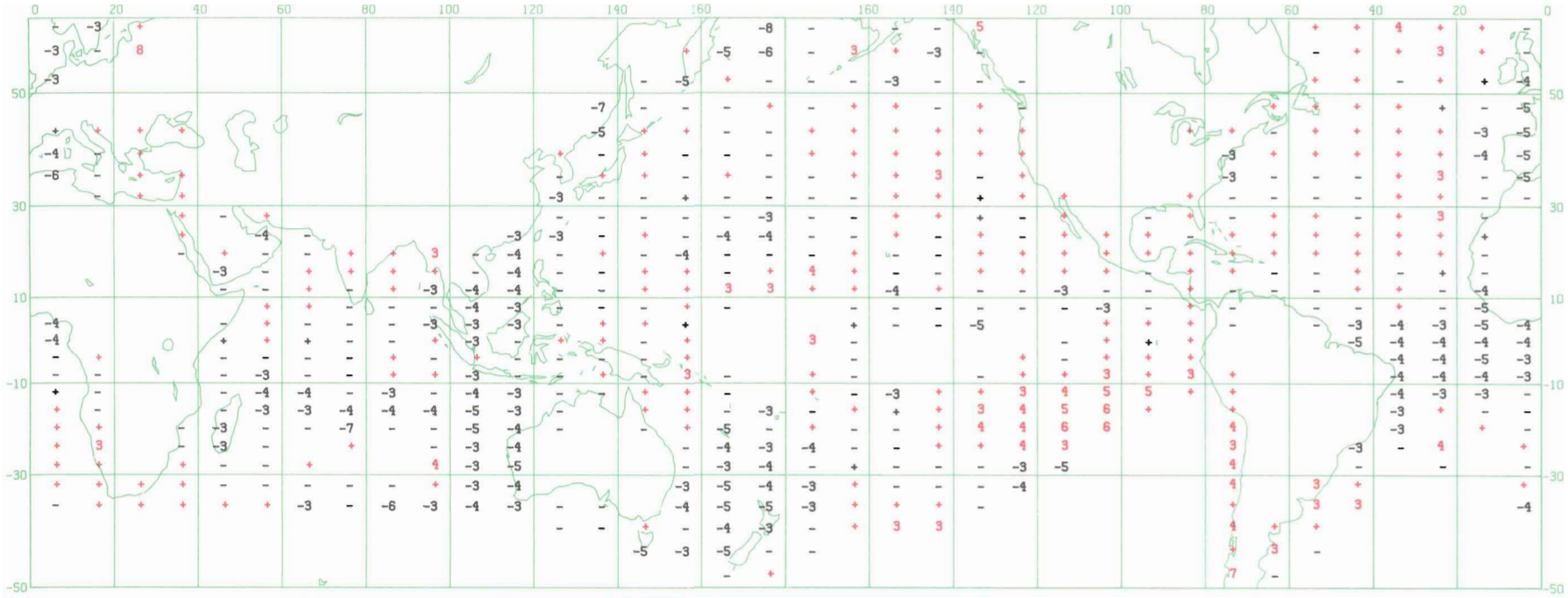

Figure 10a. SST DJF1 CORRELATION

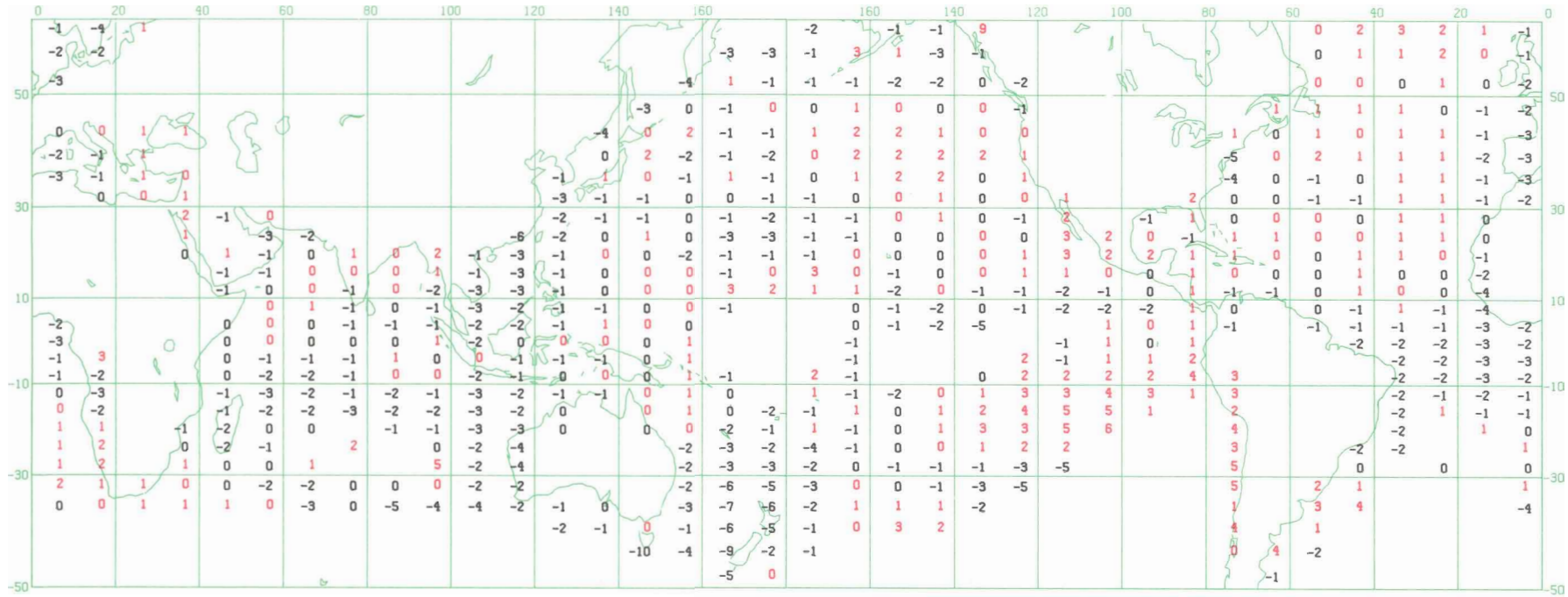

Figure 10b. SST DJF1 REGRESSION (tenths of °C/MB)

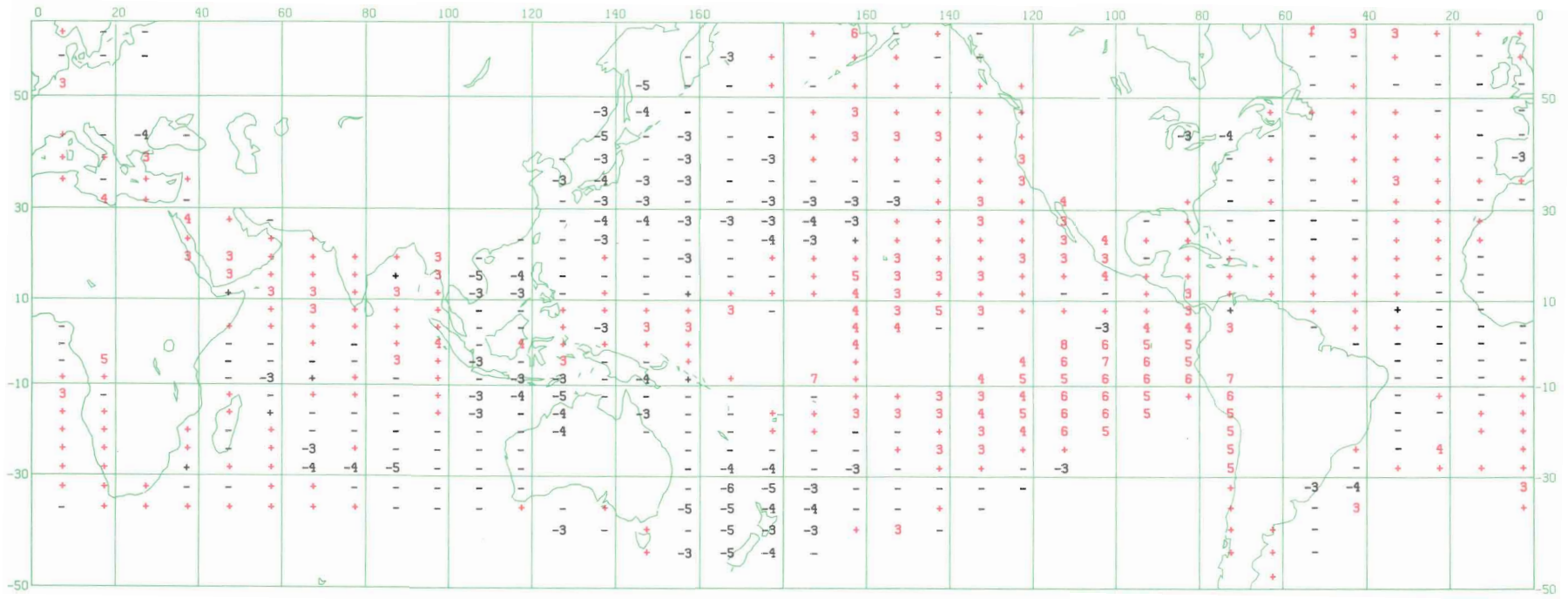

Figure IIa. SST MAM1 CORRELATION

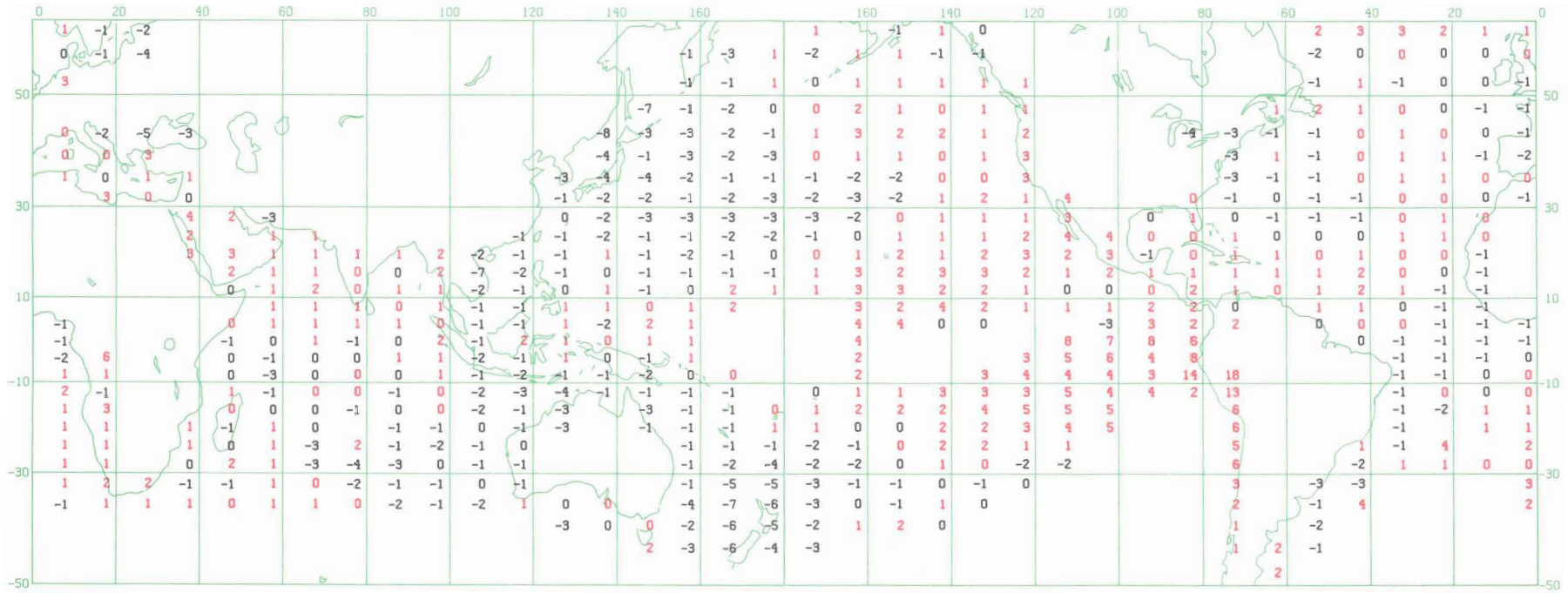

Figure IIb. SST MAM1 REGRESSION (tenths of °C/MB)

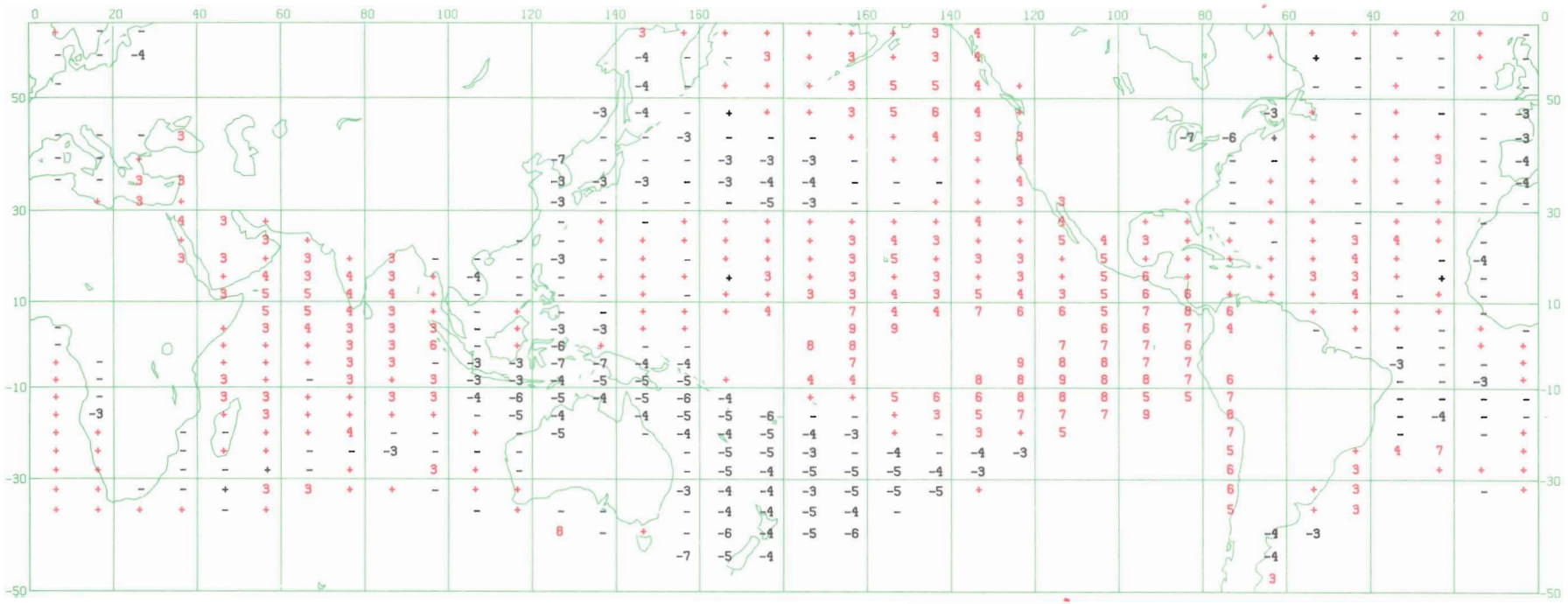

Figure 12a. SST JJA CORRELATION

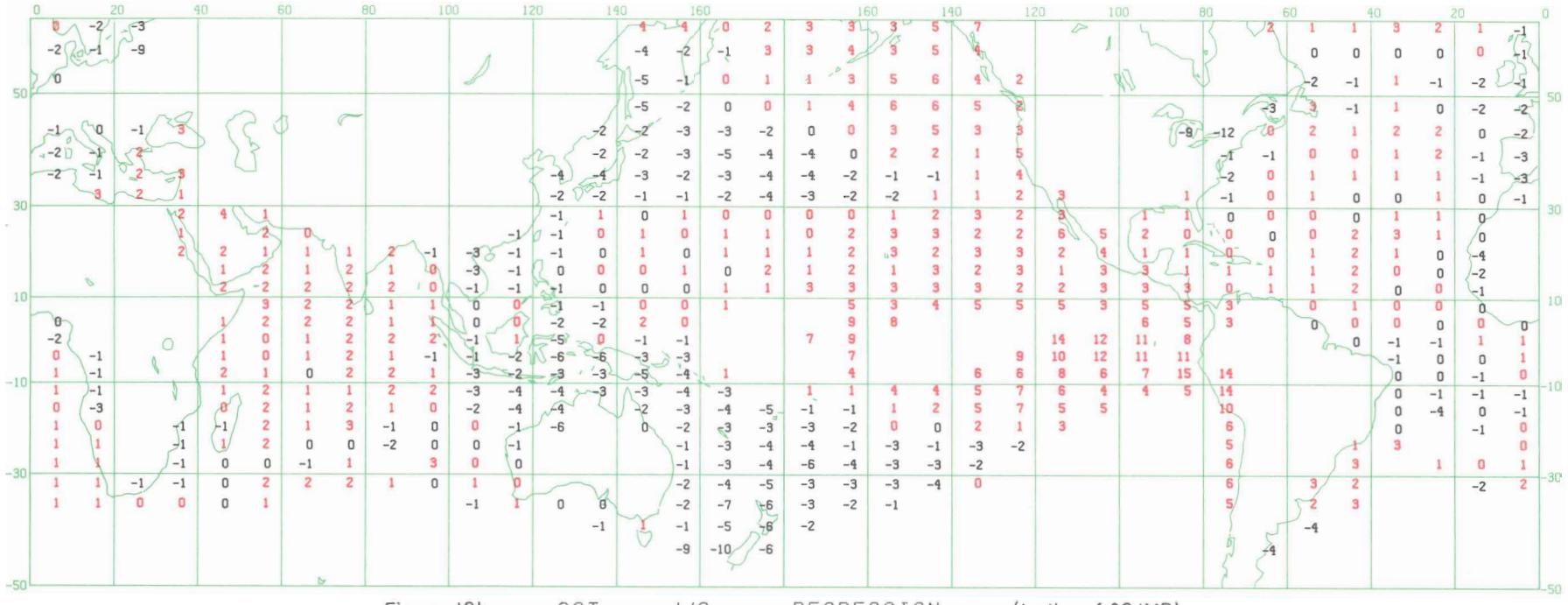

Figure 12b. SST JJA REGRESSION (tenths of °C/MB)

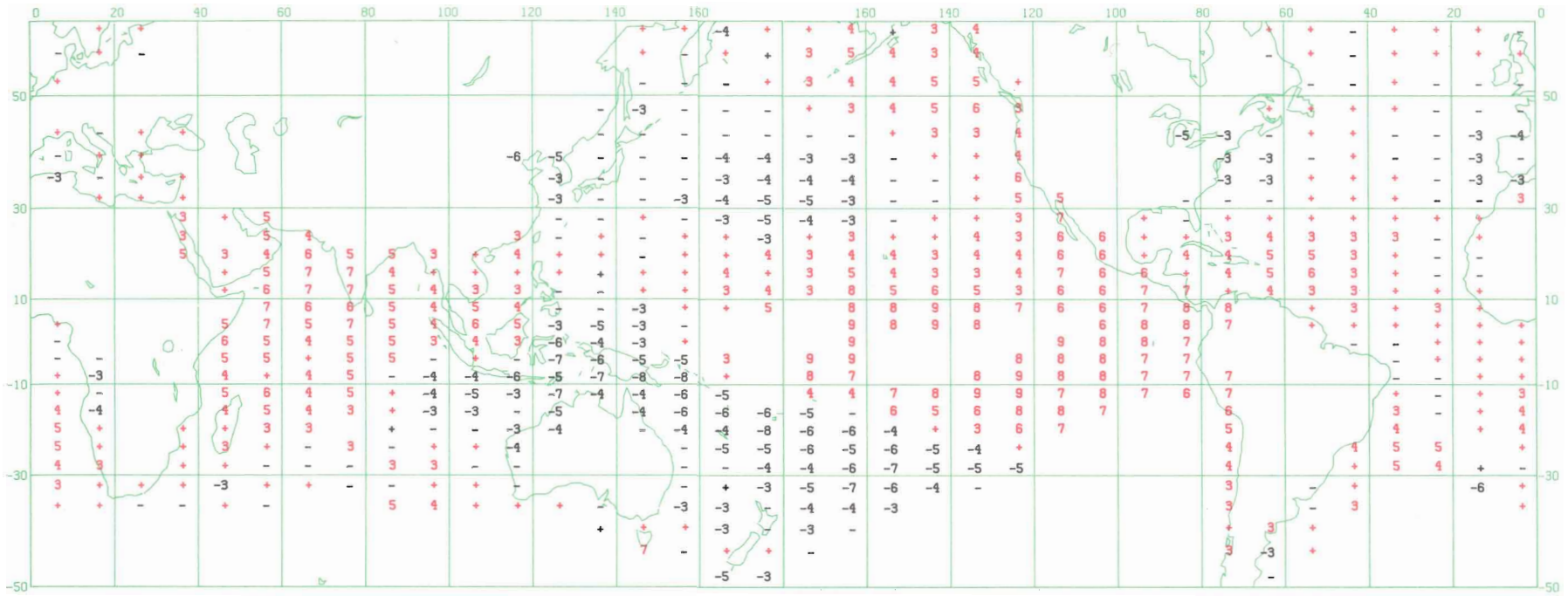

Figure 13a. SST SON CORRELATION

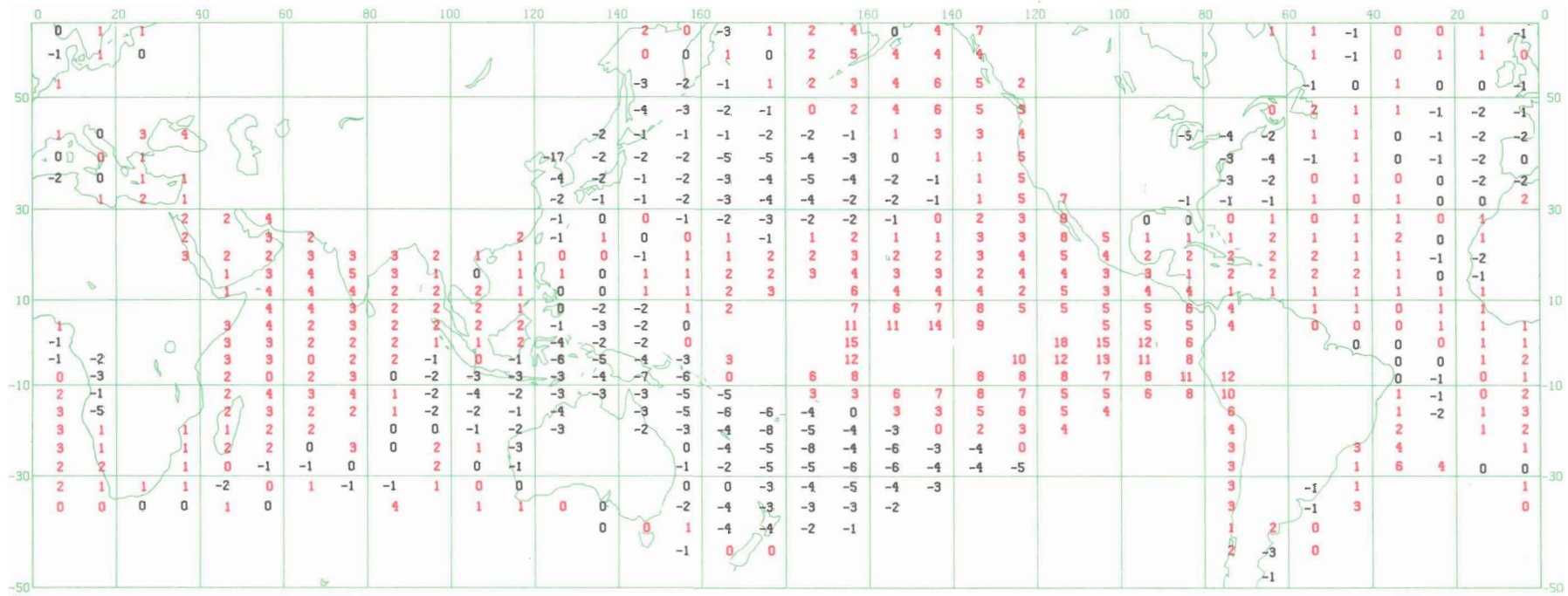

Figure 13b. SST SON REGRESSION (tenths of °C/MB)

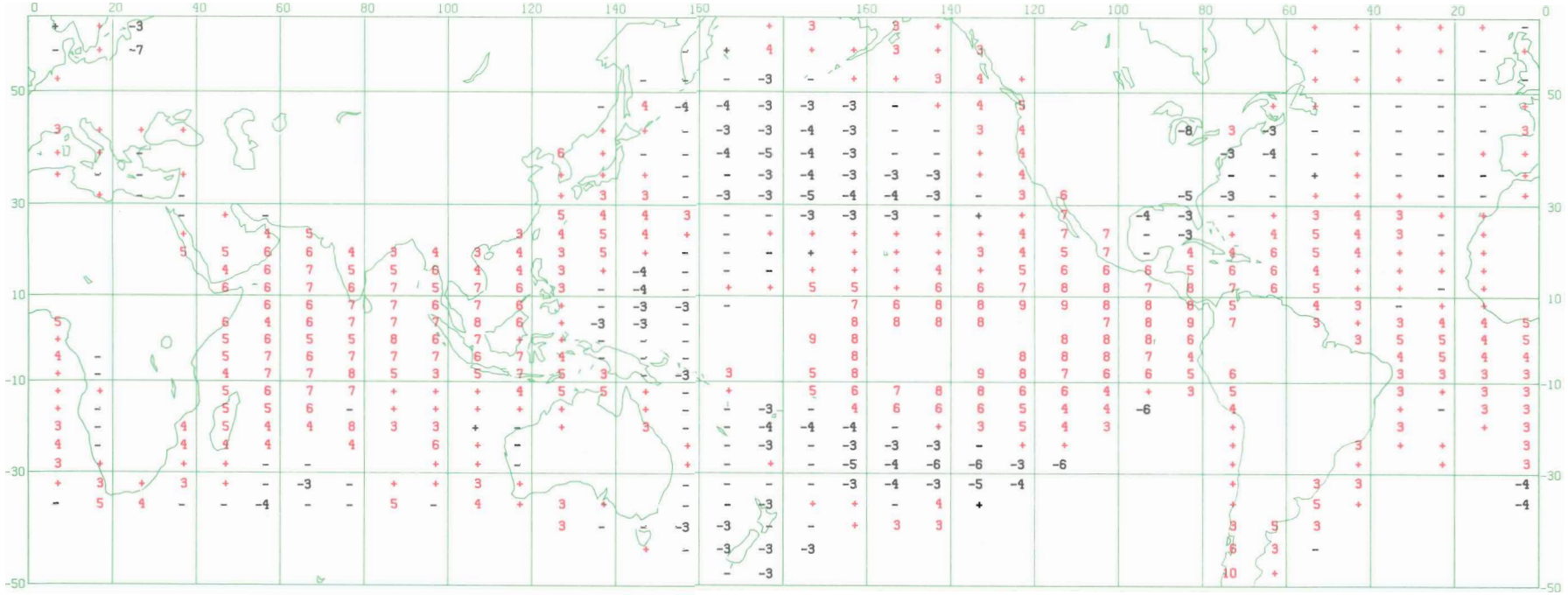

Figure 14a. SST DJF2 CORRELATION

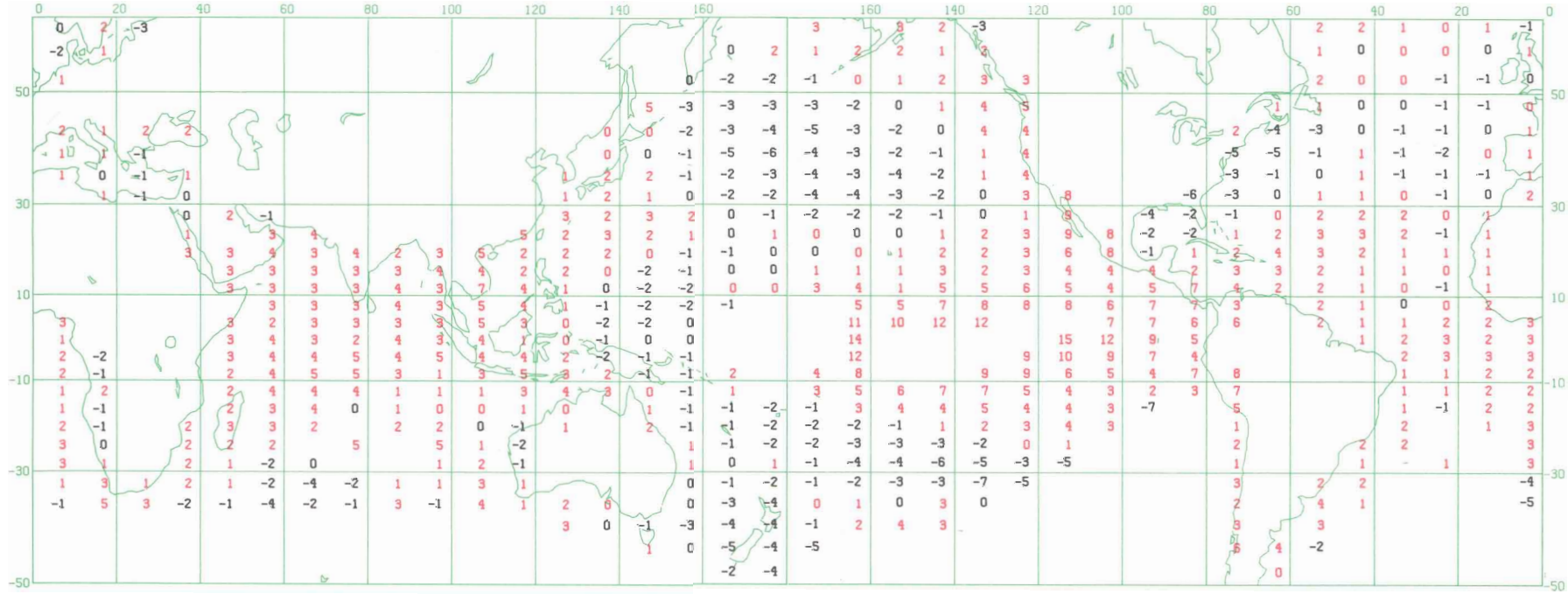

Figure 14b. SST DJF2 REGRESSION (tenths of °C/MB)

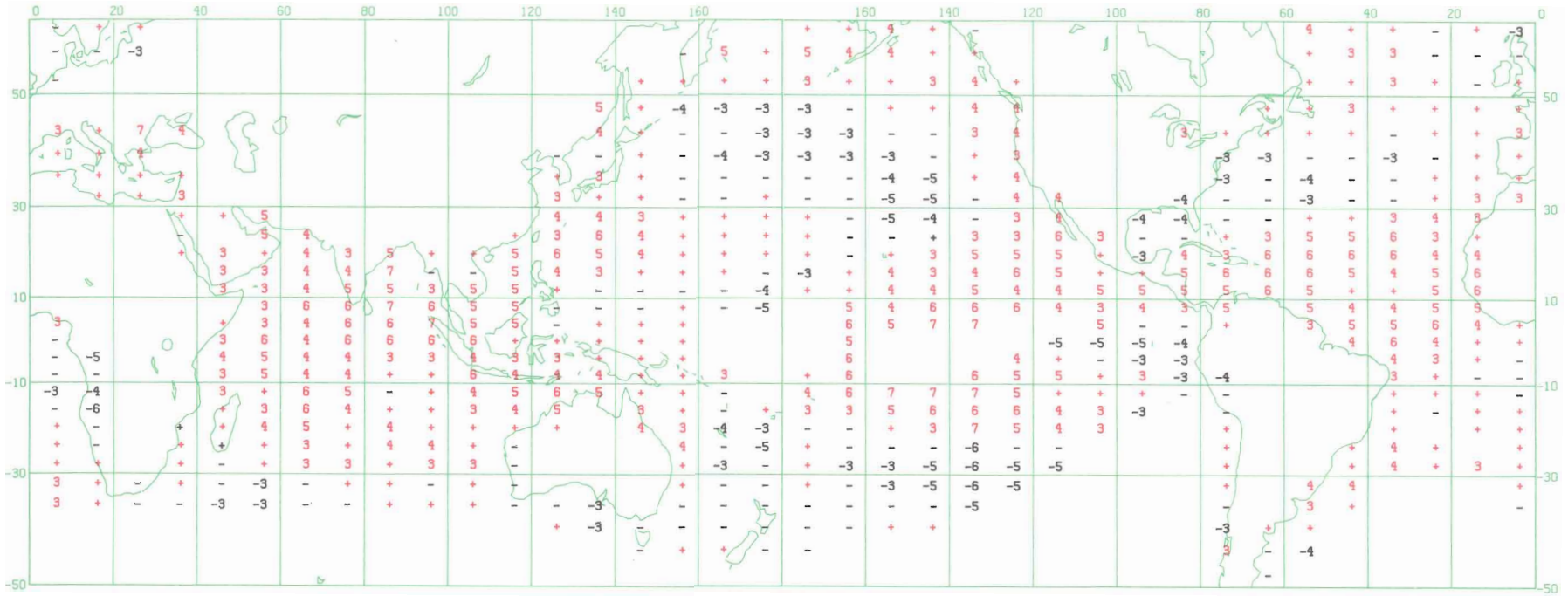

Figure 15a. SST MAM2 CORRELATION

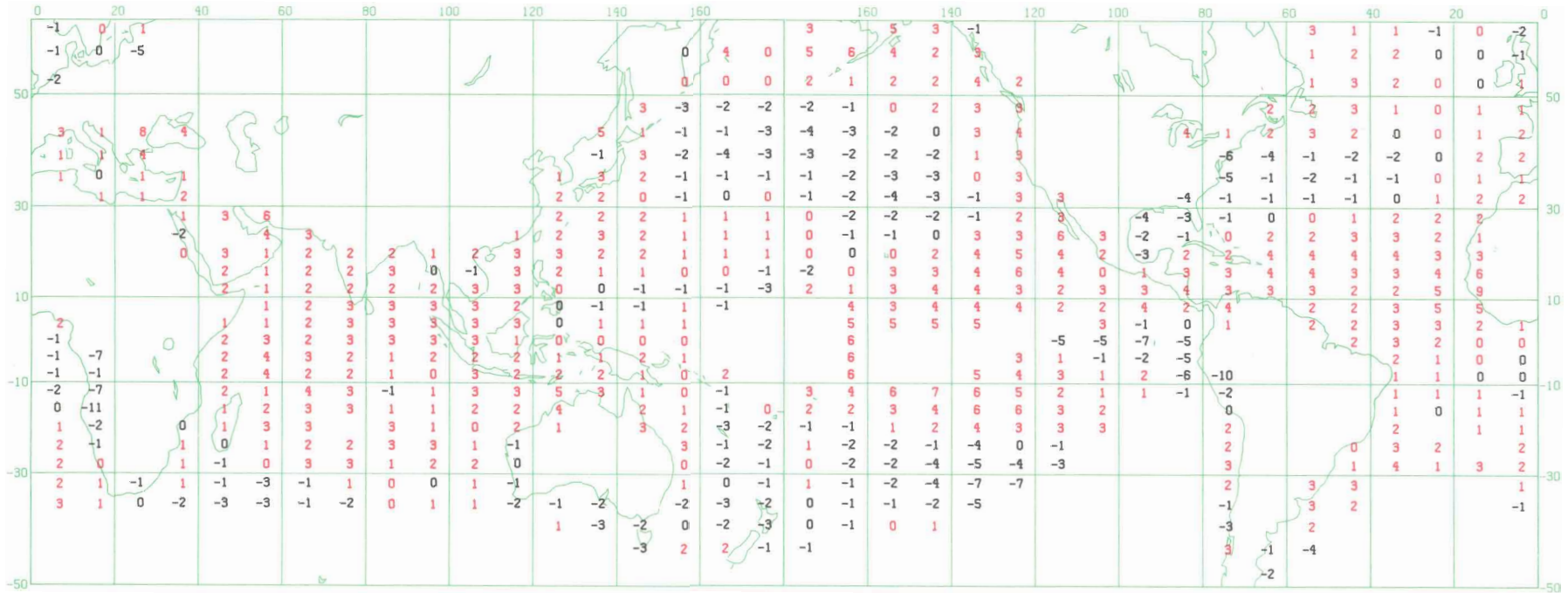

Figure 15b. SST MAM2 REGRESSION (tenths of °C/MB)

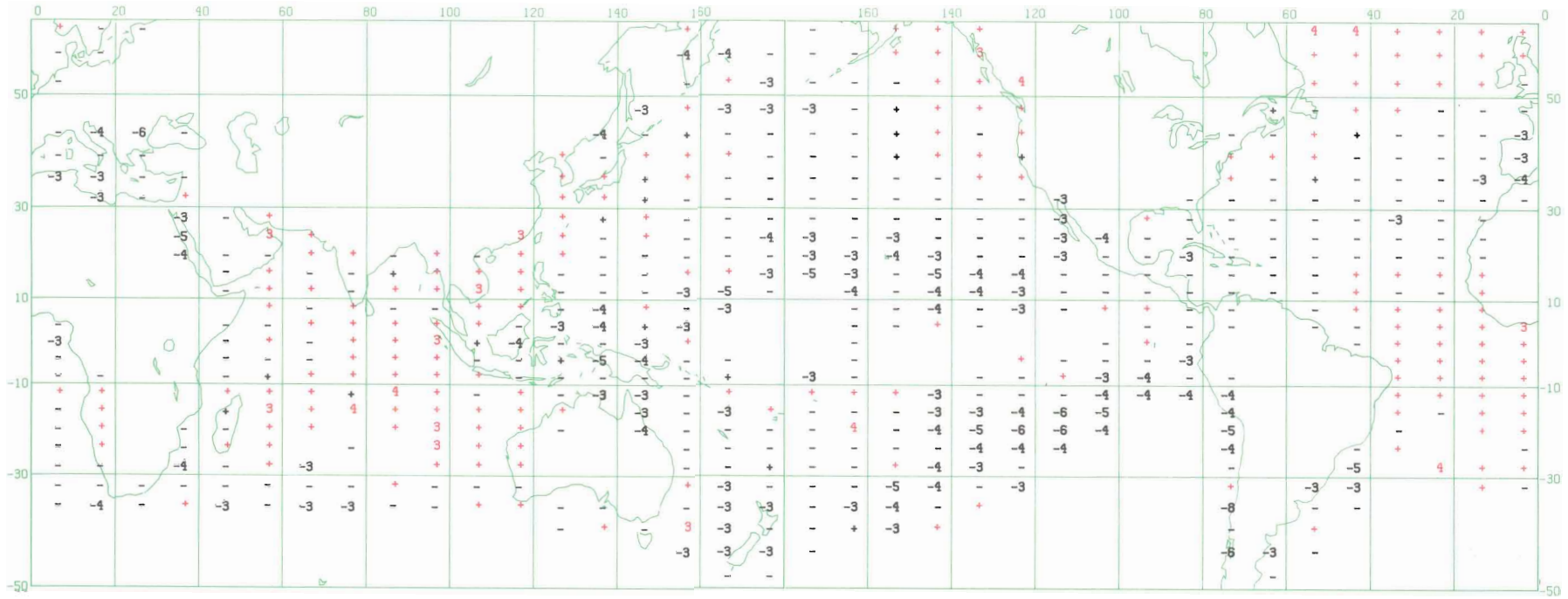

Figure 16a. PRESSURE DJF1 CORRELATION

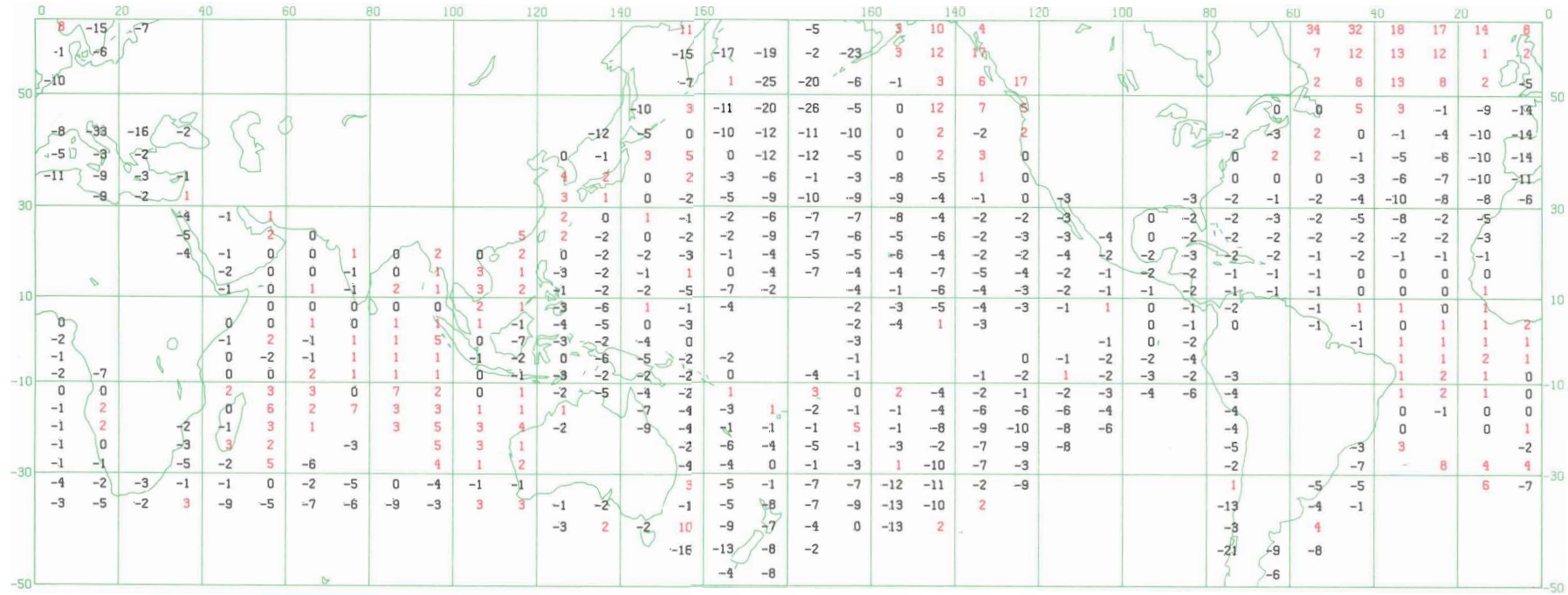

Figure 16b. PRESSURE DJF1 REGRESSION (tenths of MB/MB)

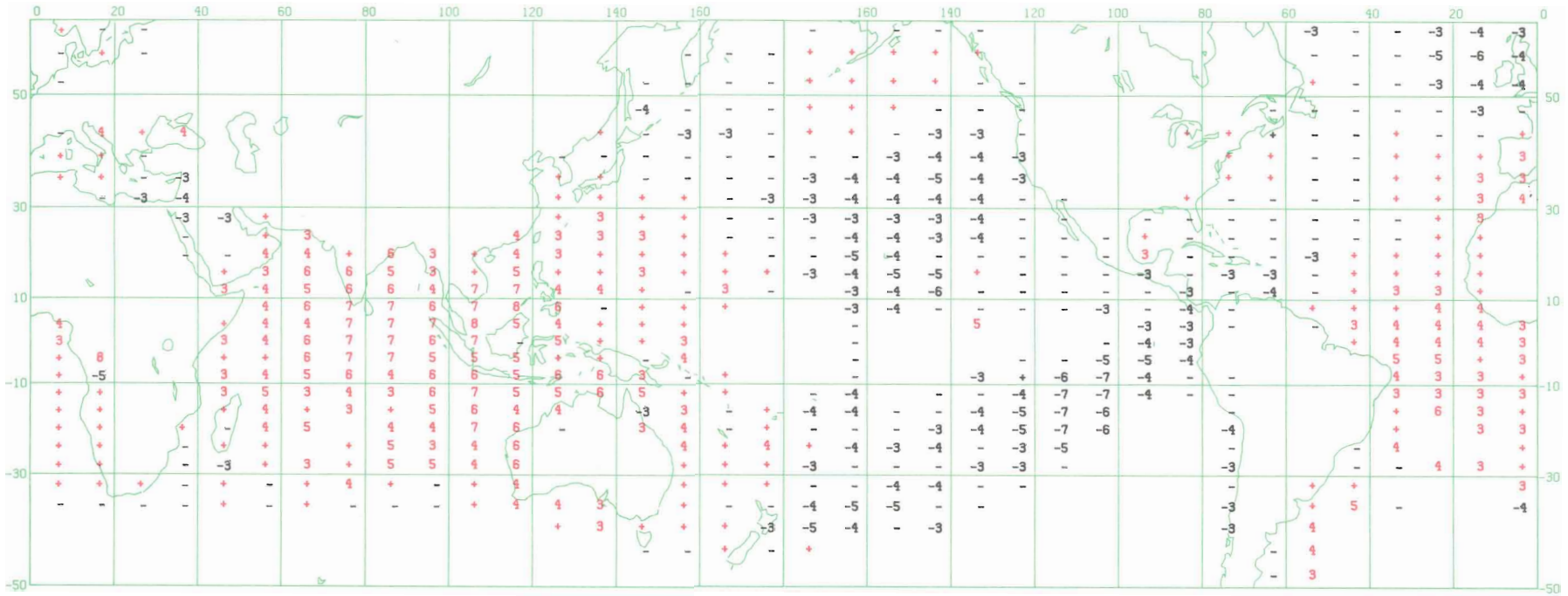

Figure 17a. PRESSURE MAM1 CORRELATION

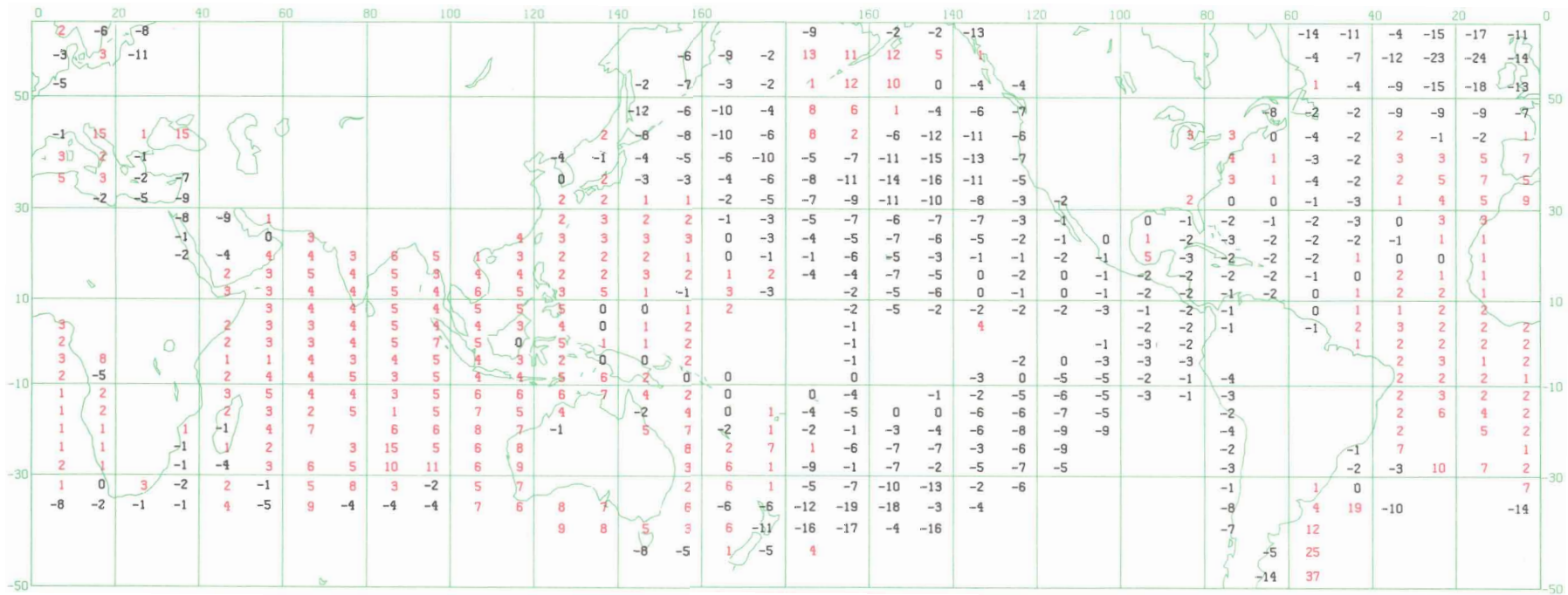

Figure 17b. PRESSURE MAM1 REGRESSION (tenths of MB/MB)

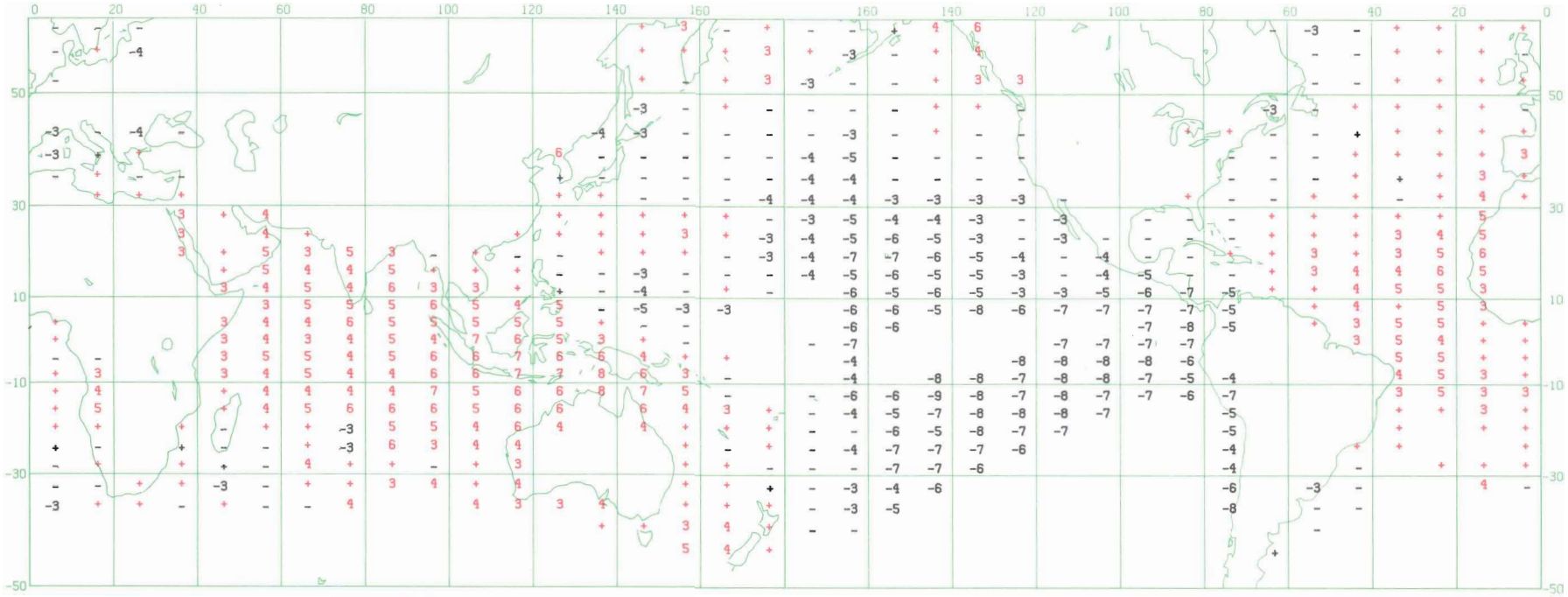

Figure 18a. PRESSURE JJA CORRELATION

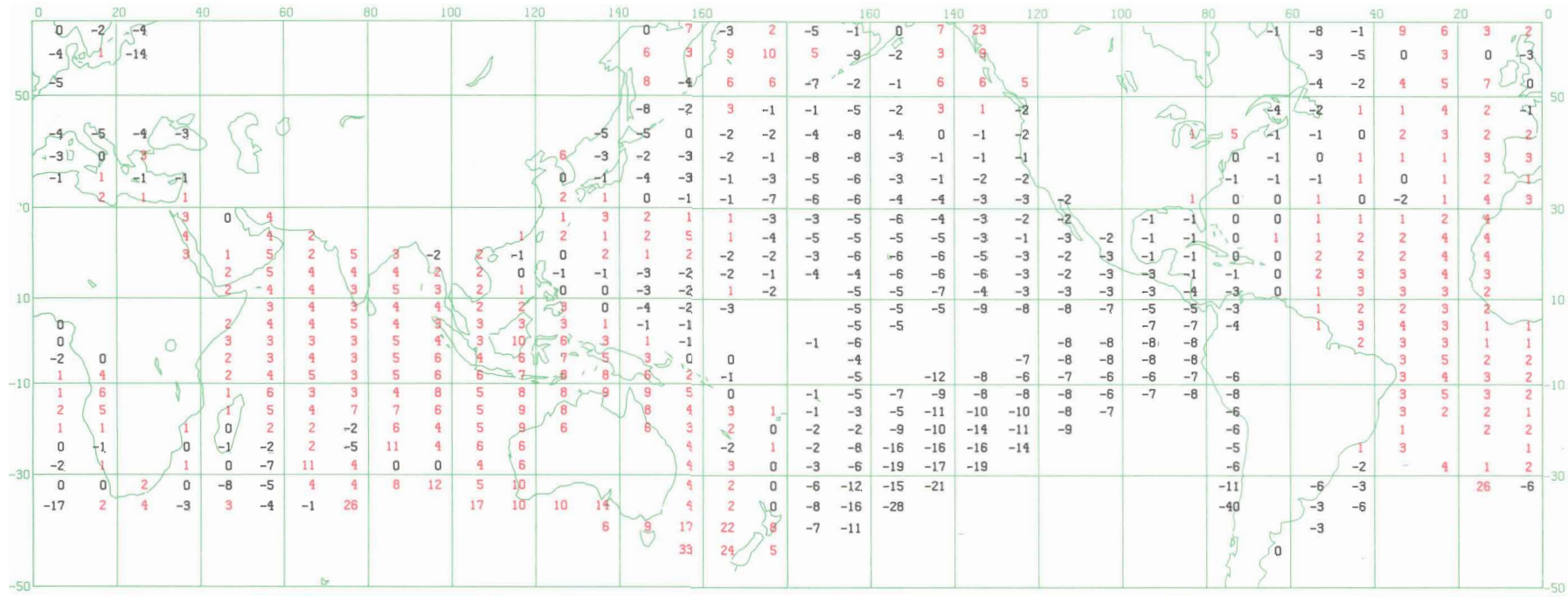

Figure 18b. PRESSURE JJA REGRESSION (tenths of MB/MB)

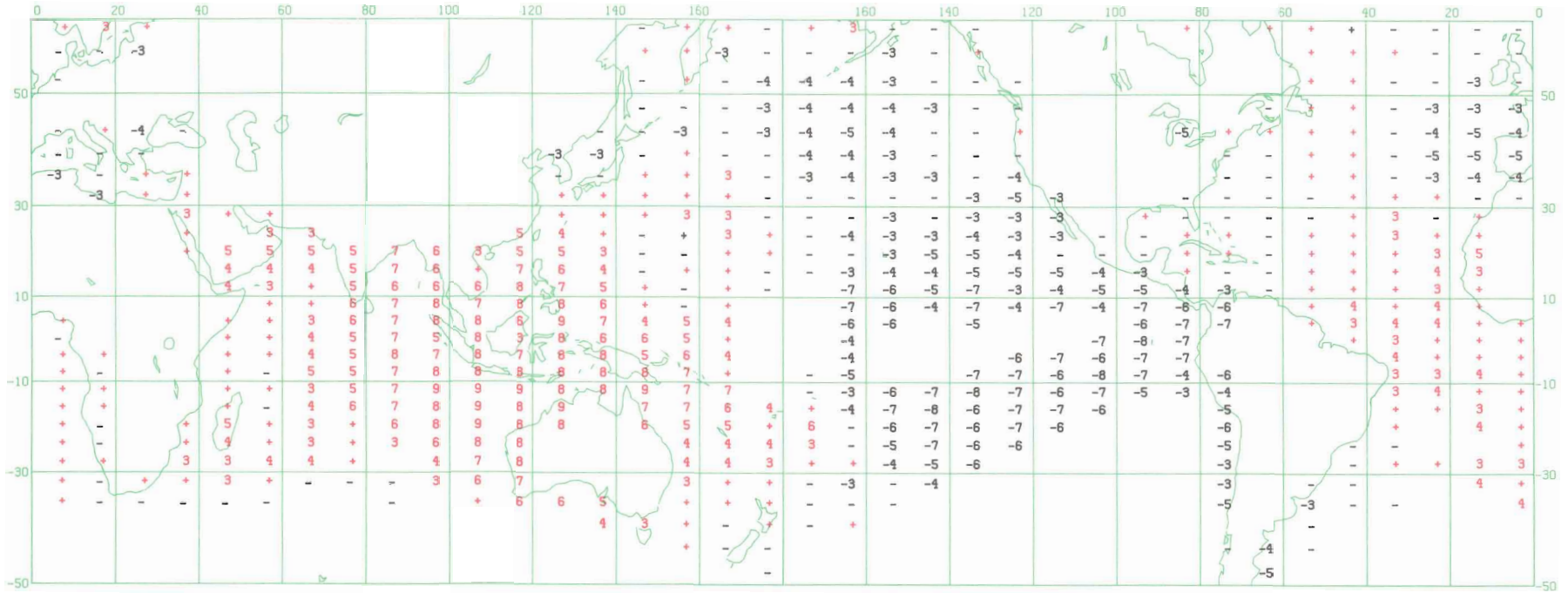

Figure 19a. PRESSURE SON CORRELATION

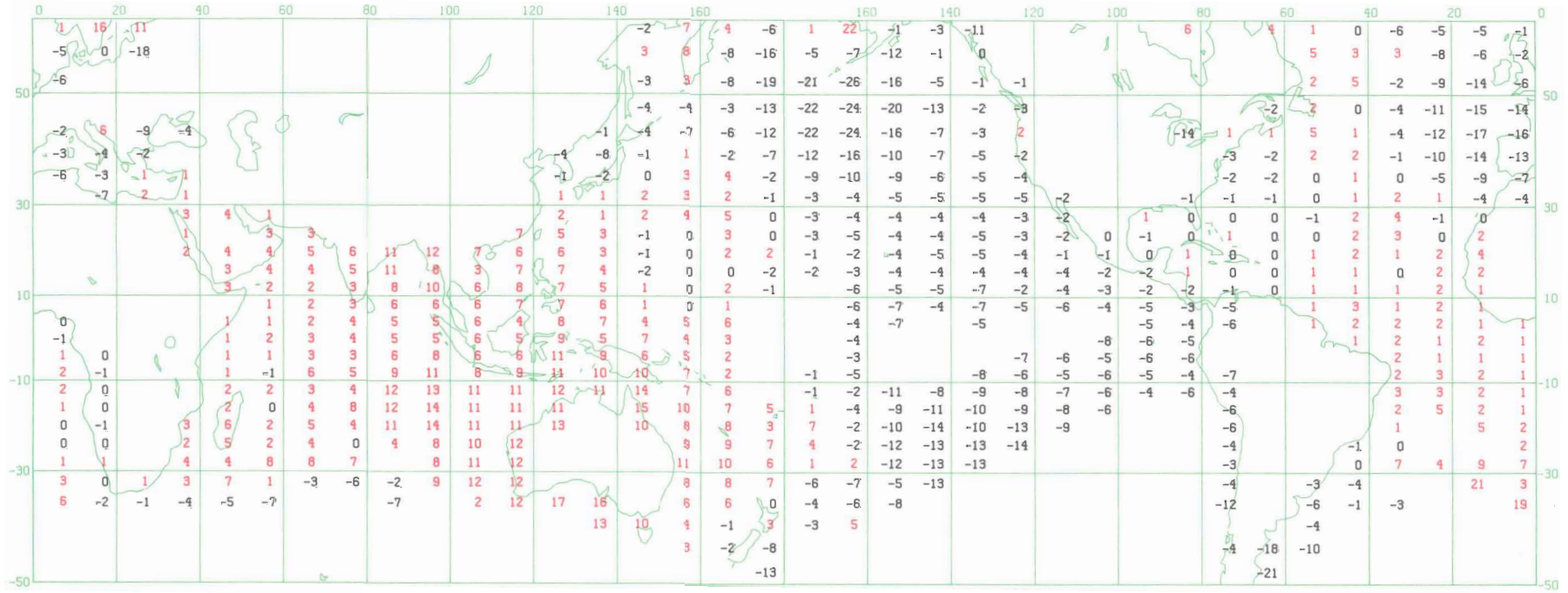

Figure 19b. PRESSURE SON REGRESSION (tenths of MB/MB)

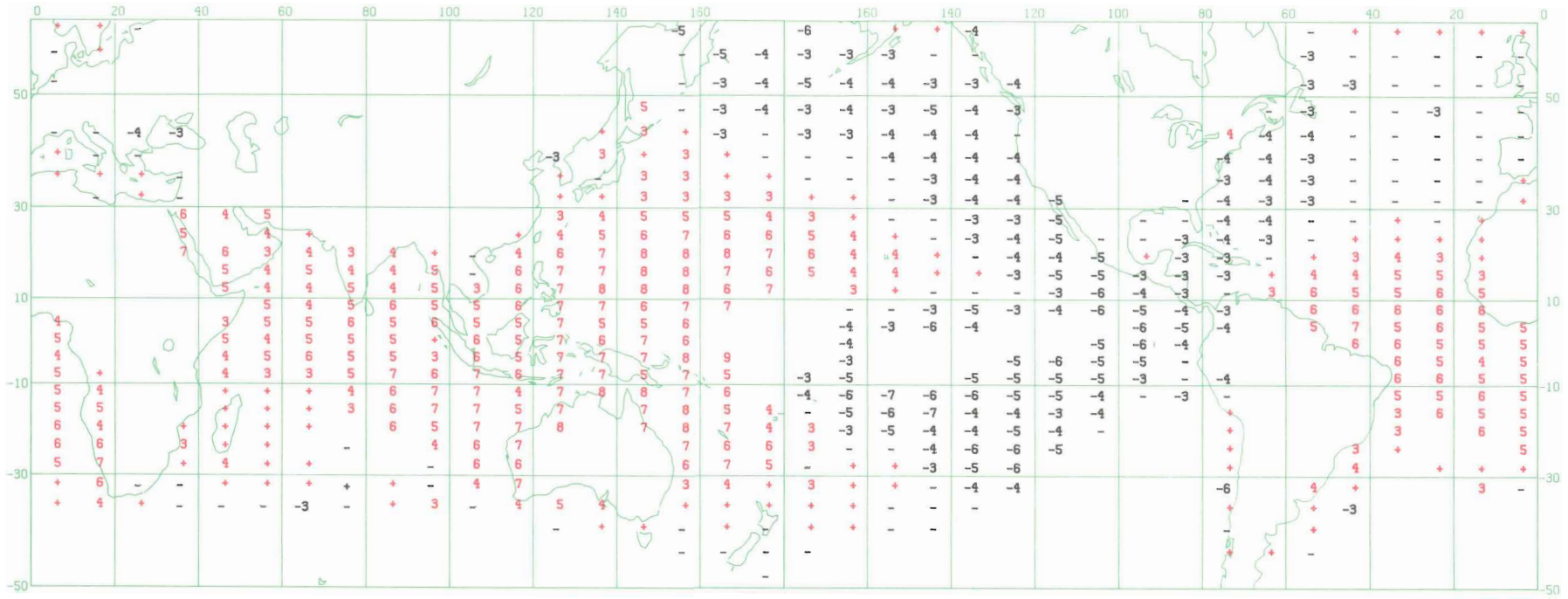

Figure 20a. PRESSURE DJF2 CORRELATION

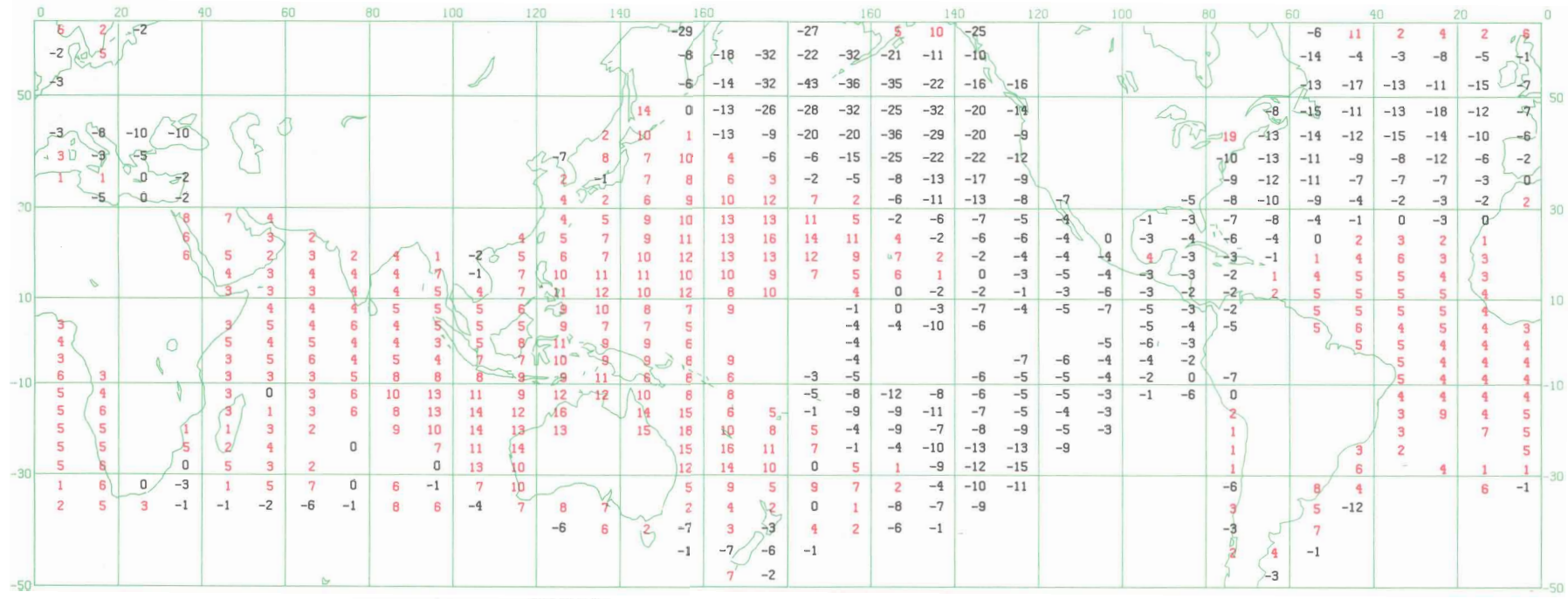

Figure 20b. PRESSURE DJF2 REGRESSION (tenths of MB/MB)

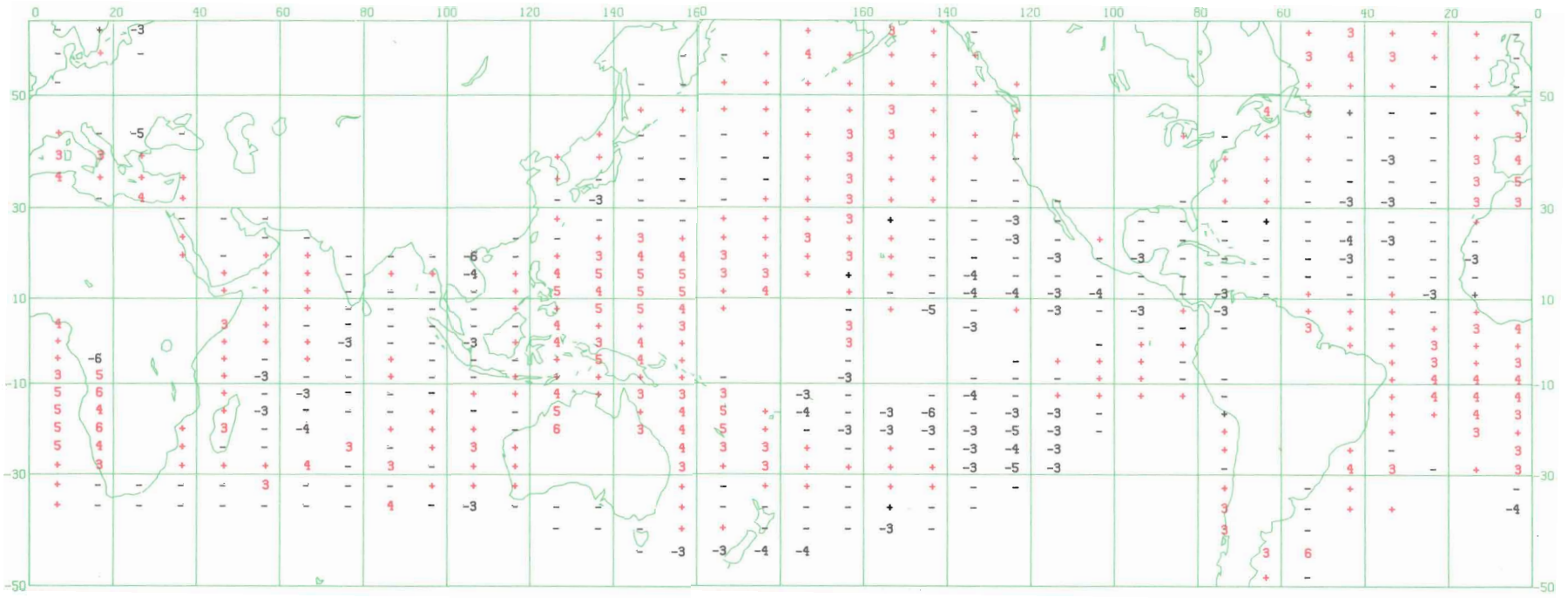

Figure 21a. PRESSURE MAM2 CORRELATION

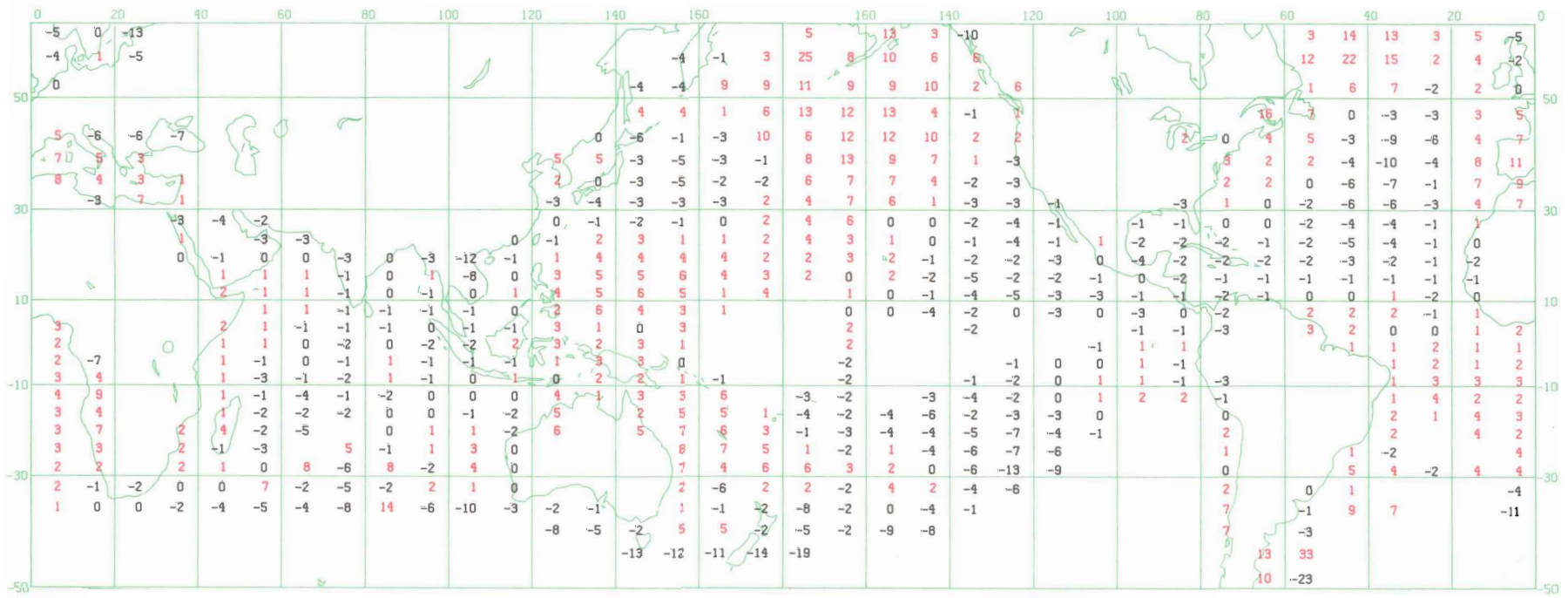

Figure 21b. PRESSURE MAM2 REGRESSION (tenths of MB/MB)

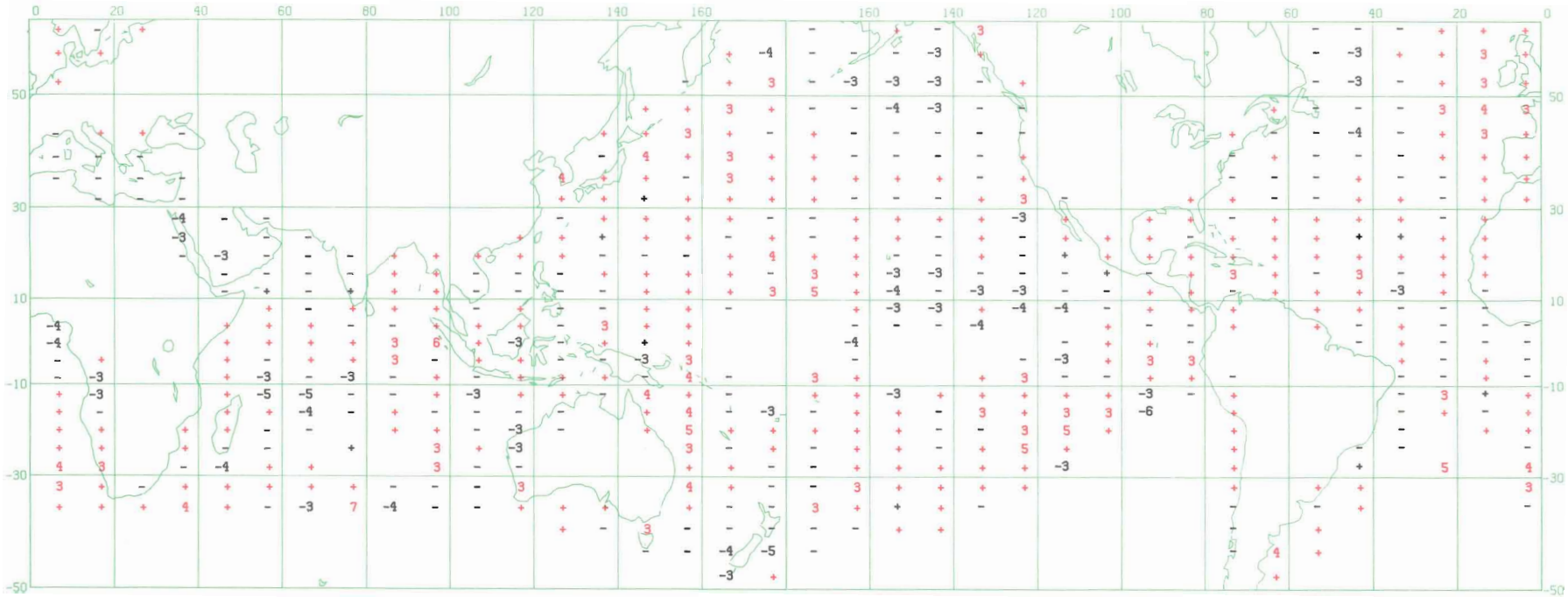

Figure 22a. SST MINUS AIR TEMP DJF1 CORRELATION

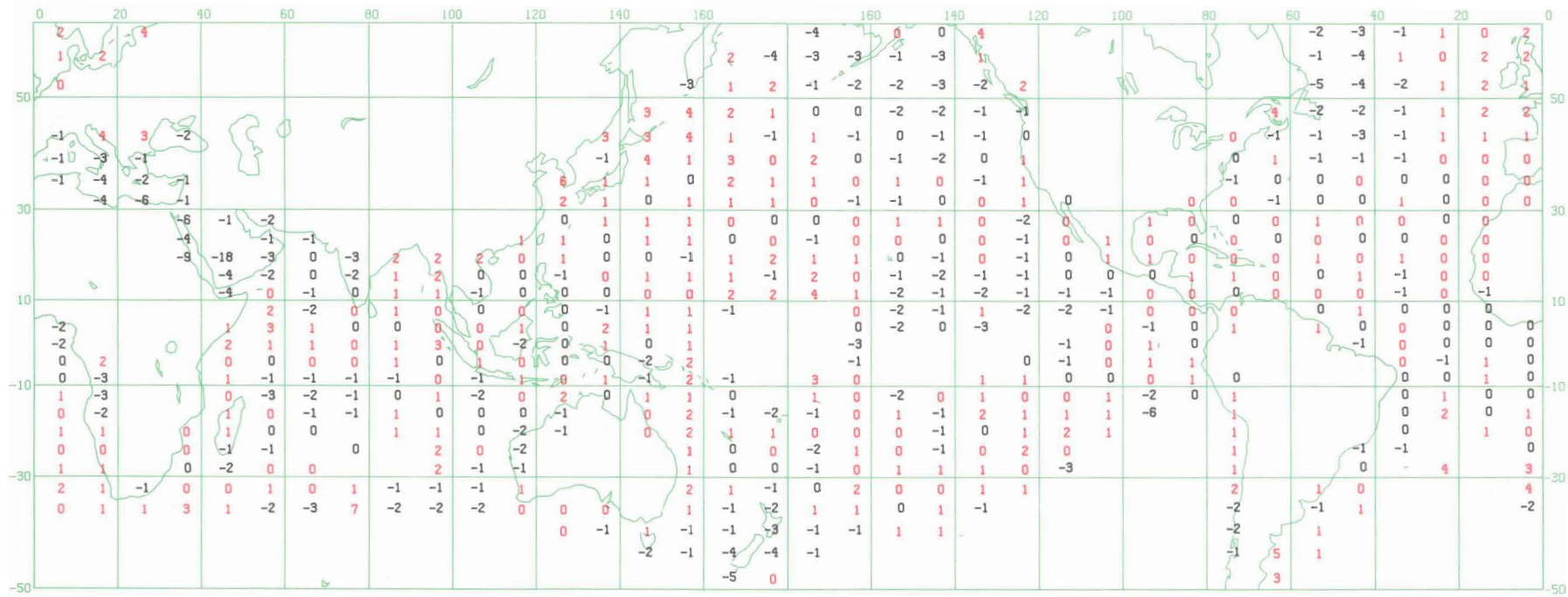

Figure 22b. SST MINUS AIR TEMP DJF1 REGRESSION (tenths of °C/MB)

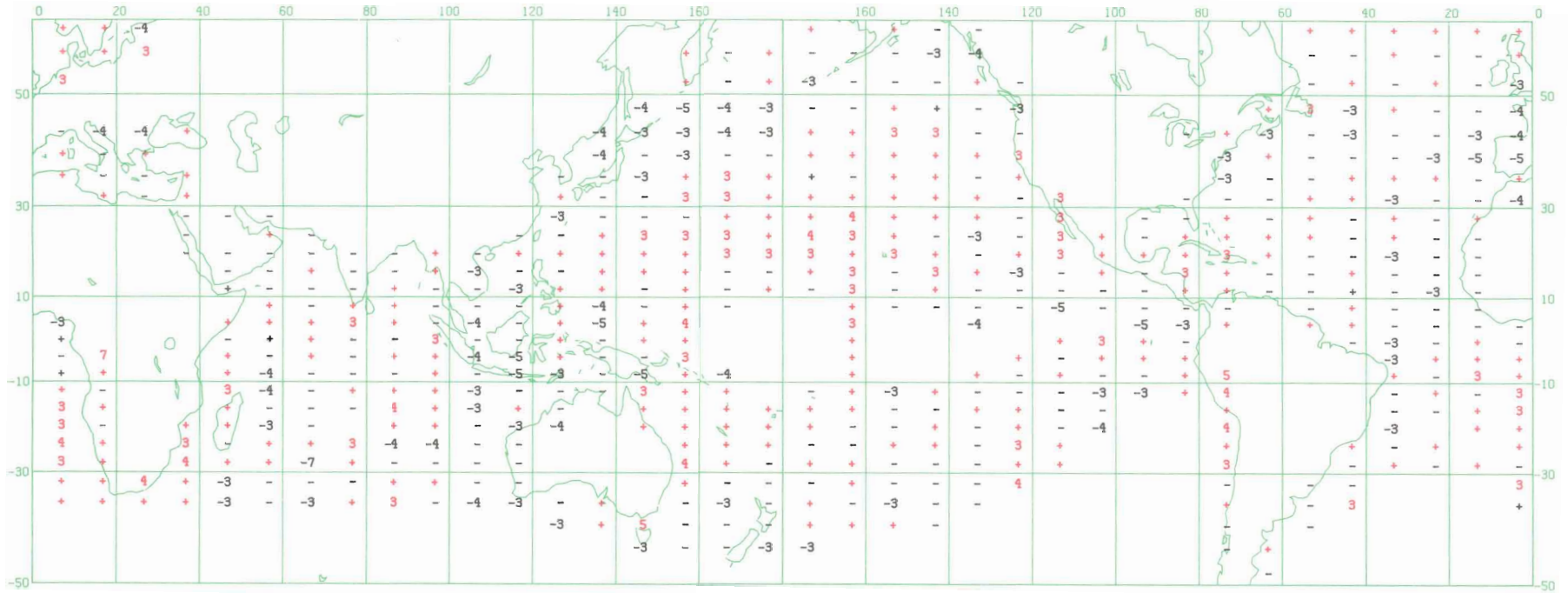

Figure 23a. SST MINUS AIR TEMP MAM1 CORRELATION

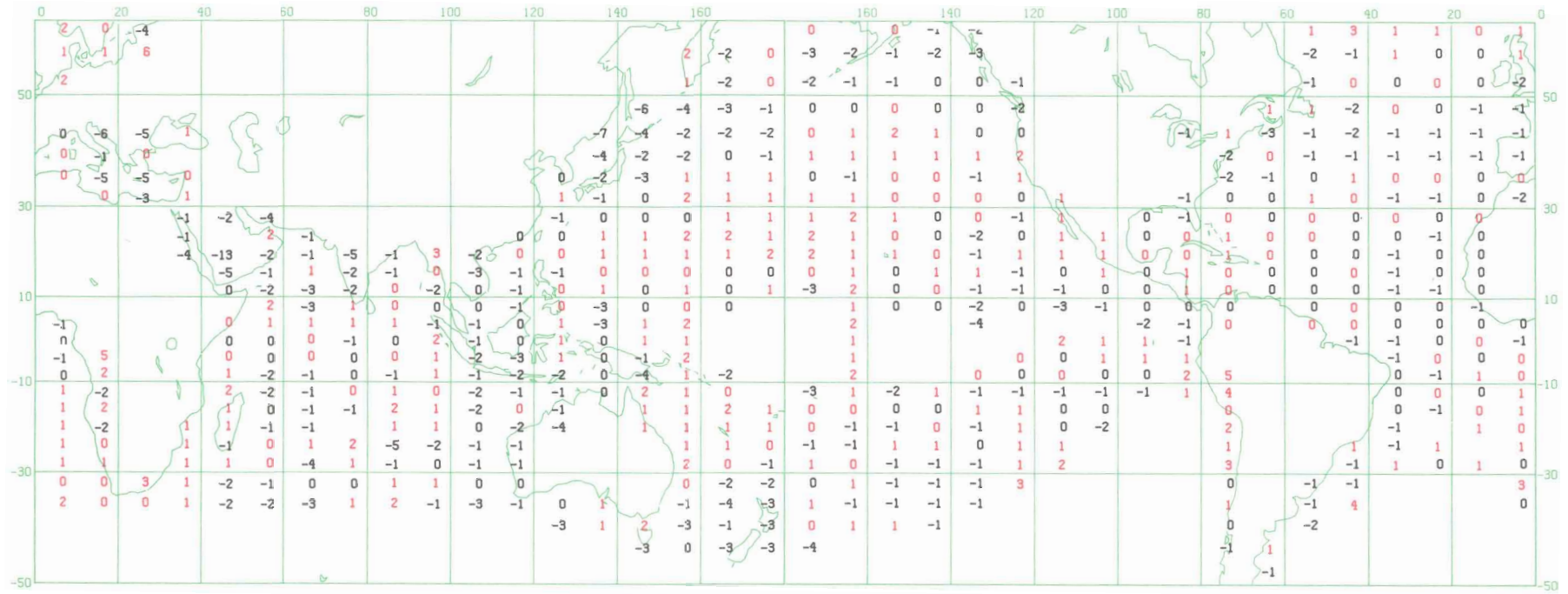

Figure 23b. SST MINUS AIR TEMP MAM1 REGRESSION (tenths of °C/MB)

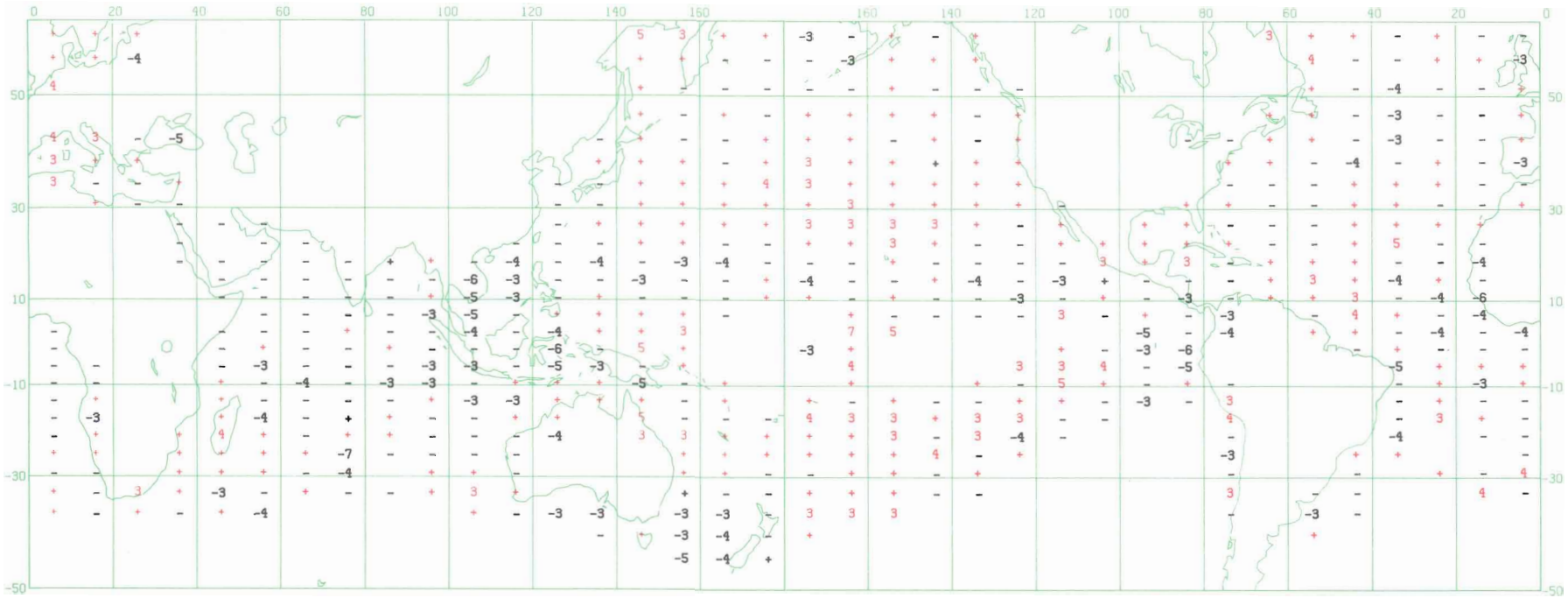

Figure 24a. SST MINUS AIR TEMP JJA CORRELATION

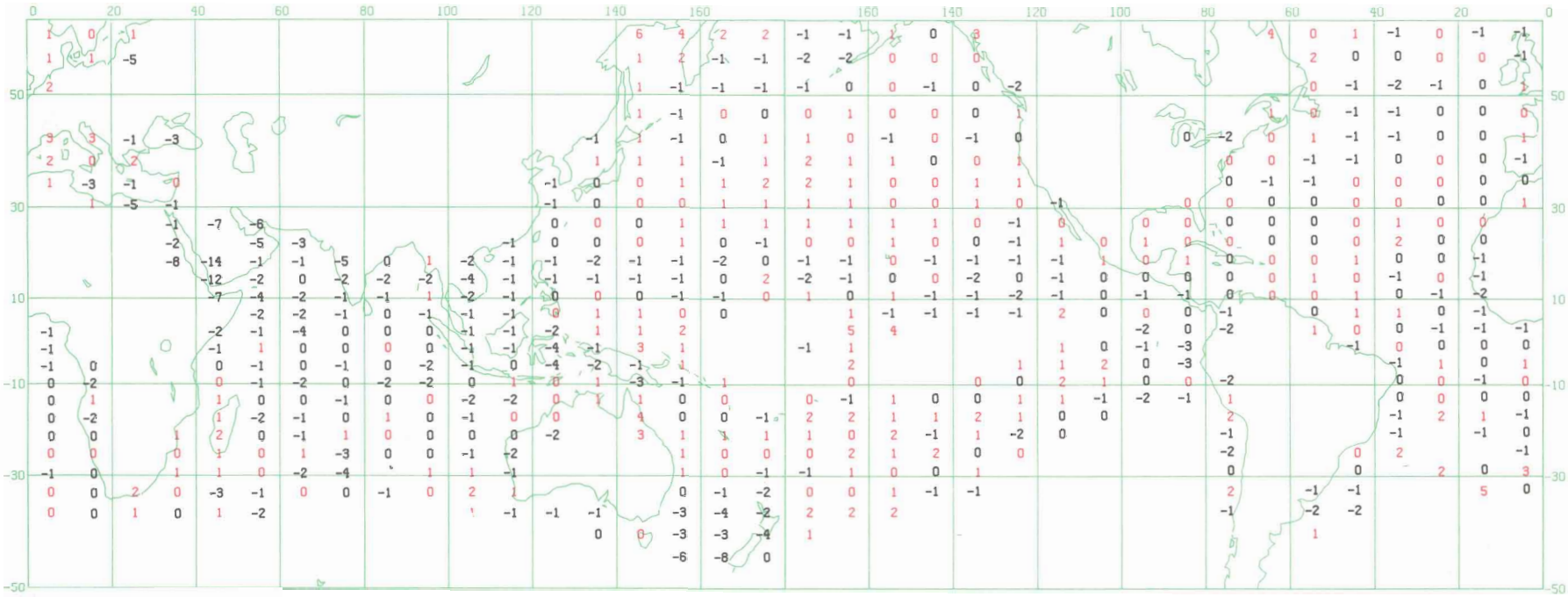

Figure 24b. SST MINUS AIR TEMP JJA REGRESSION (tenths of °C/MB)

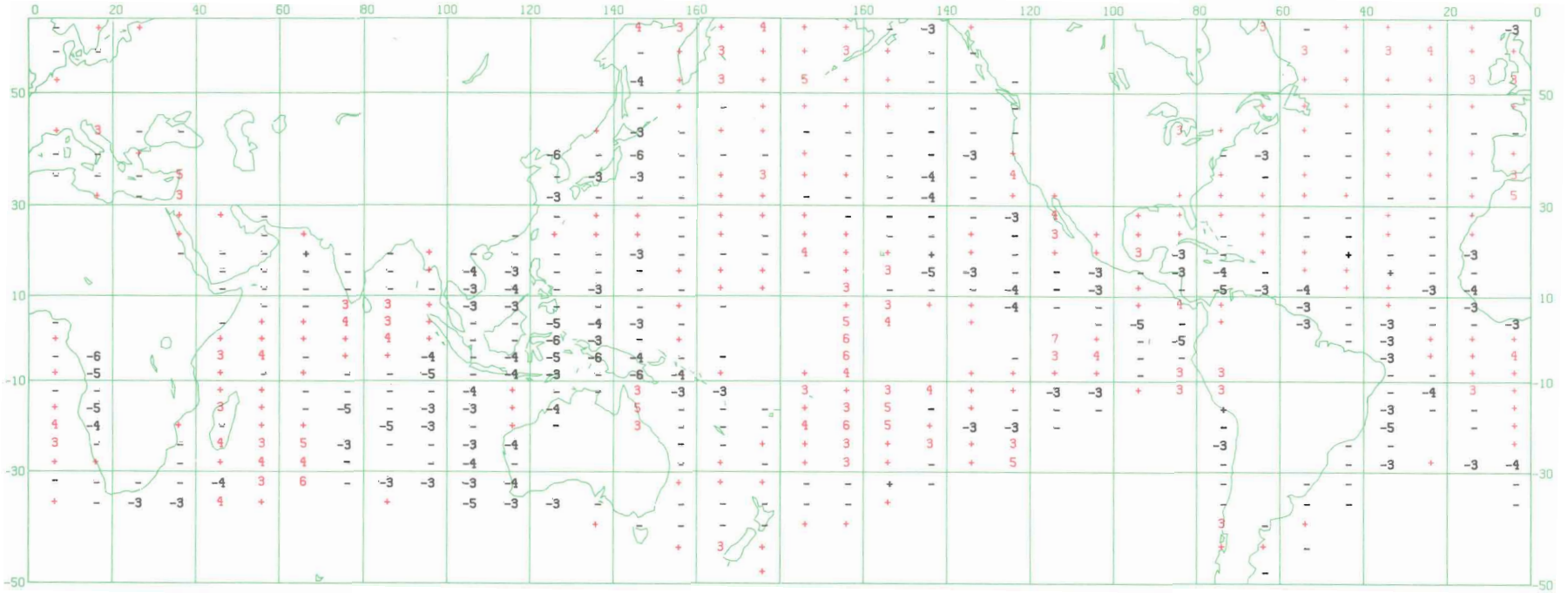

Figure 25a. SST MINUS AIR TEMP SON CORRELATION

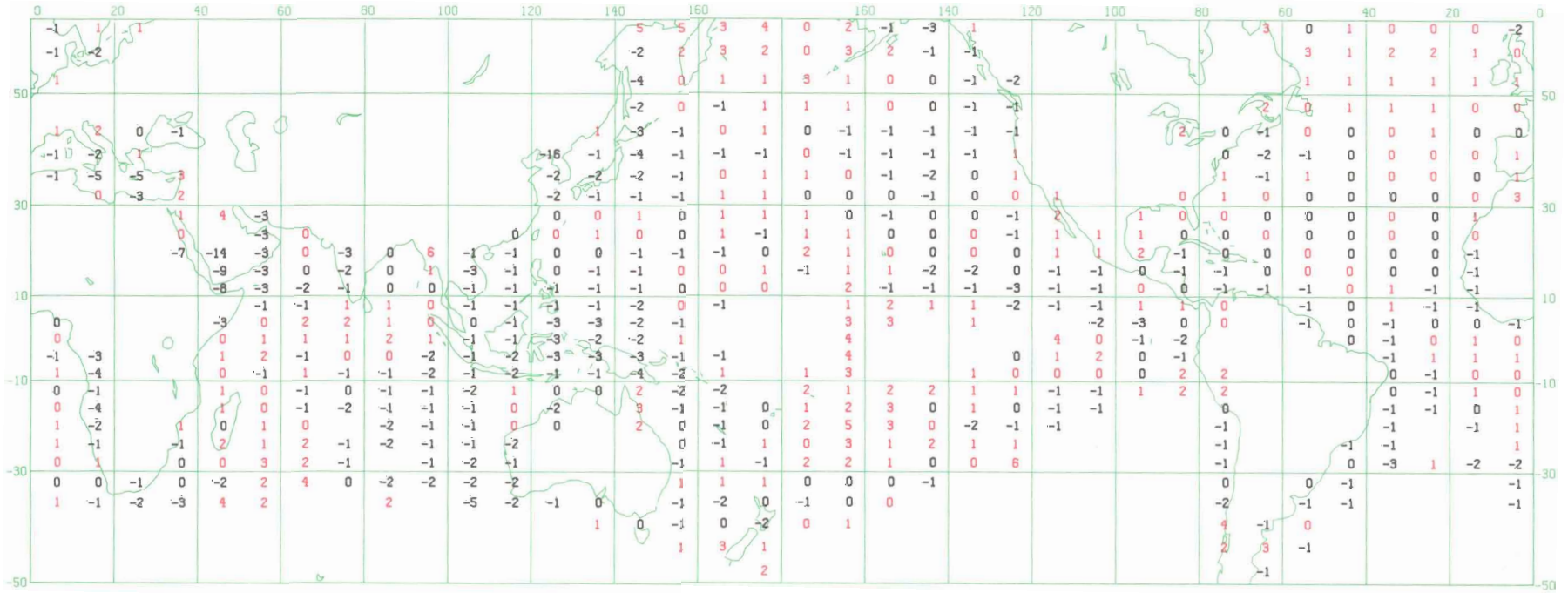

Figure 25b. SST MINUS AIR TEMP SON REGRESSION (tenths of °C/MB)

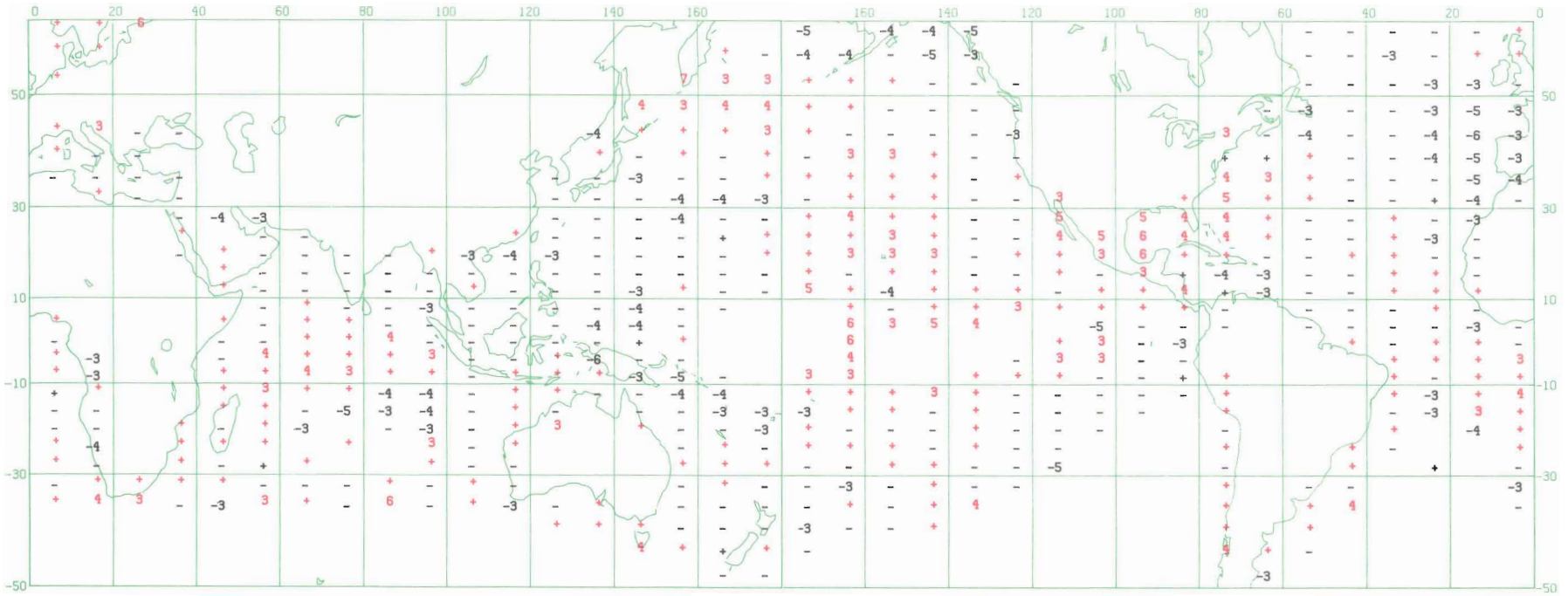

Figure 26a. SST MINUS AIR TEMP DJF2 CORRELATION

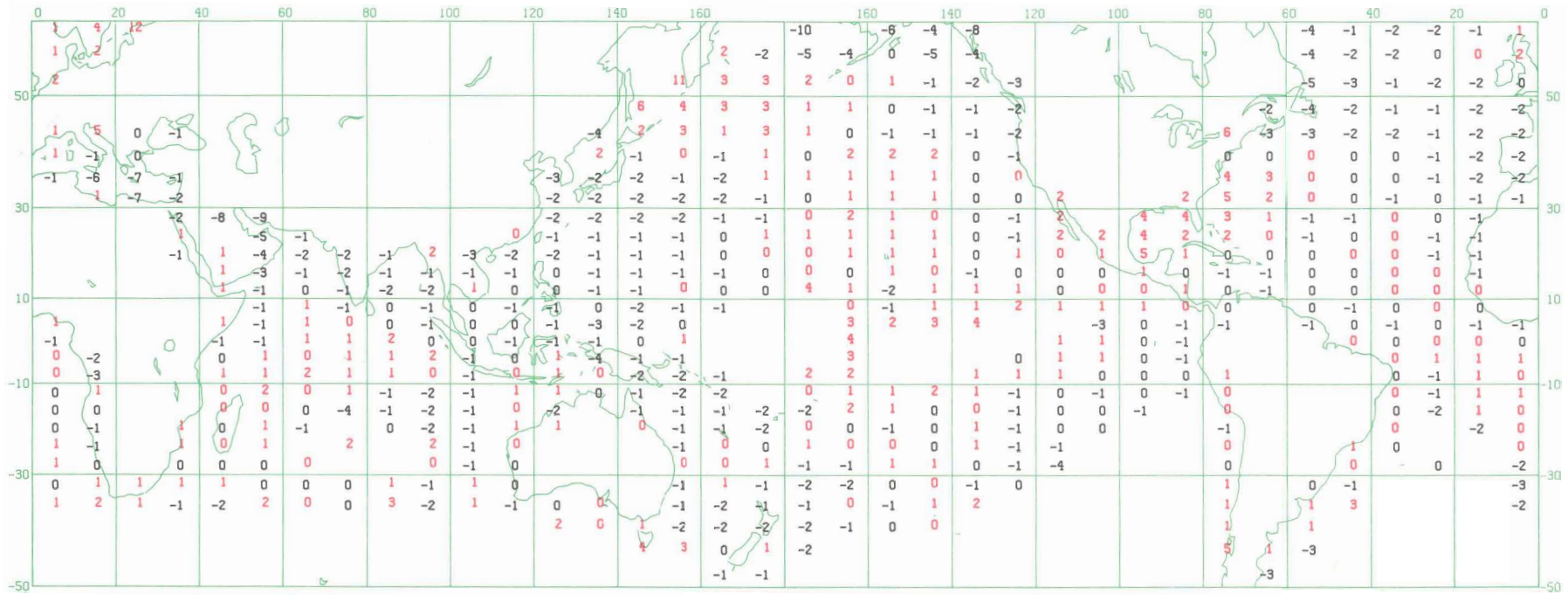

Figure 26b. SST MINUS AIR TEMP DJF2 REGRESSION (tenths of °C/MB)

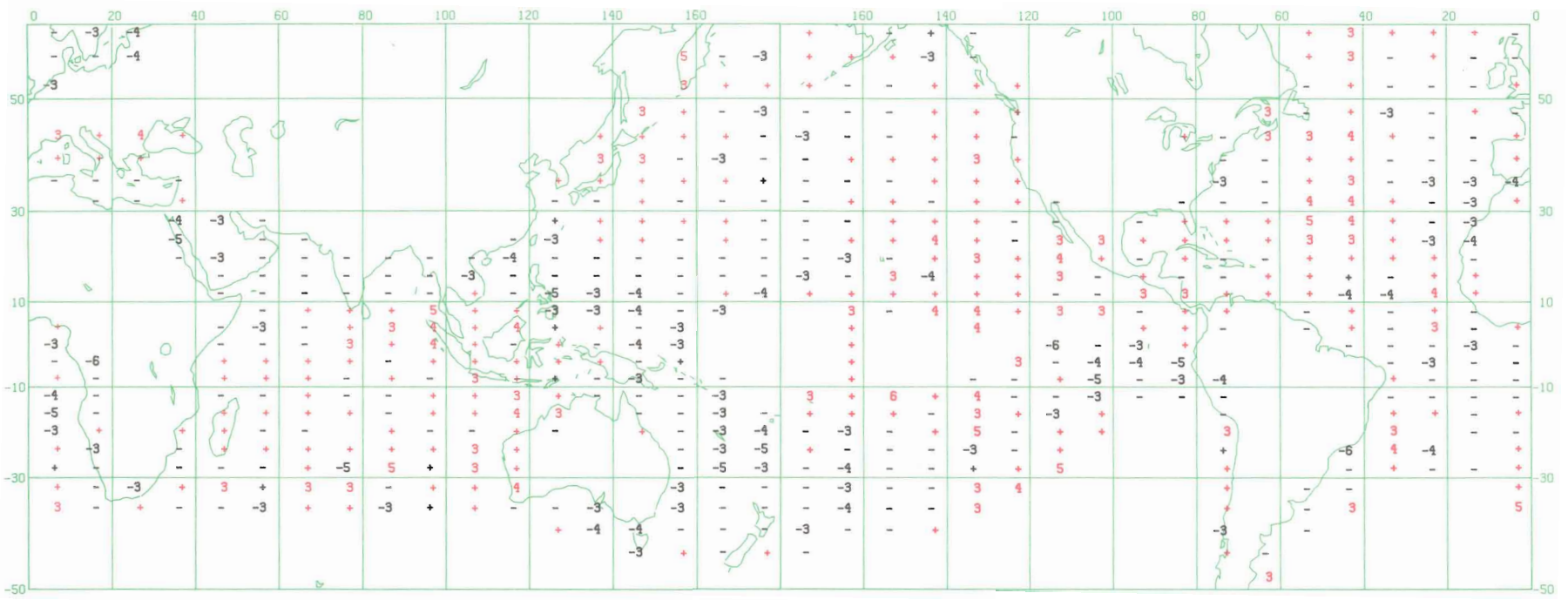

Figure 27a. SST MINUS AIR TEMP MAM2 CORRELATION

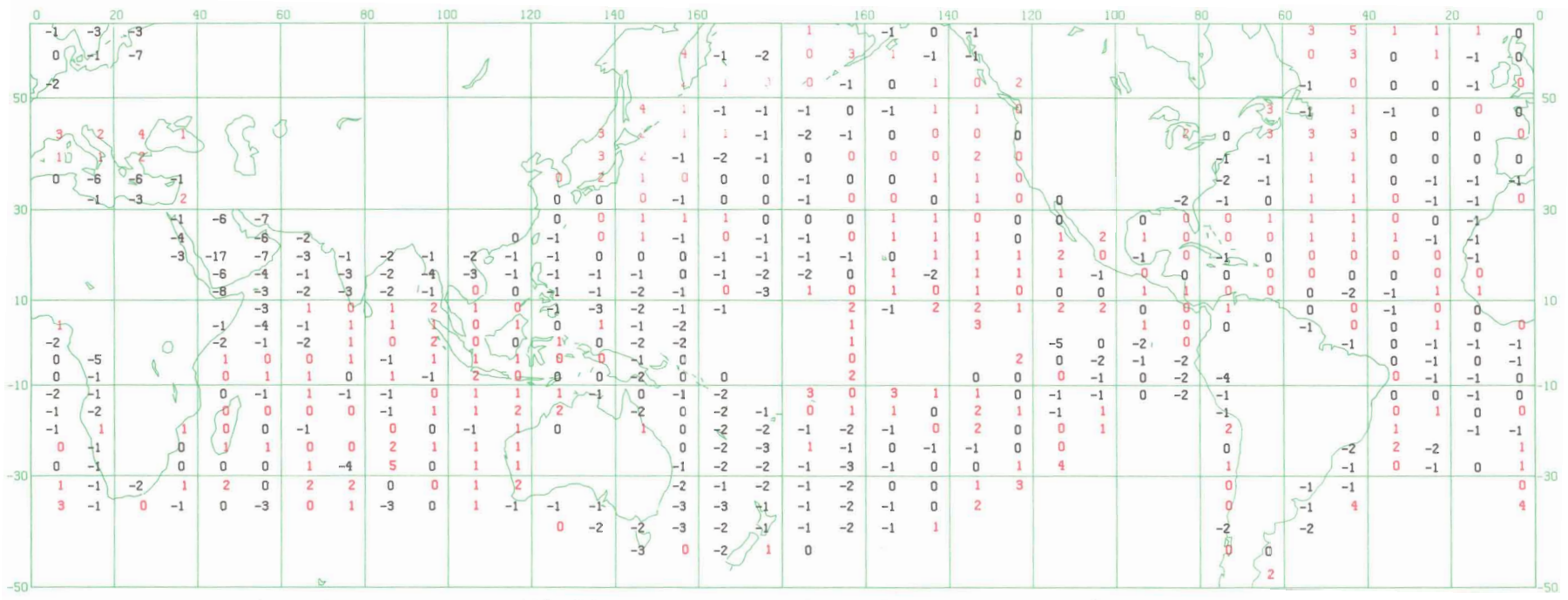

Figure 27b. SST MINUS AIR TEMP MAM2 REGRESSION (tenths of °C/MB)

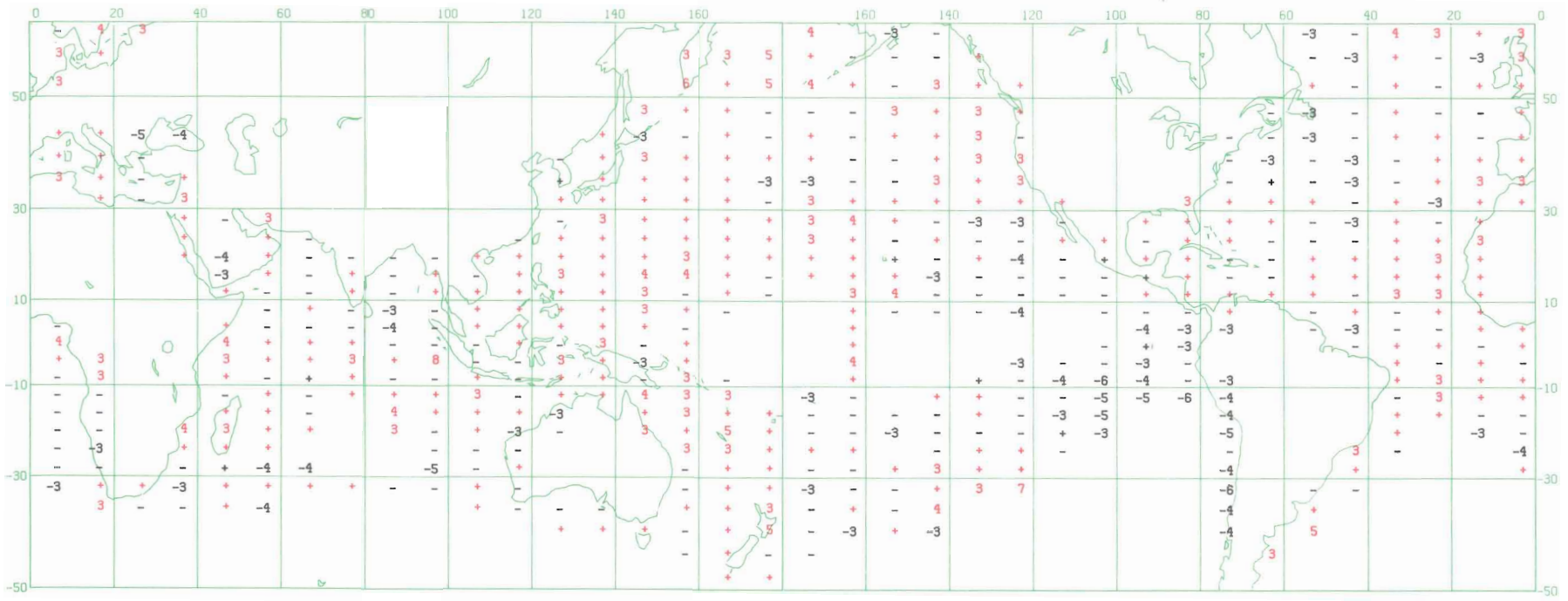

Figure 28a. CLOUDINESS DJF1 CORRELATION

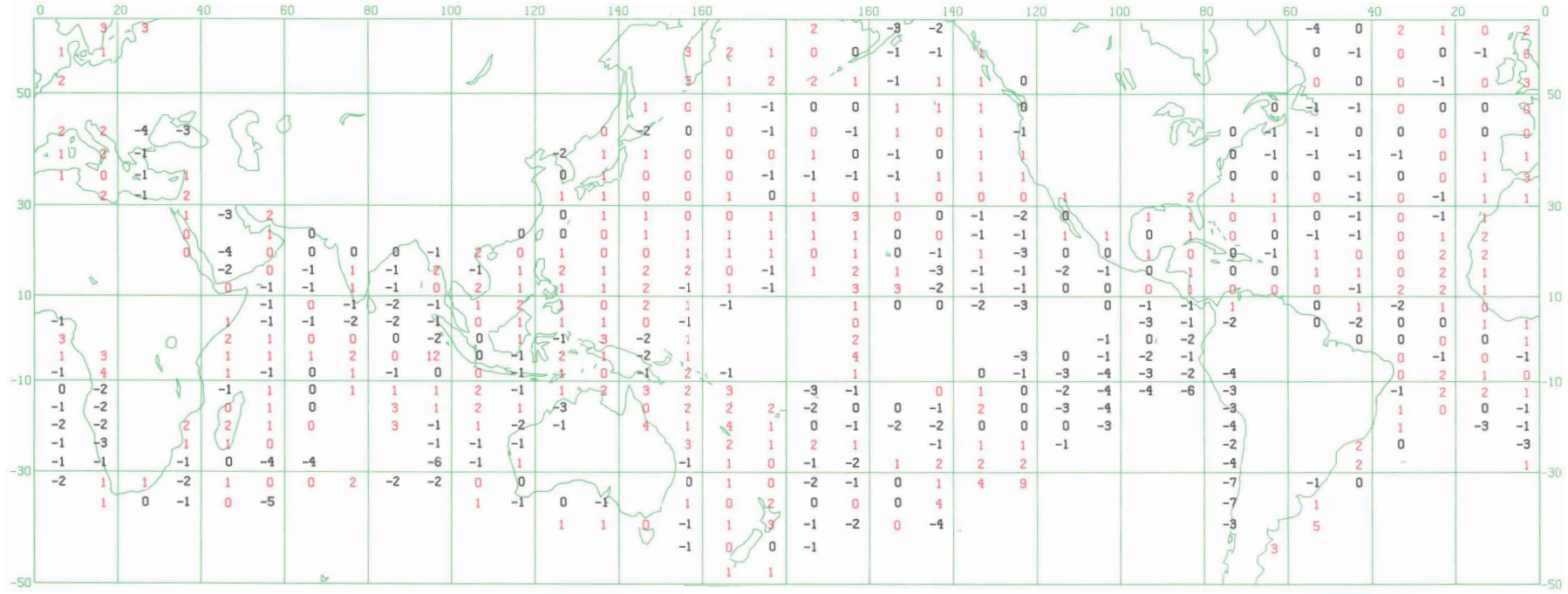

Figure 28b. CLOUDINESS DJF1 REGRESSION (tenths of OKTAS/MB)

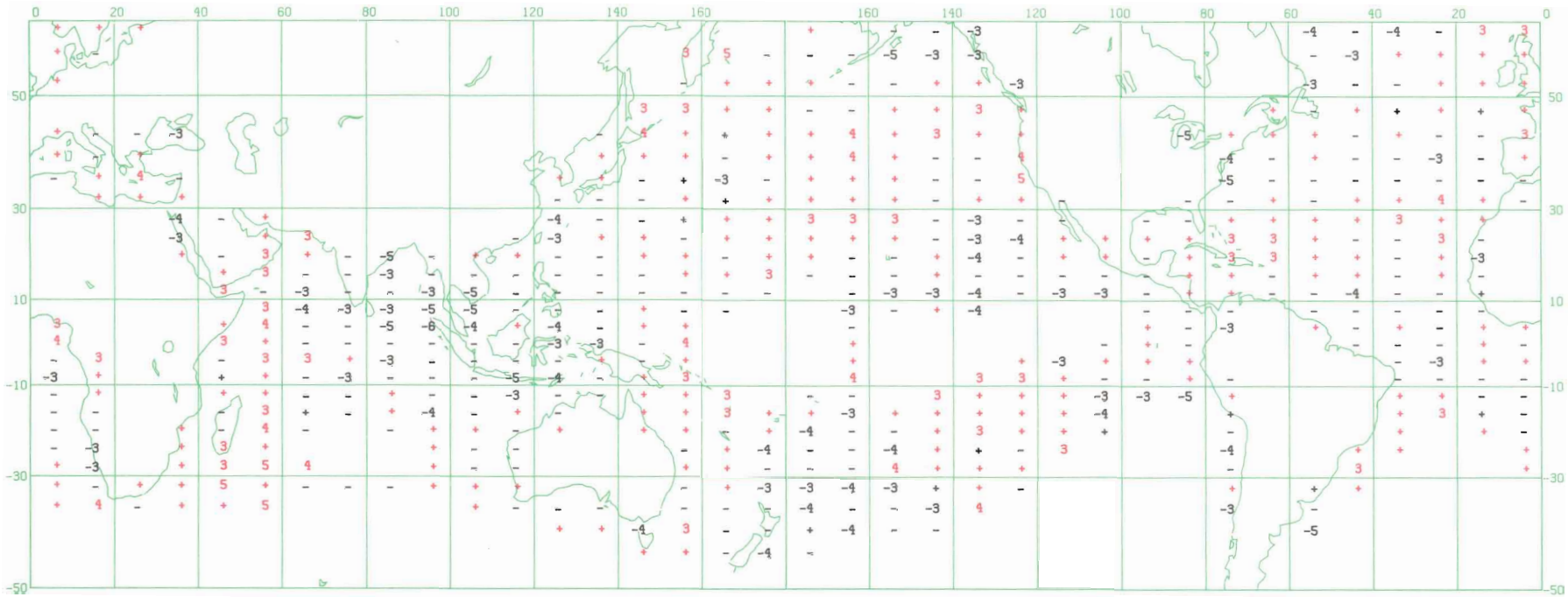

Figure 29a. CLOUDINESS MAM1 CORRELATION

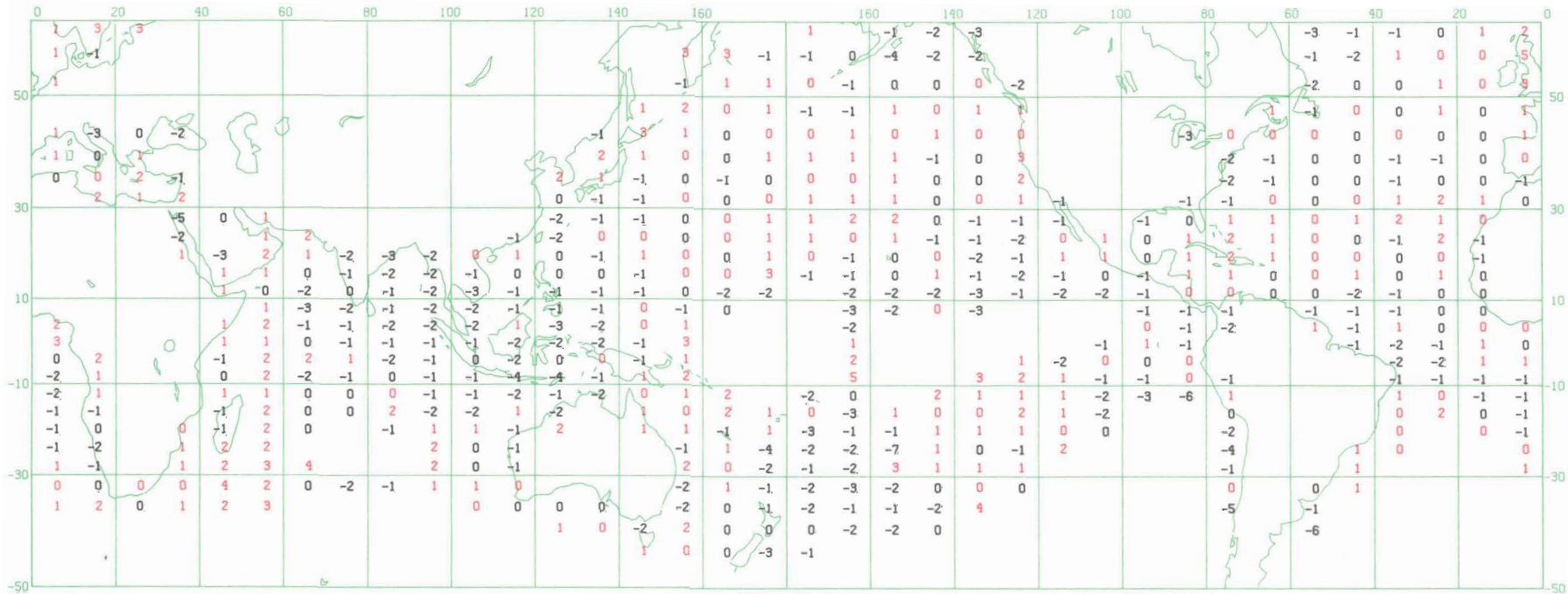

Figure 29b. CLOUDINESS MAM1 REGRESSION (tenths of OKTAS/MB)

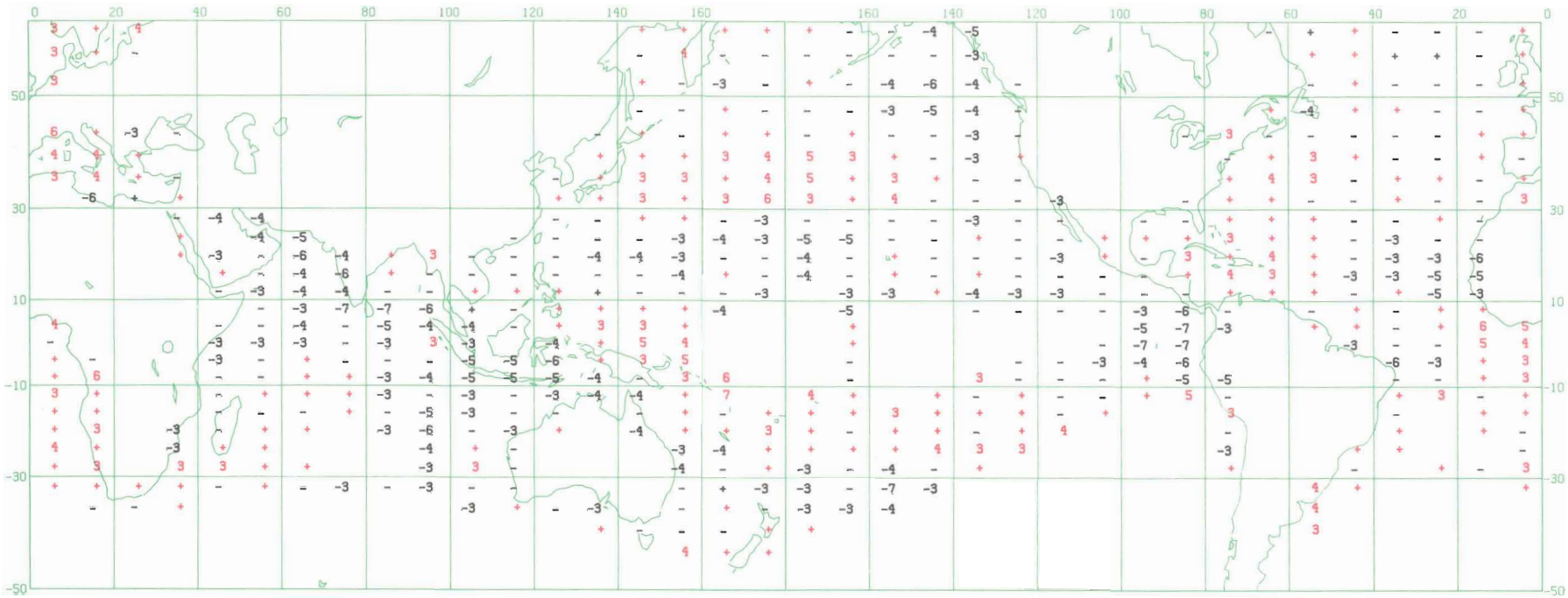

Figure 30a. CLOUDINESS JJA CORRELATION

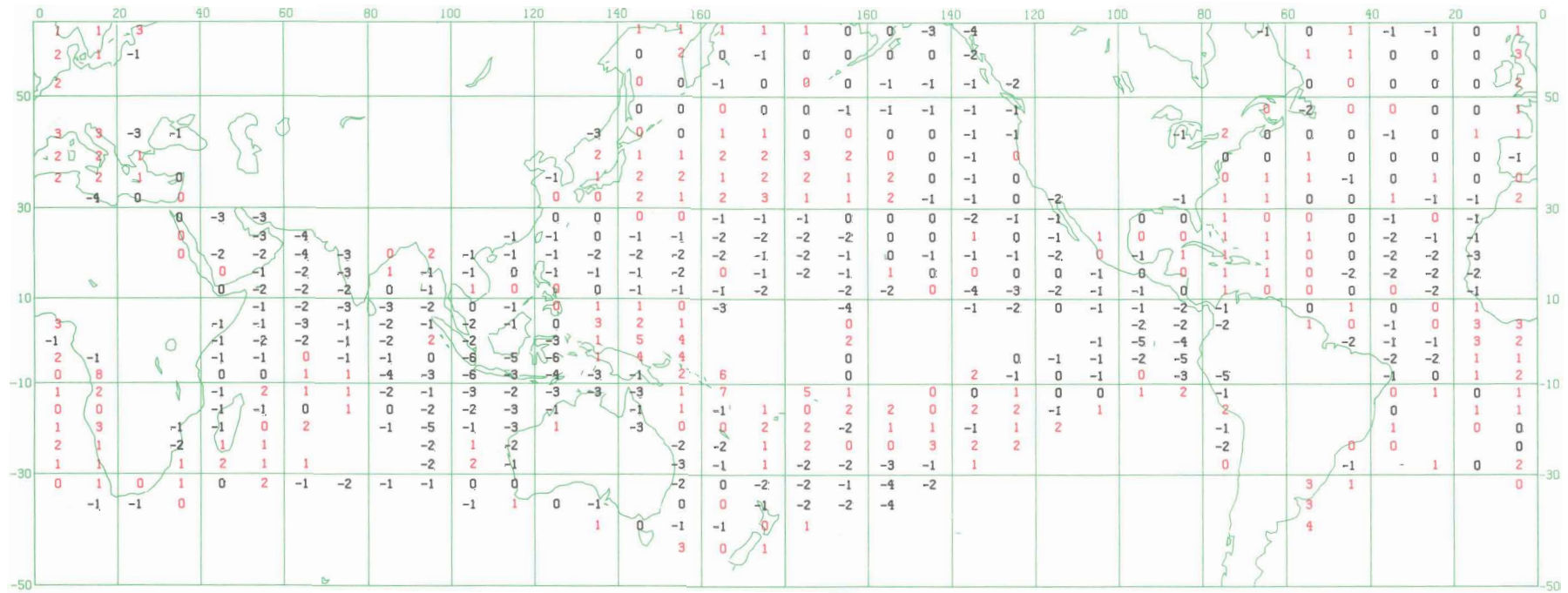

Figure 30b. CLOUDINESS JJA REGRESSION (tenths of OKTAS/MB)

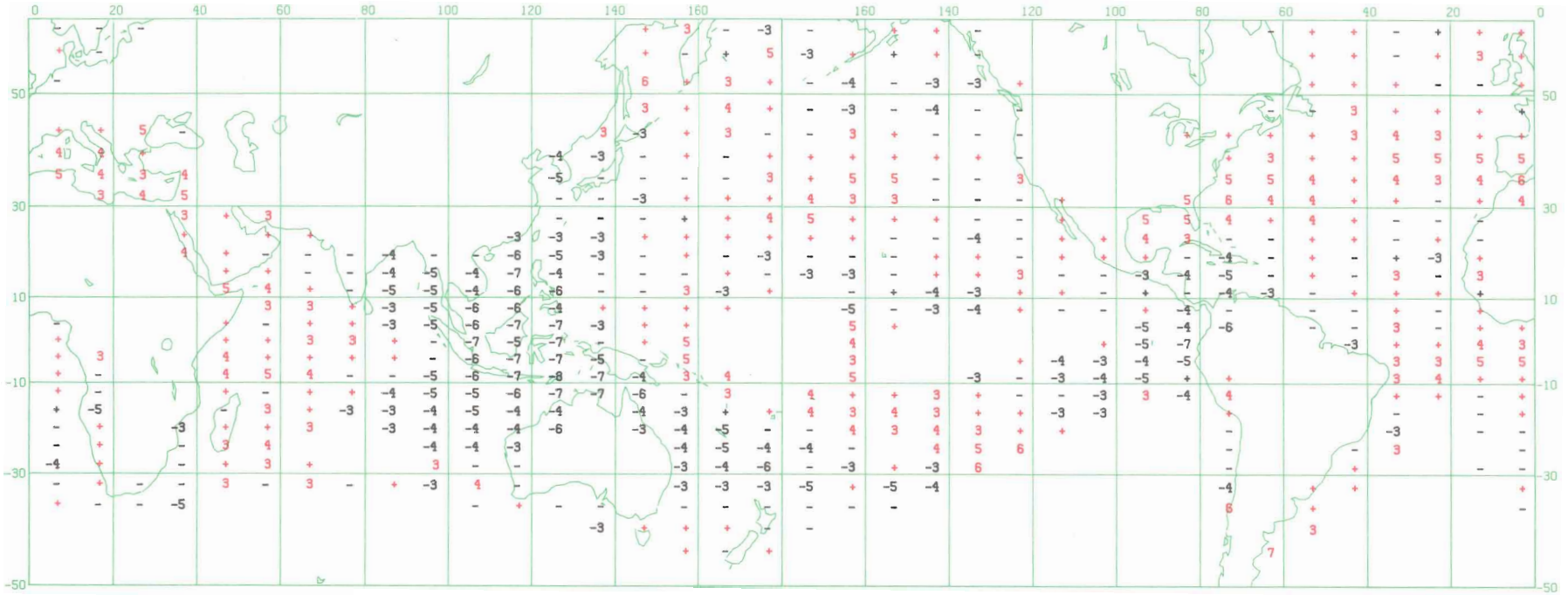

Figure 31a. CLOUDINESS SON CORRELATION

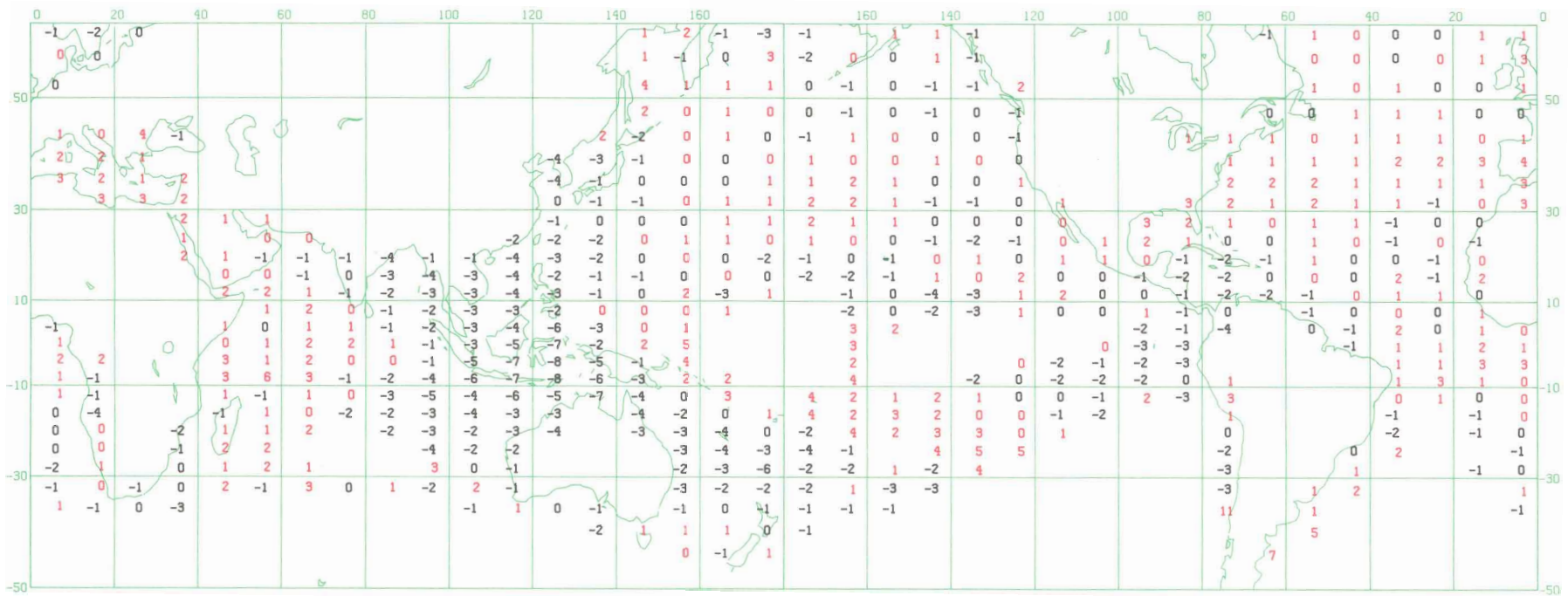

Figure 31b. CLOUDINESS SON REGRESSION (tenths of OKTAS/MB)

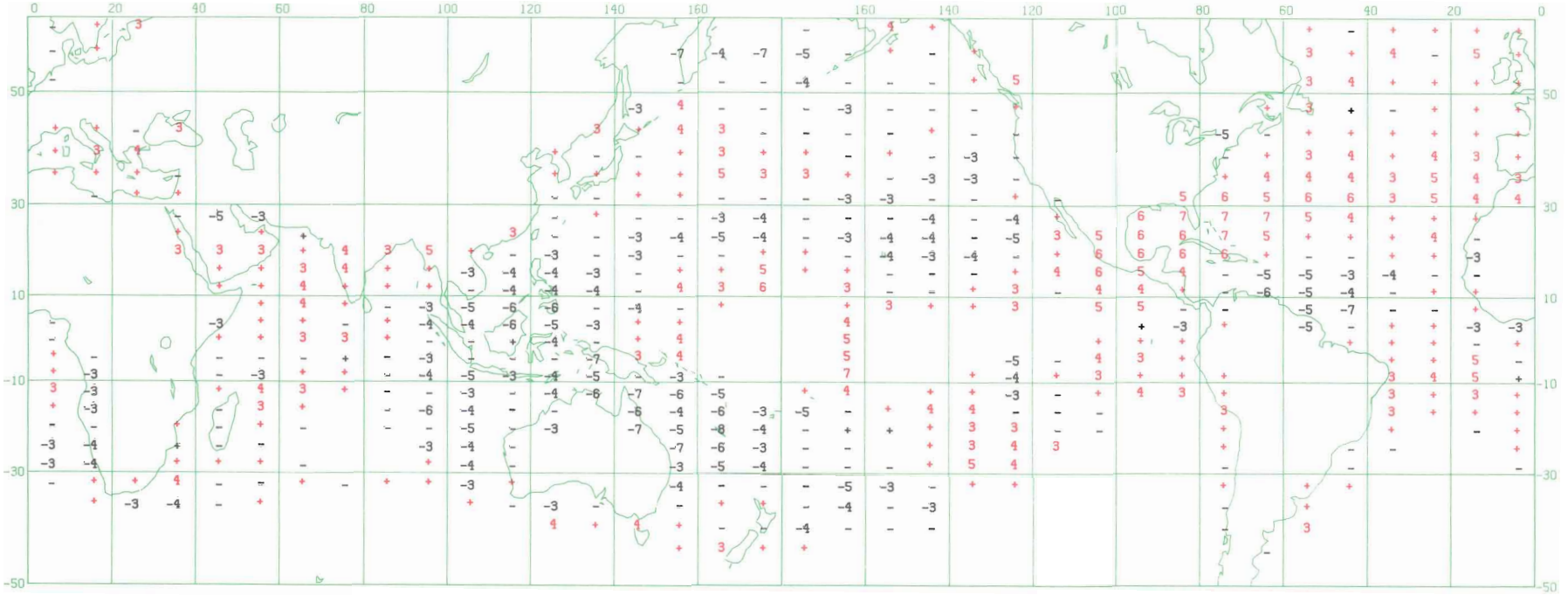

Figure 32a. CLOUDINESS DJF2 CORRELATION

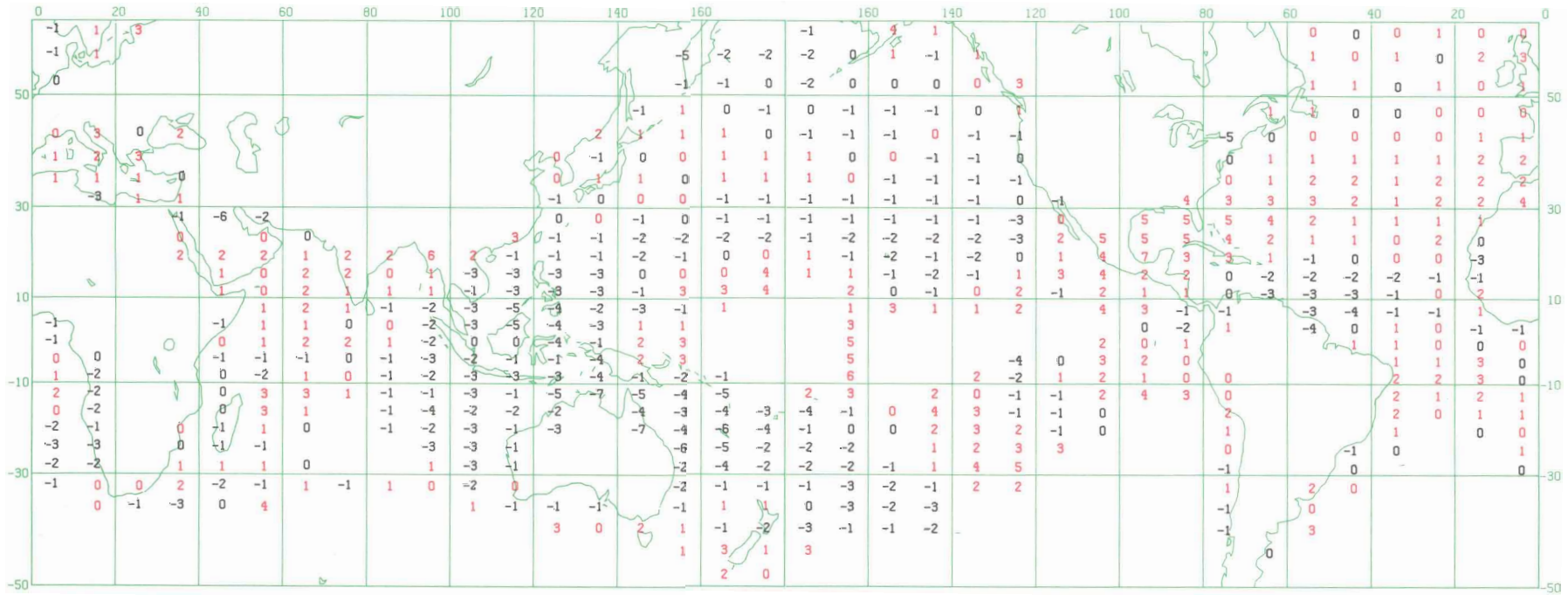

Figure 32b. CLOUDINESS DJF2 REGRESSION (tenths of OKTAS/MB)

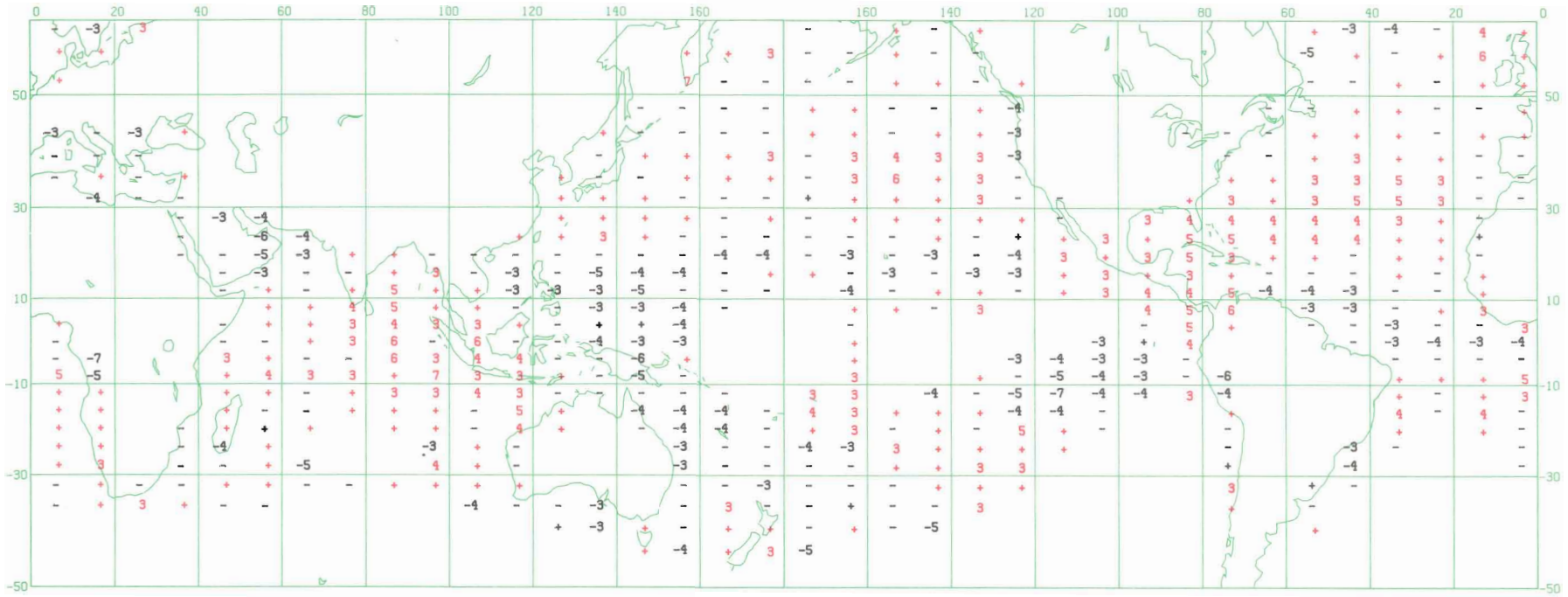

Figure 33a. CLOUDINESS MAM2 CORRELATION

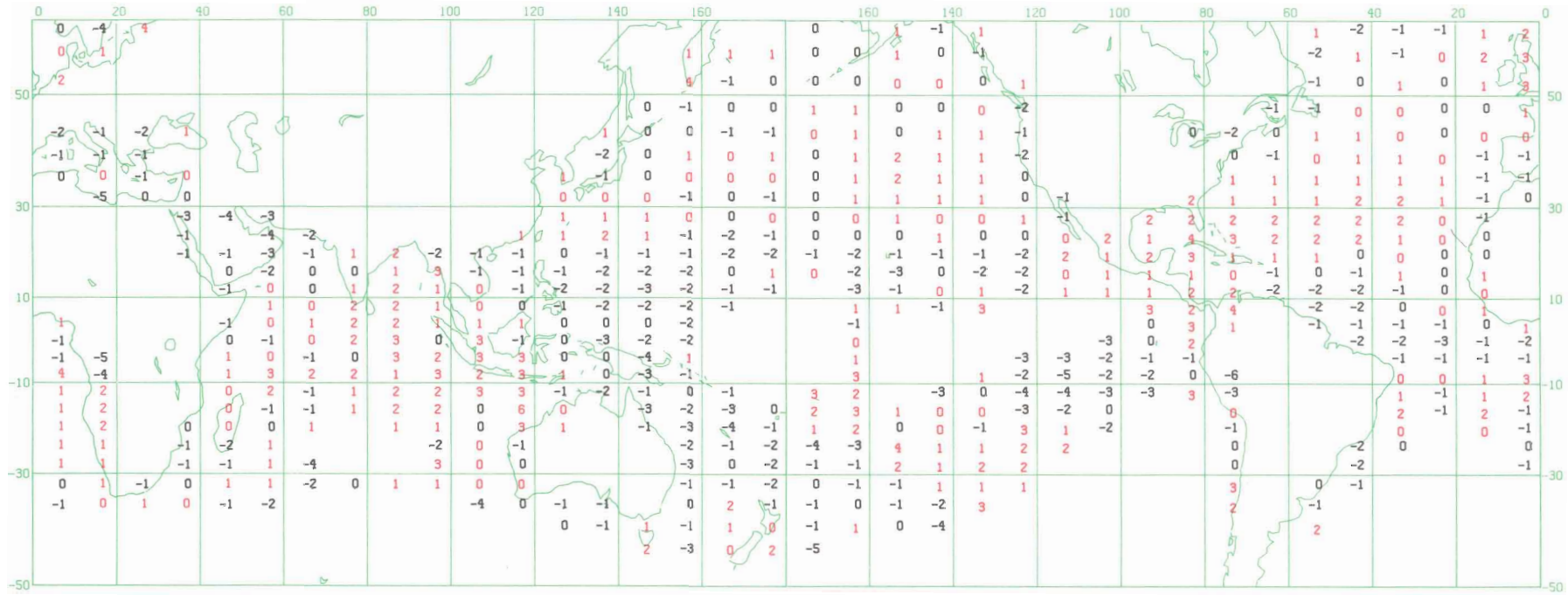

Figure 33b. CLOUDINESS MAM2 REGRESSION (tenths of OKTAS/MB)

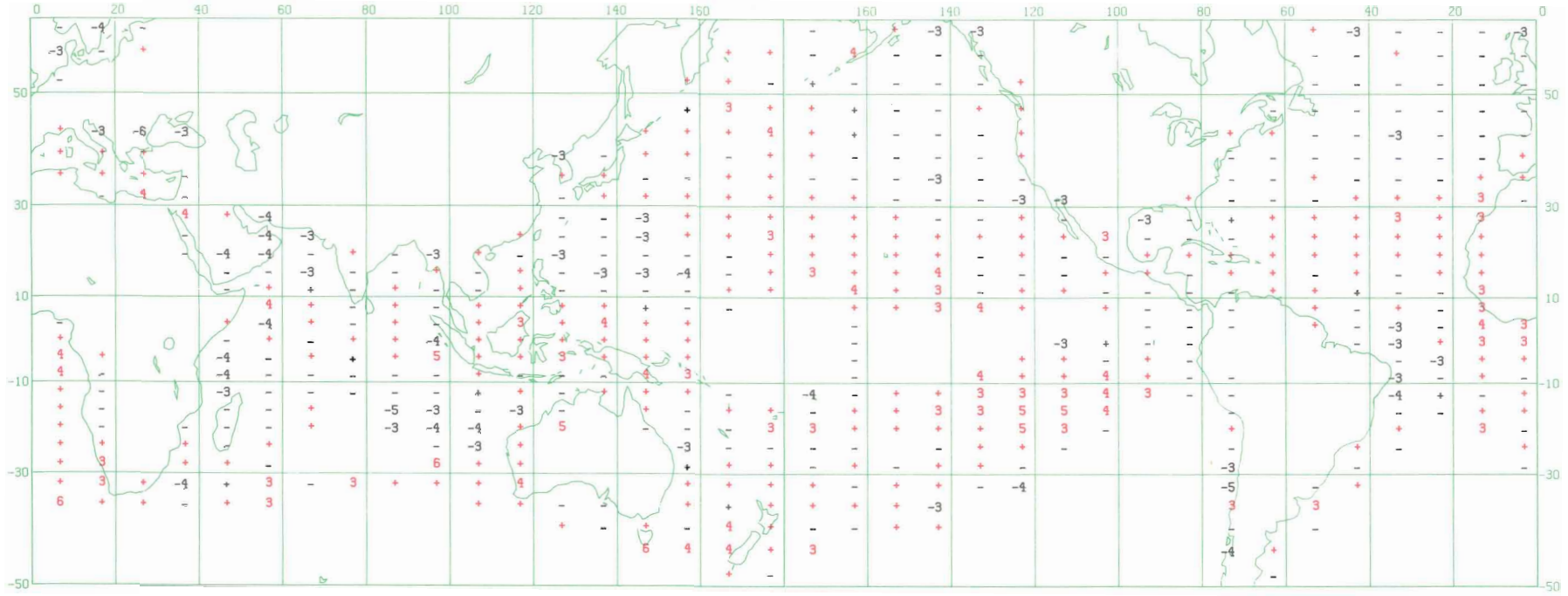

Figure 34a. U-COMPONENT OF WIND DJF1 CORRELATION

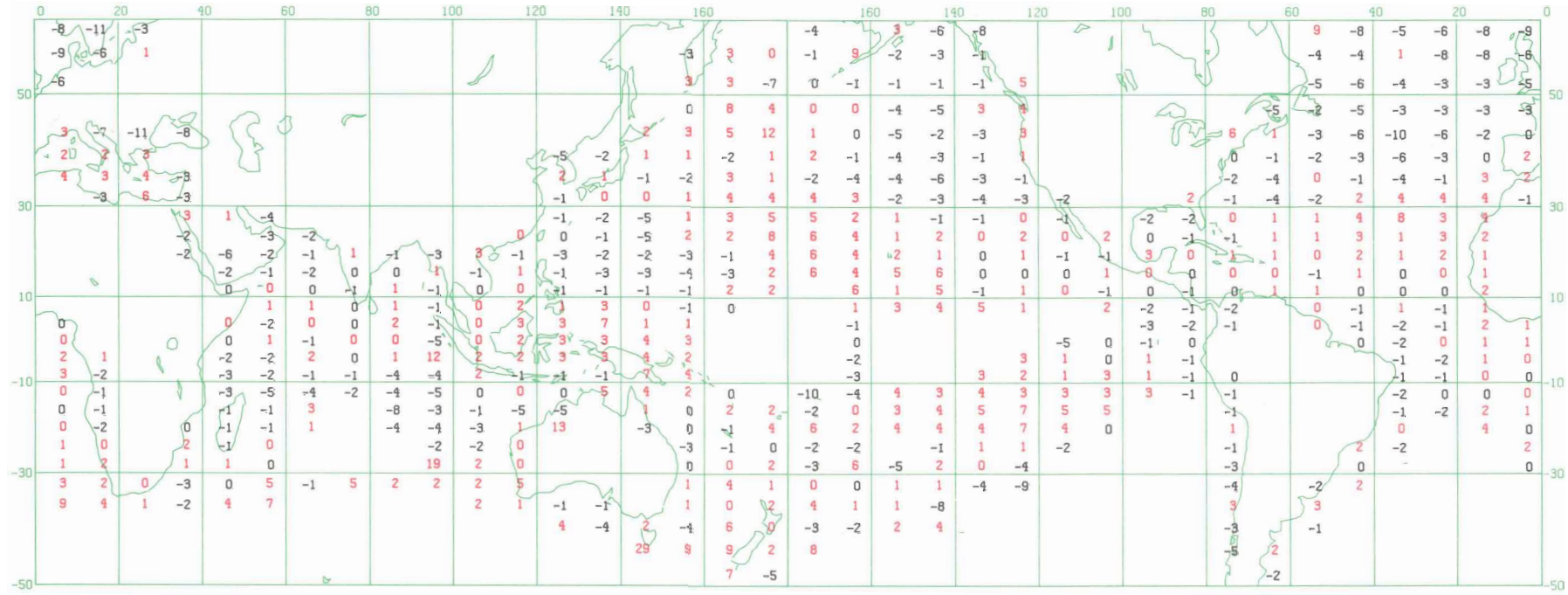

Figure 34b. U-COMPONENT OF WIND DJF1 REGRESSION (tenths of MS^{-1}/MB)

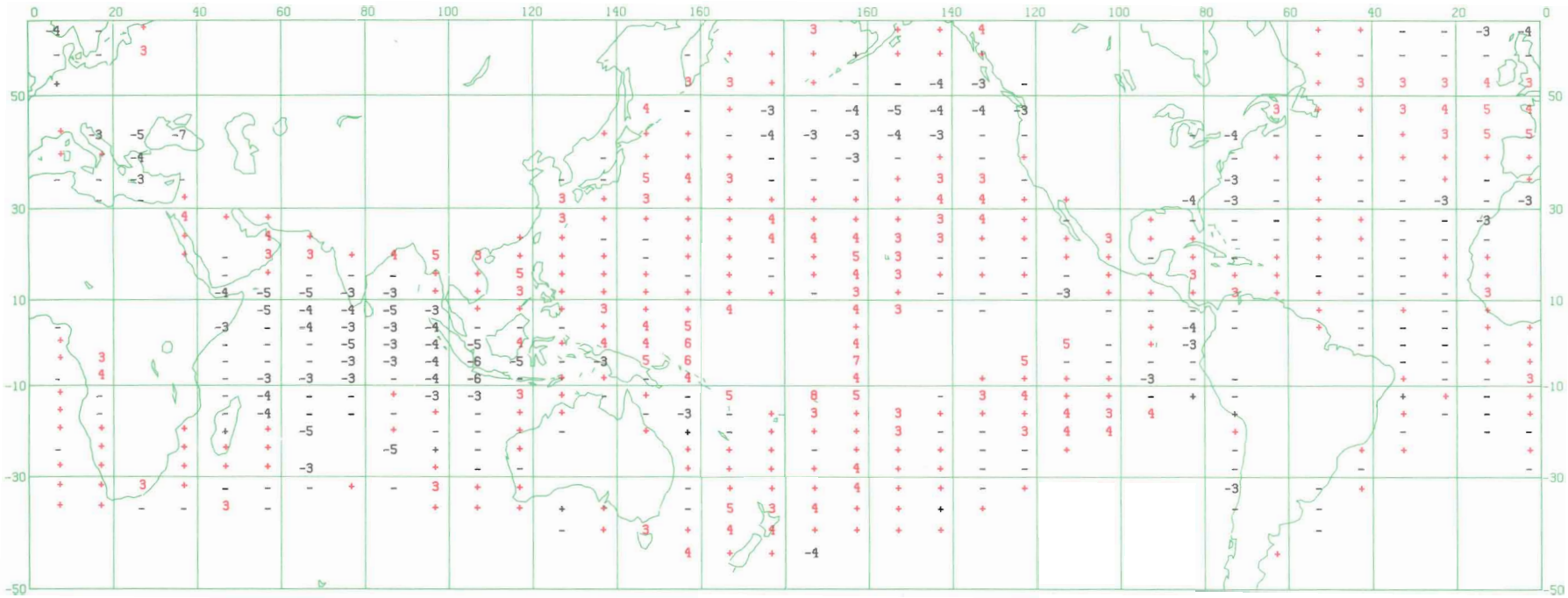

Figure 35a. U-COMPONENT OF WIND MAM1 CORRELATION

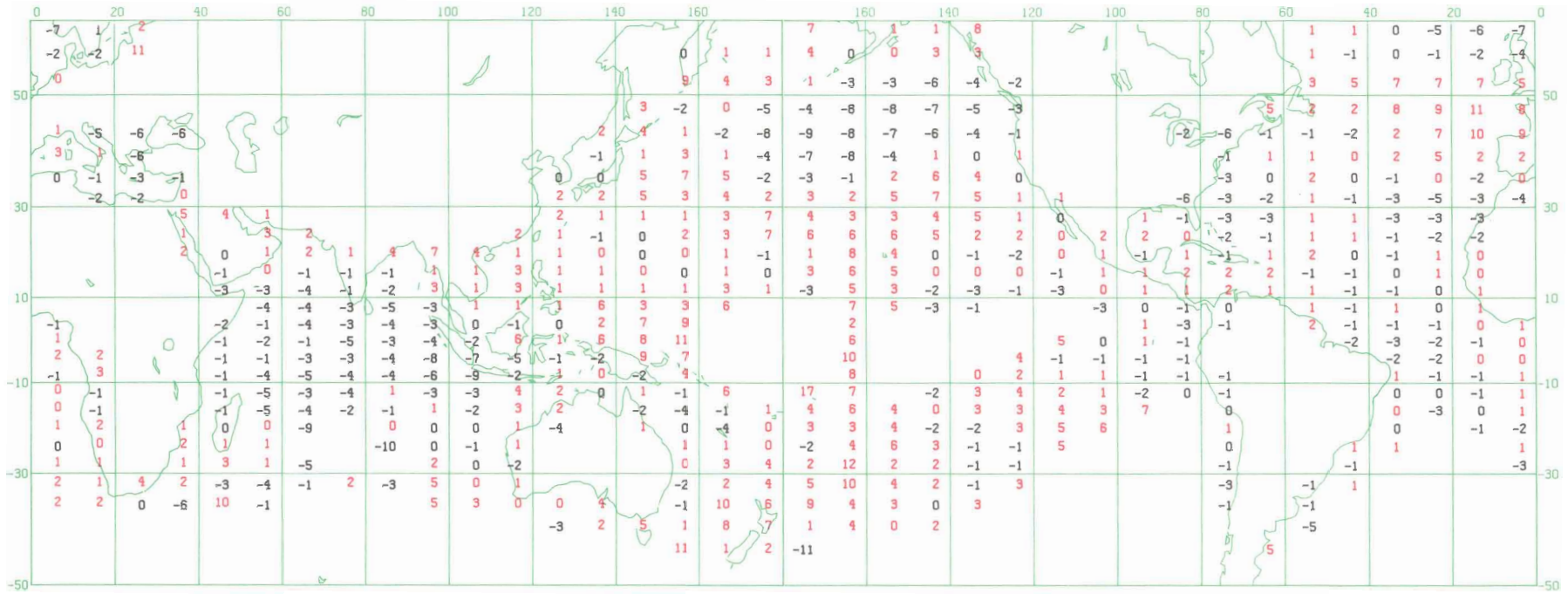

Figure 35b. U-COMPONENT OF WIND MAM1 REGRESSION (tenths of $M S^{-1}/MB$)

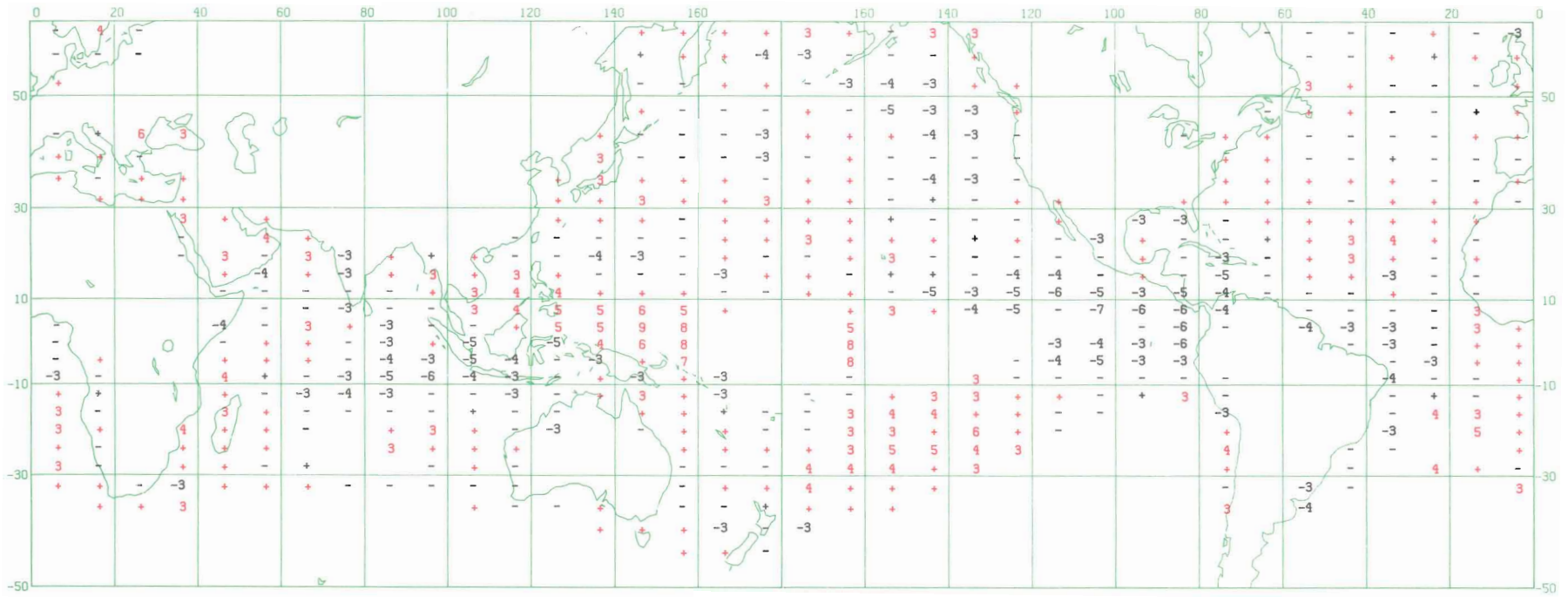

Figure 36a. U-COMPONENT OF WIND JJA CORRELATION

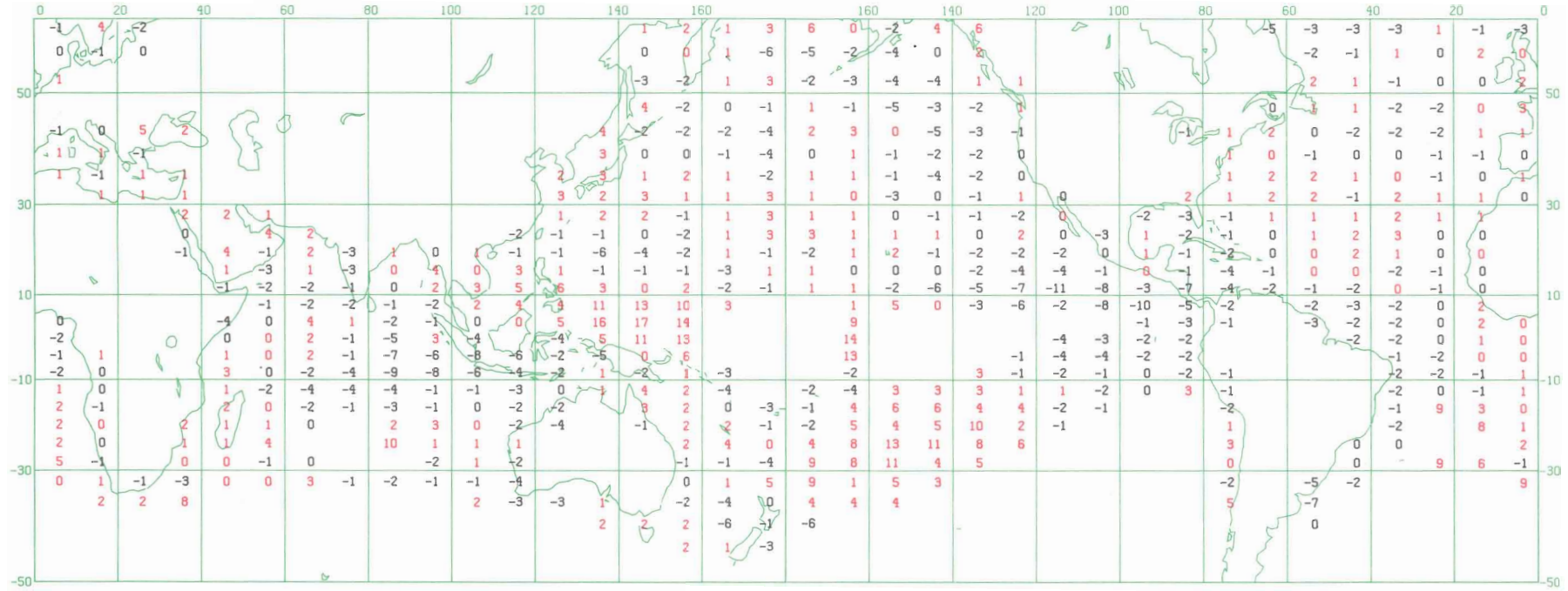

Figure 36b. U-COMPONENT OF WIND JJA REGRESSION (tenths of $M S^{-1}/MB$)

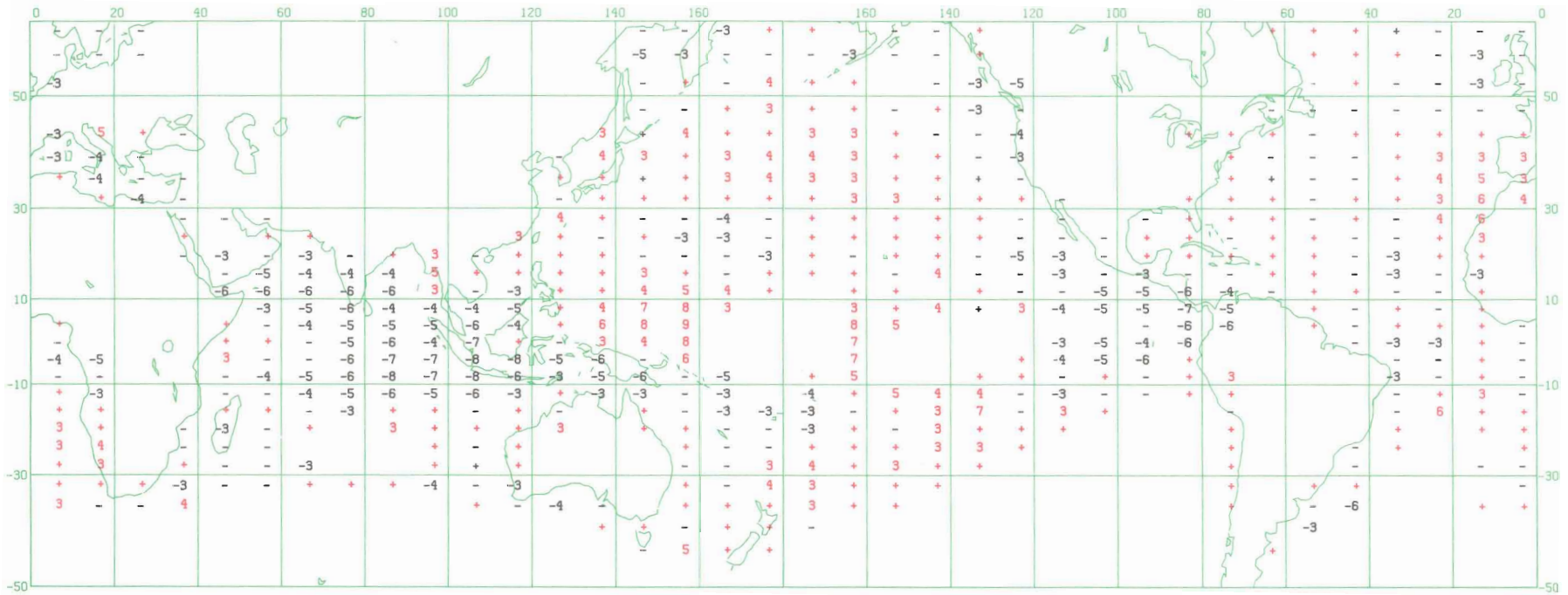

Figure 37a. U-COMPONENT OF WIND SON CORRELATION

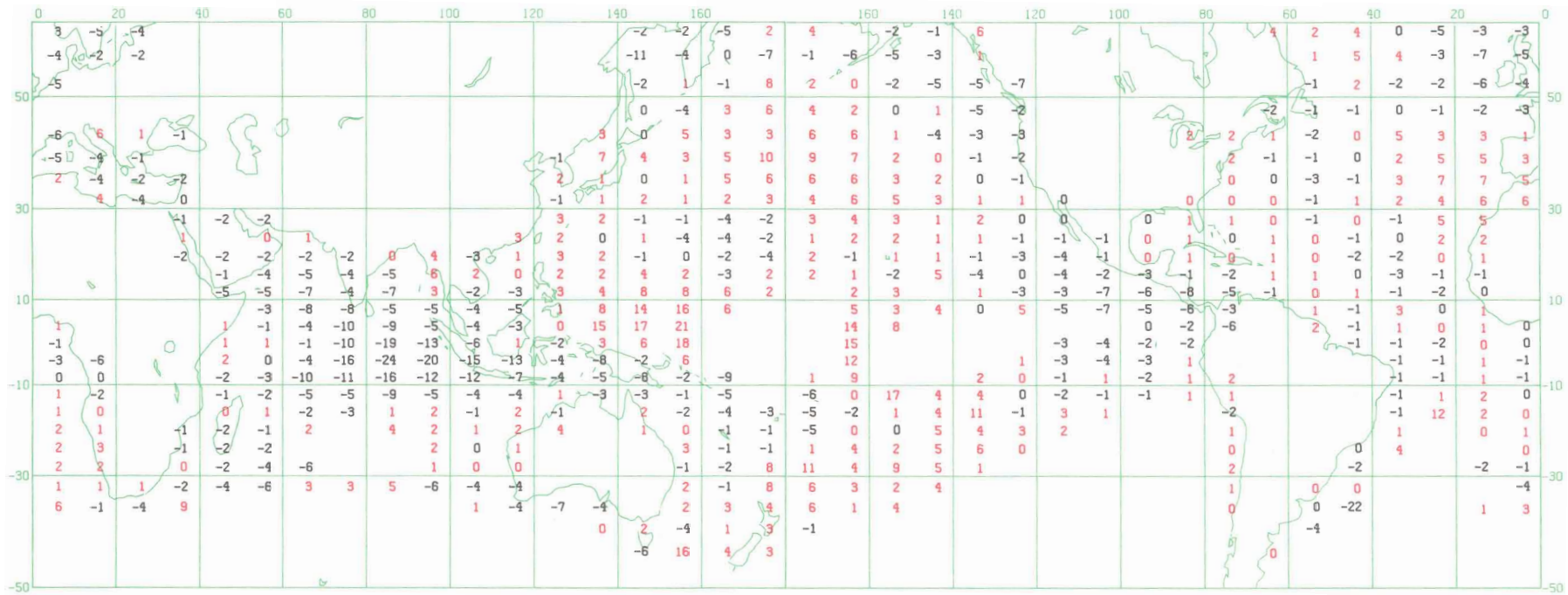

Figure 37b. U-COMPONENT OF WIND SON REGRESSION (tenths of M S^{-1}/MB)

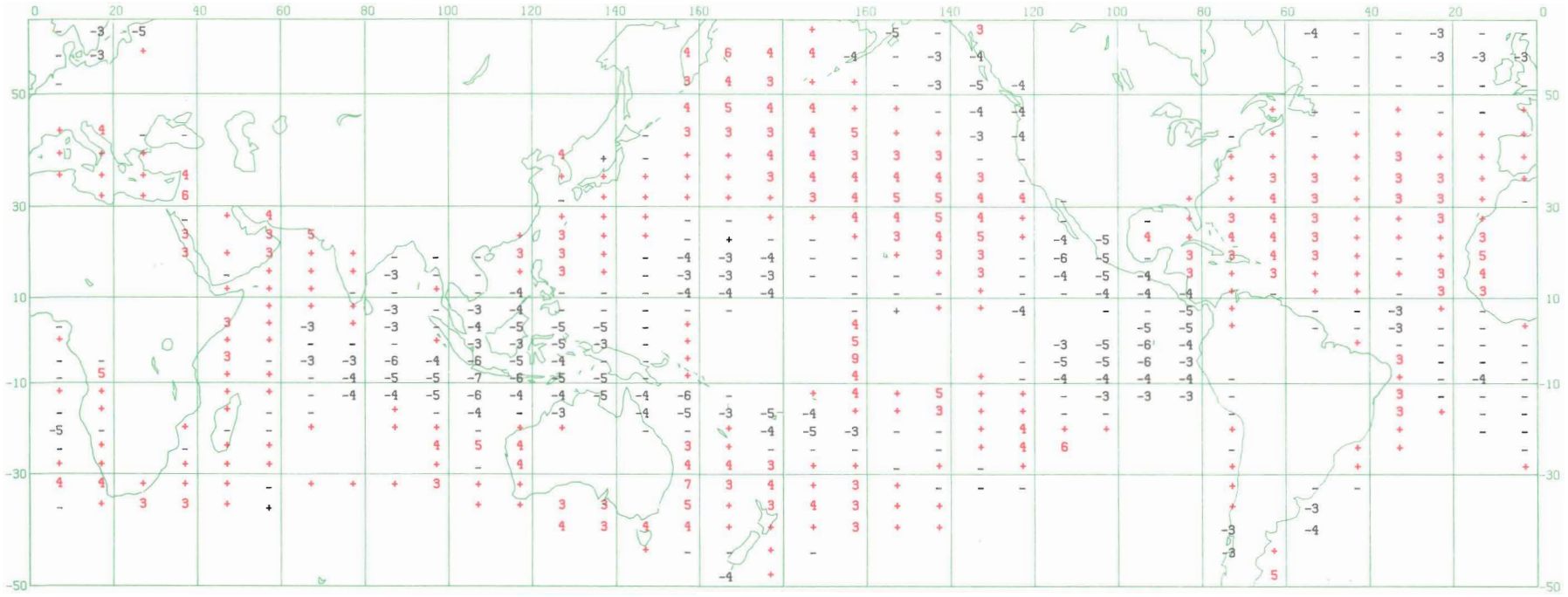

Figure 38a. U-COMPONENT OF WIND DJF2 CORRELATION

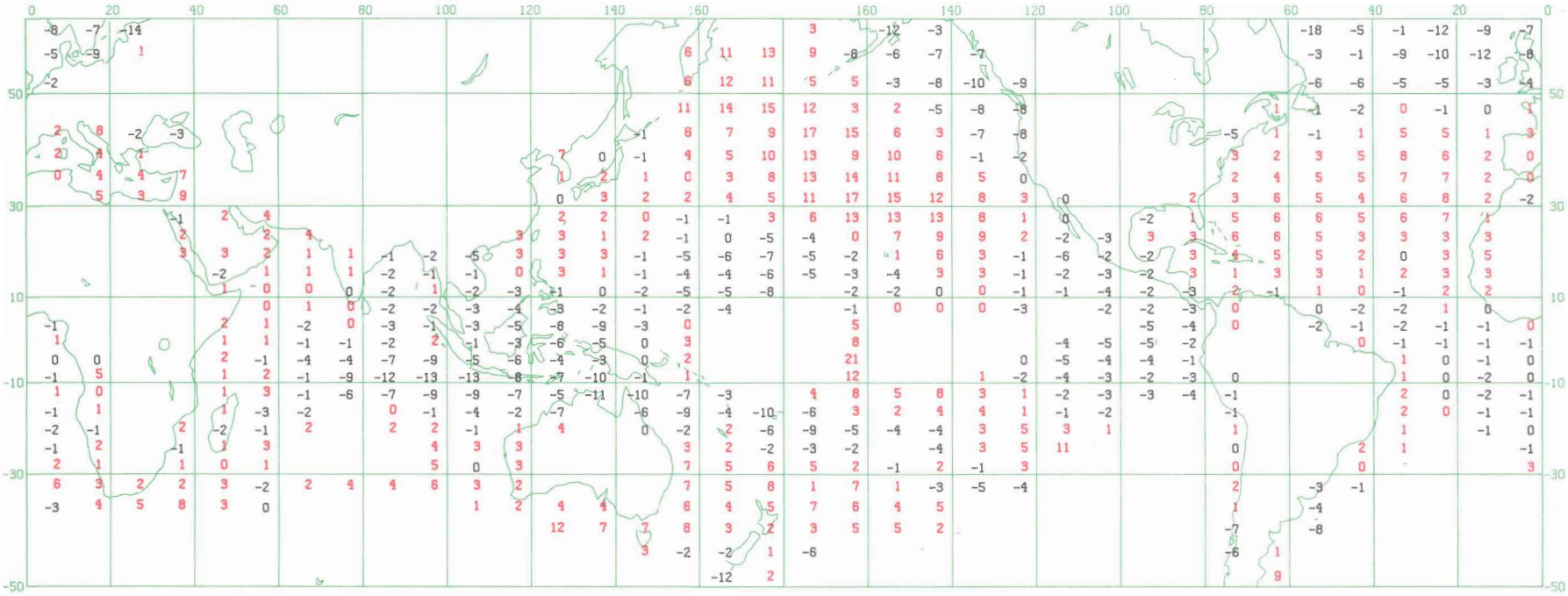

Figure 38b. U-COMPONENT OF WIND DJF2 REGRESSION (tenths of $M S^{-1}$/MB)

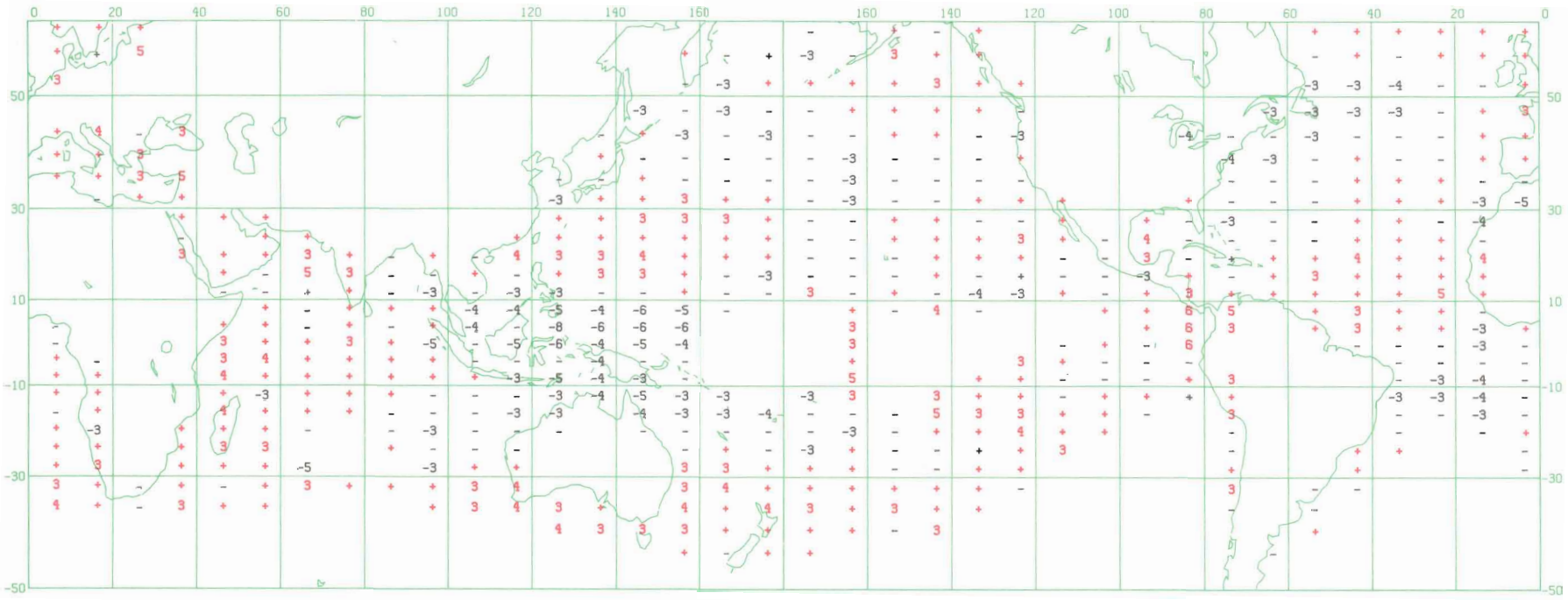

Figure 39a. U-COMPONENT OF WIND MAM2 CORRELATION

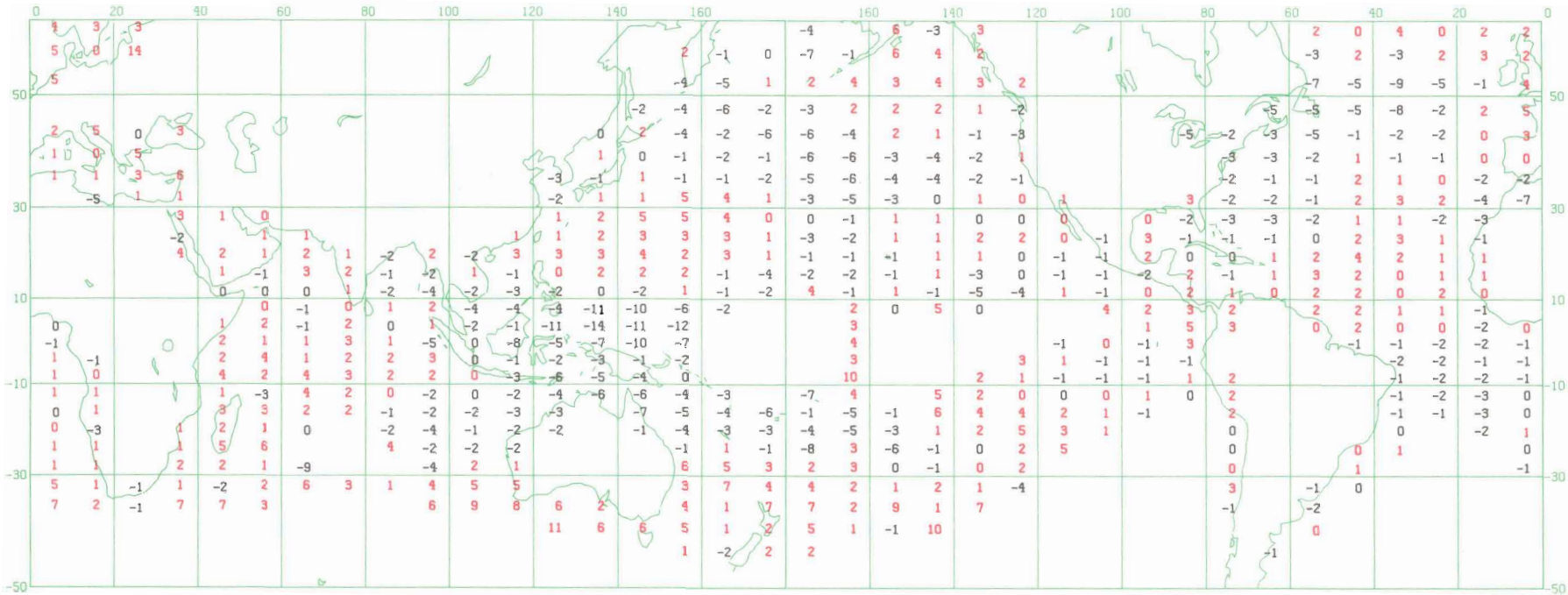

Figure 39b. U-COMPONENT OF WIND MAM2 REGRESSION (tenths of M S^{-1}/MB)

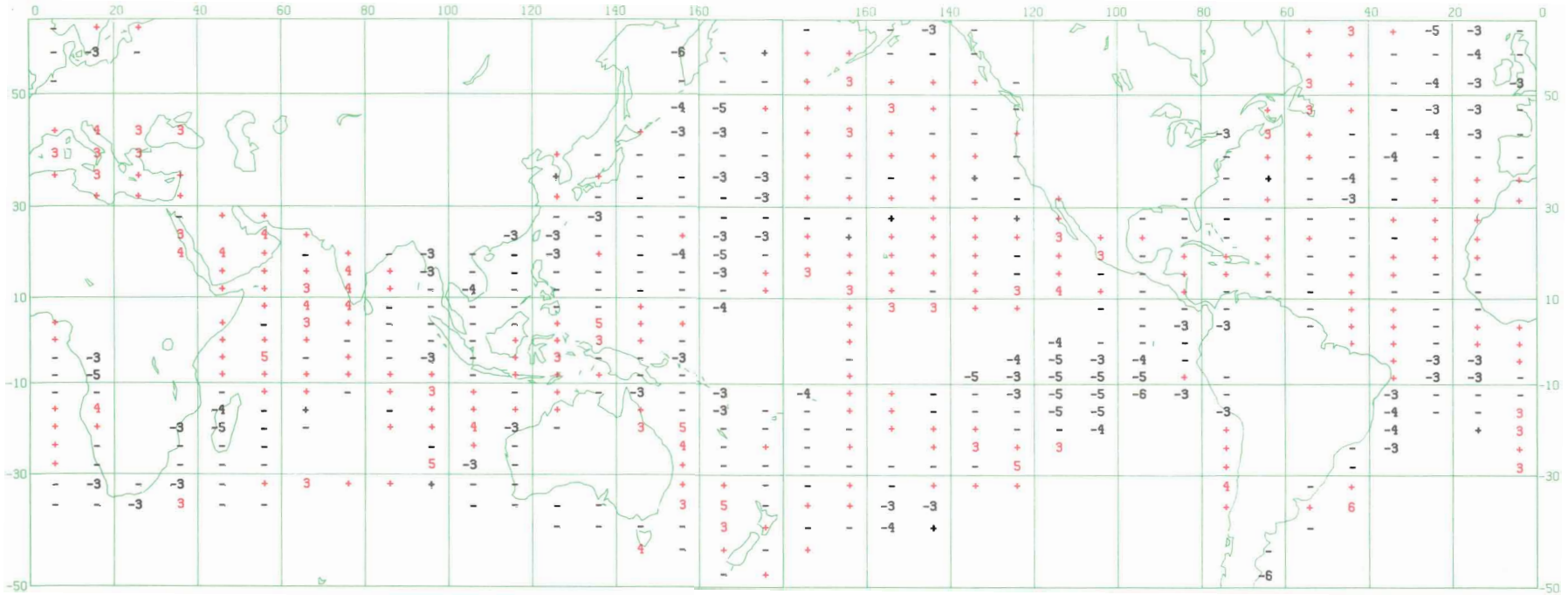

Figure 40. V-COMPONENT OF WIND DJF1 CORRELATION

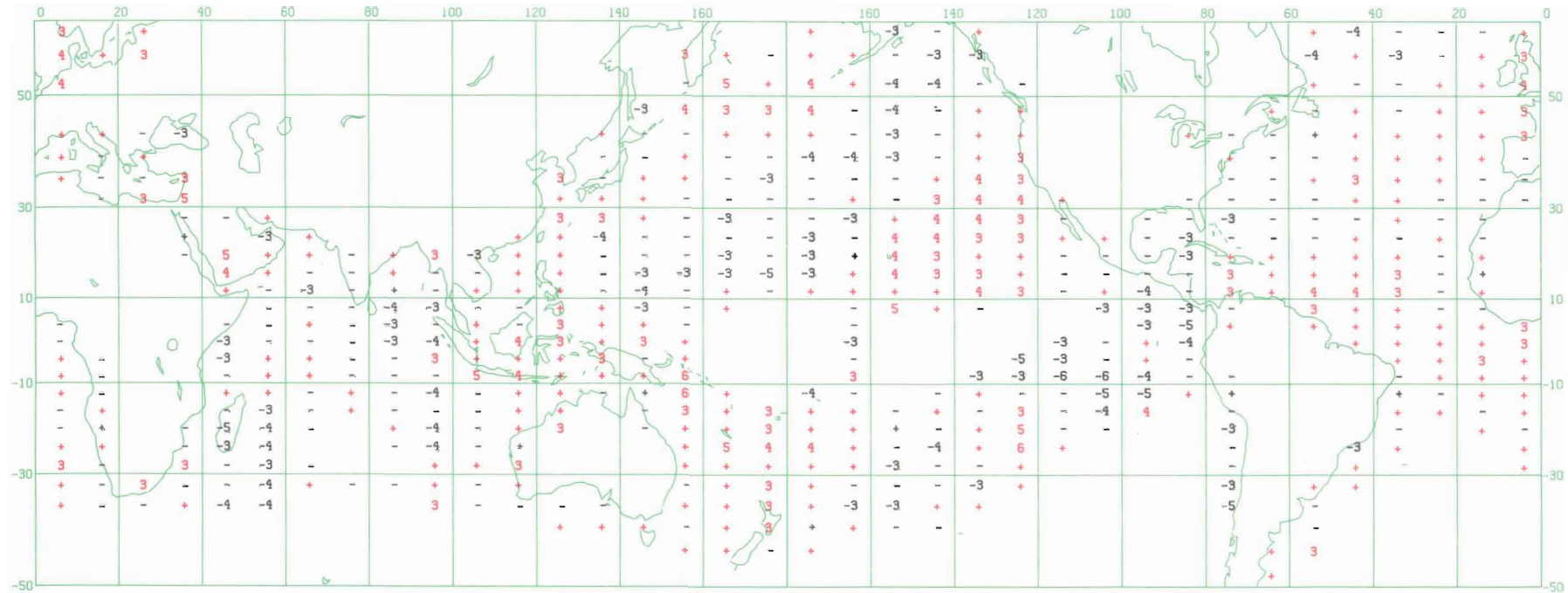

Figure 41. V-COMPONENT OF WIND MAM1 CORRELATION

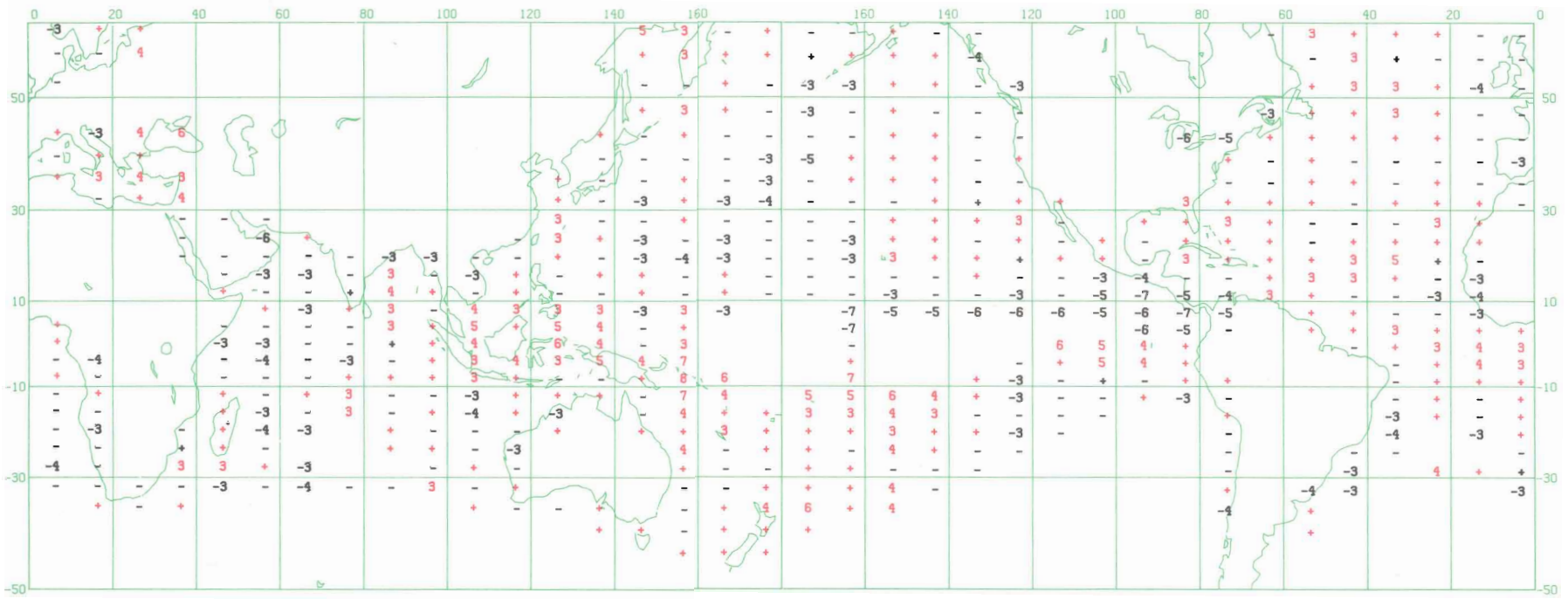

Figure 42. V-COMPONENT OF WIND JJA CORRELATION

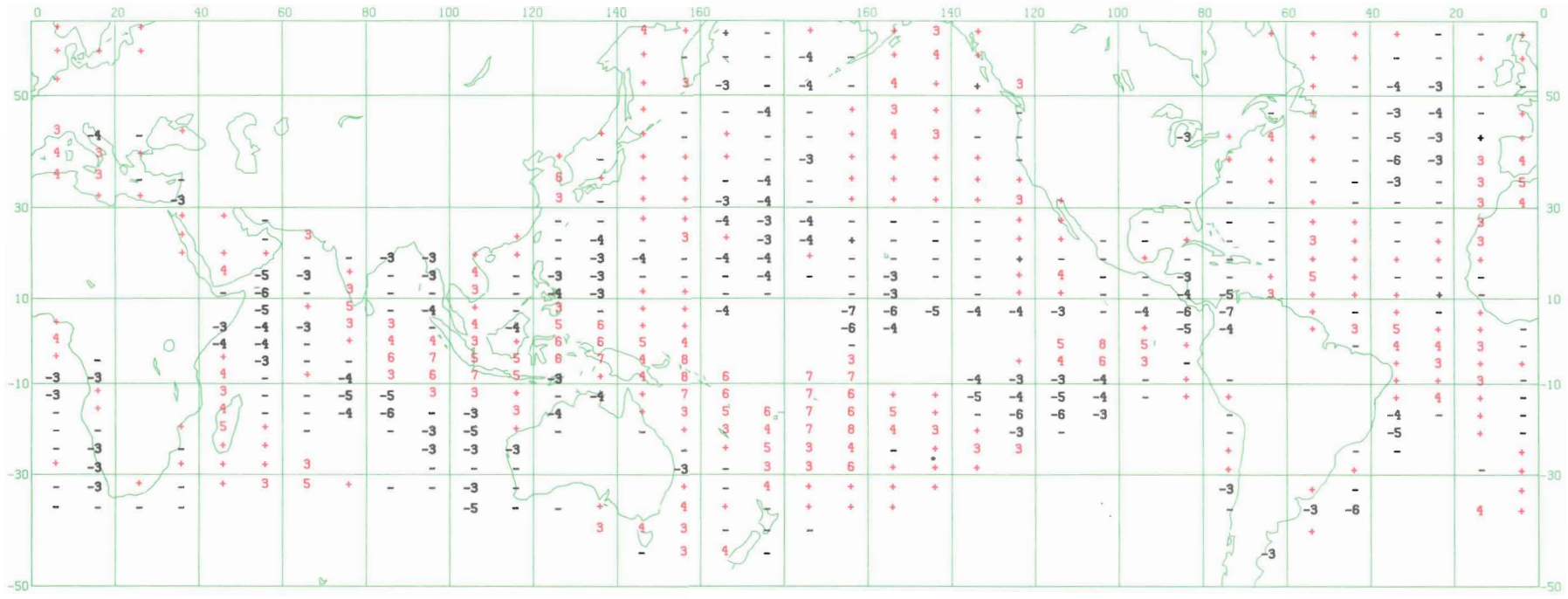

Figure 43. V-COMPONENT OF WIND SON CORRELATION

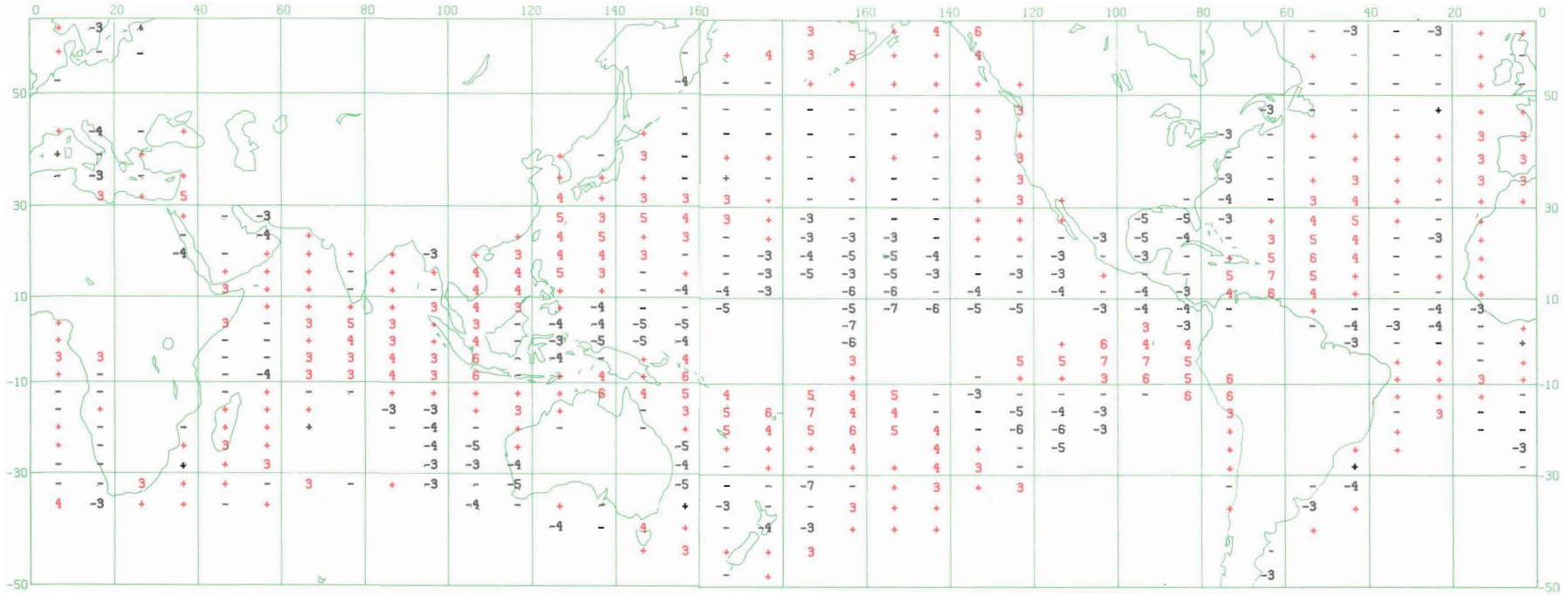

Figure 44. V-COMPONENT OF WIND DJF2 CORRELATION

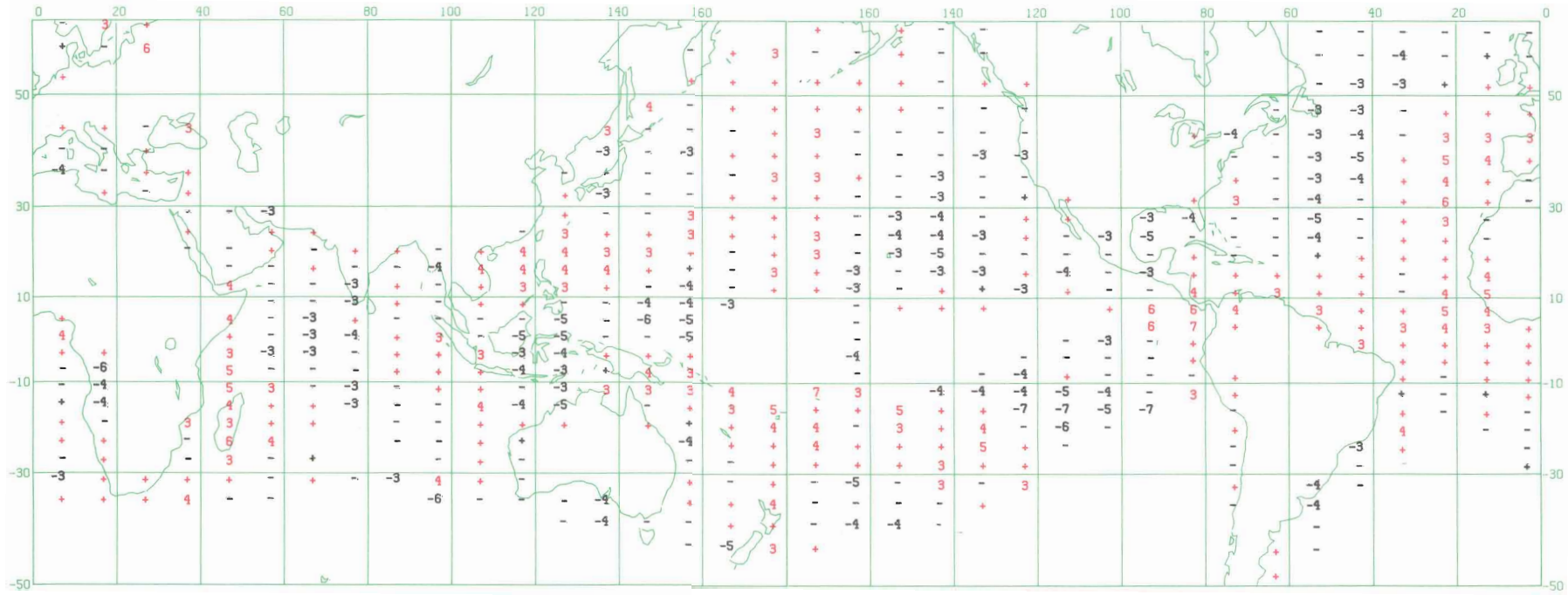

Figure 45. V-COMPONENT OF WIND MAM2 CORRELATION

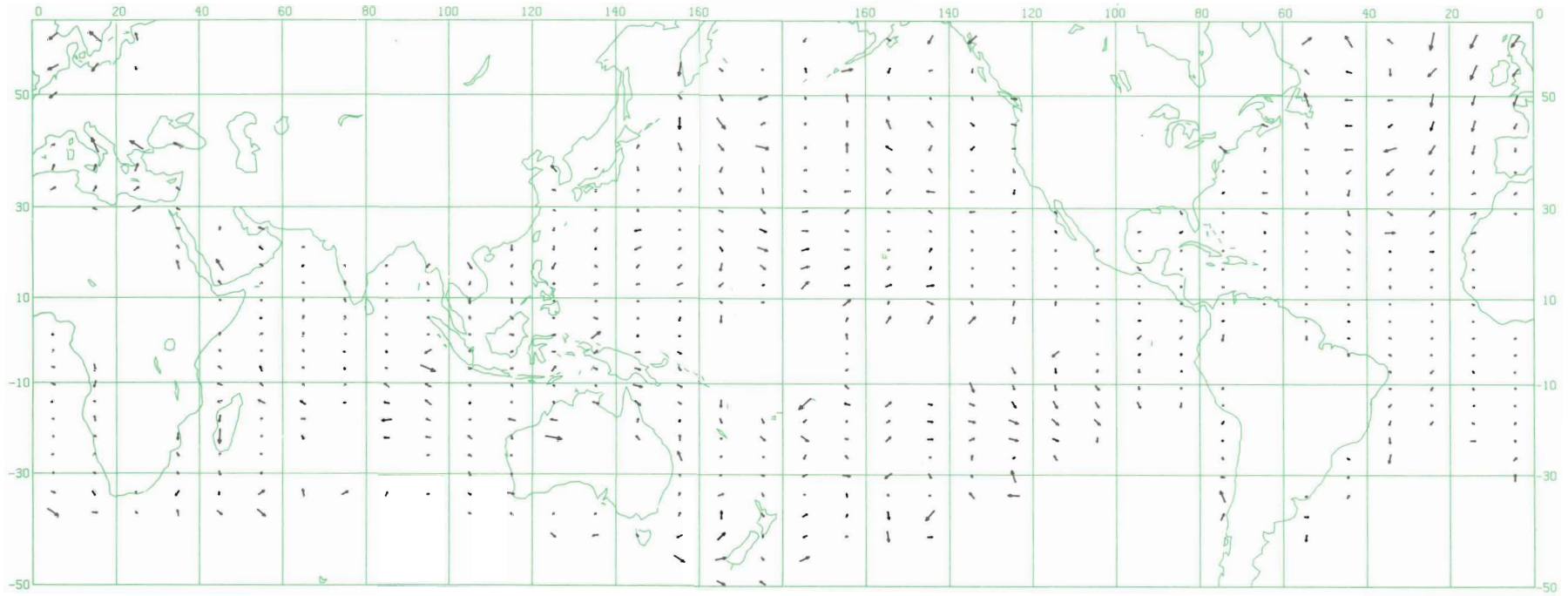

Figure 46. WIND DJF1 REGRESSION (⟶ 3 M S^{-1}/MB)

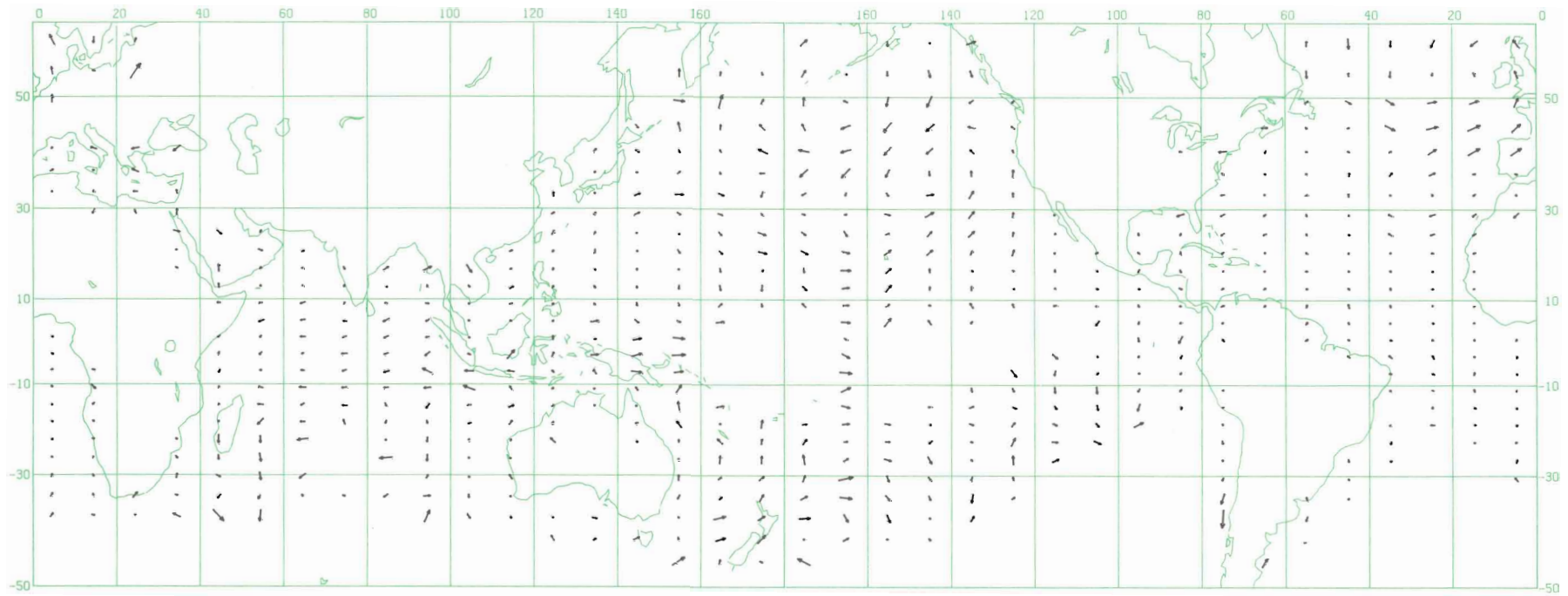

Figure 47. WIND MAM1 REGRESSION (⟶ 3 M S^{-1}/MB)

Figure 48. WIND JJA REGRESSION (⟶ 3 M S^{-1}/MB)

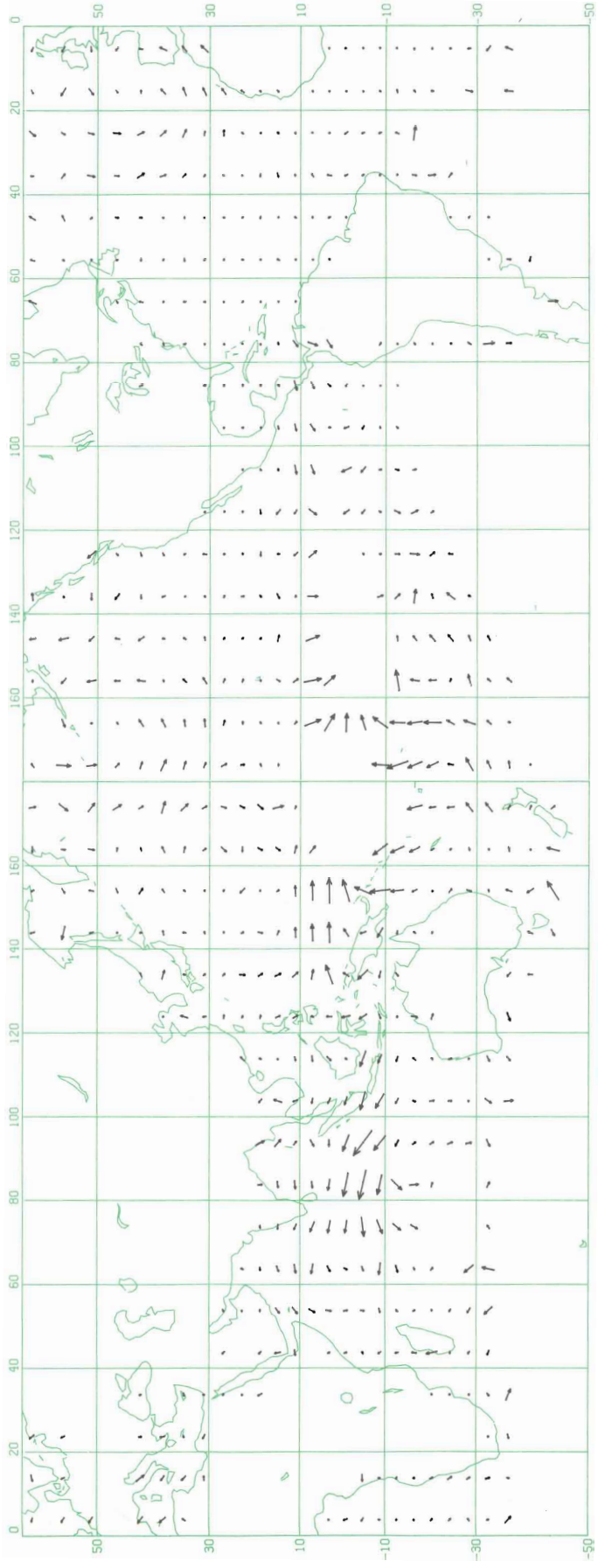

Figure 49. WIND SON REGRESSION (⟶ 3 M S^{-1}/MB)

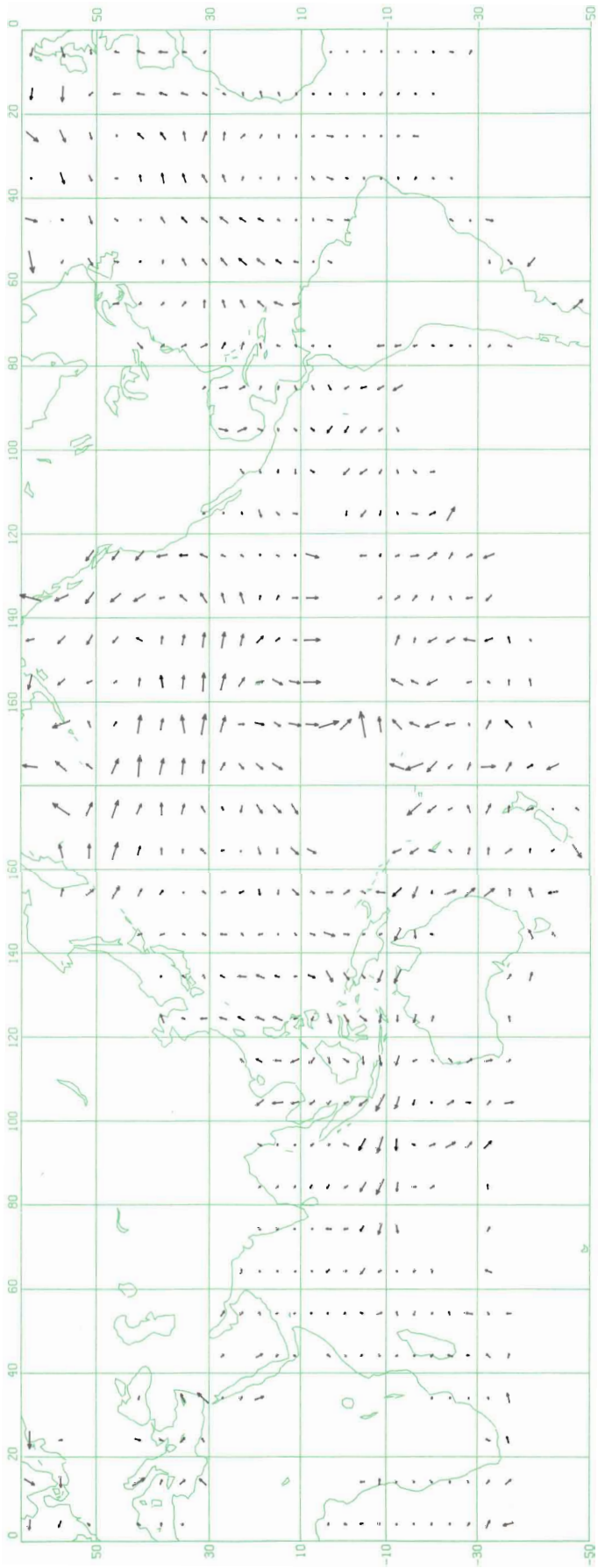

Figure 50. WIND DJF2 REGRESSION (⟶ 3 M S^{-1}/MB)

Figure 51. WIND MAM2 REGRESSION (⟶ 3 M S^{-1}/MB)